UNIVERSITY OF CALIFORNIA
RIVERSIDE

Harnessing Radical Chemistry for the Facile Identification of Post Translational Modification Sites in Proteins by Photodissociation Mass Spectrometry

A Dissertation submitted in partial satisfaction
of the requirements for the degree of

Doctor of Philosophy

in

Chemistry

by

Jolene Katie Diedrich

August 2011

Dissertation Committee:
Dr. Ryan R. Julian, Chairperson
Dr. Yinsheng Wang
Dr. Quan J. Cheng

The Dissertation of Jolene Katie Diedrich is approved:

_____

_____

_____

Committee Chairperson

University of California, Riverside

Acknowledgements

My love of science began with my parents and it was them that first showed me how much fun science could be, from explosions to dissections, science was always fascinating and something to look forward to. My journey into science as a career was further inspired by my high school chemistry and mathematics teachers Ms Greenman and Mrs Everlith. It was because of both of these women that I decided to pursue a degree in chemistry. During my senior year at the University of Denver I had the opportunity to get a taste of research in the university setting. I had the opportunity to be presented with two separate research projects and under the guidance of Dr Keith Miller and Dr Balsingham Murugaverl I learned how to approach and work through a novel research project from start to finish. Up to this point I had never considered the possibility of grad school but fell in love with the idea of continuing the journey. A year later I found myself at UCR in the lab of Ryan Julian and I couldn't have ended up in a better place.

I want to thank my PI Ryan Julian for being a great mentor to me the last five years. Thank you for inspiring me in research and helping me to grow as a scientist. Ryan taught me how to think out of the box and how to approach

scientific problems from a position that may be atypical but often results in beautiful data. Experiments often didn't work out as hoped or even planned but learning to laugh at my unusual results and my unique way of doing chemistry not only inspired me to keep trying but made successful experiments that much more fulfilling. The unexpected results were often the beginning of new exciting projects. I will be forever grateful for all the time and energy that Ryan spent guiding me through this process.

I want to thank my labmates, past and present (Tony, Emily, Helen, Zhenjiu, Ben, Geoff, Eric, Yuanqi, Vic, Arun, and Omar). It was because of all of you that I looked forward to coming into lab day after day, thanks for making grad school an incredible experience. I especially want to thank Tony and Ben for spending endless hours in discussions with me, from research challenges to personal life, conversations never ceased to be dull. Geoff, you have been an incredible mentor to me, thank you for taking me under your wing and sharing your knowledge with me. I am the scientist that I am today because of all the time and insight that you shared.

I want to thank Julia Bailey-Seers and Sean Cutler for allowing me to participate in the IGERT program. Zhenbiao Yang allowed me to spend a few months rotating in his lab and I thank him for the chance to get a glimpse of

performing research in a biology lab. I want to thank Augusta Jamin for guiding me through this process, her help was invaluable. I thank all the IGERT students for their camaraderie as we forged bridges between disciplines. We quickly discovered that communication was a challenge but it was one that we could face together.

I want to thank all my family and friends for all their love and support and for always being there as a voice of encouragement. In particular, I want to thank Odessa and Greg for being two of the best friends that I could ever have. They were there for me through all the highs and lows of the last several years, always there to listen to me vent about life and research. I would not have made it through grad school without their support.

I thank the following institutions for funding: UC Riverside (RRJ), the National Science Foundation CAREER Award (RRJ, CHE-0747481) and IGERT fellowship (JKD, DGE-0504249), and the UCR Graduate Division. The ECD data shown in Chapter 2 was collected by Tony Ly using FT-ICR instrumentation in the lab of Joseph Loo at UCLA. The work in Chapter 4 was performed in collaboration with Arun Agarwal. The brominated Cytochrome C used in Chapter 5 was modified by Eric Knudsen.

The text of this dissertation, in part or in full, is a reprint of the material as it appears in the following publications:

Ch. 2: Diedrich, J. K.; Julian, R. R. *J. Am. Chem. Soc.* **2008**, *130*, 12212–12213 and Diedrich, J. K.; Julian, R. R. *Anal. Chem*. **2011**, DOI: 10.1021/ac201647w

Ch. 3: Diedrich, J. K.; Julian, R. R. *Anal. Chem.* **2010**, *82*, 4006-4014

Ch. 4: Agarwal, A.; Diedrich, J. K.; Julian, R. R. *Anal. Chem*. **2011**, DOI: 10.1021/ac201650v

Dedication

To my parents,

for inspiring me to challenge myself and for their love and support in everything.

ABSTRACT OF THE DISSERTATION

Harnessing Radical Chemistry for the Facile Identification of Post Translational Modification Sites in Proteins by Photodissociation Mass Spectrometry

by

Jolene K. Diedrich

Doctor of Philosophy, Graduate Program in Chemistry
University of California, Riverside, August 2011
Dr. Ryan R. Julian, Chairperson

Photodissociation (PD) mass spectrometry has been shown to be a useful analytical technique for determining protein modifications. Described herein is the development and application of photodissociation for various modifications. Photo-excitation with 266nm laser light normally does not yield fragmentation. However C-S, S-S, C-I, C-Br, and C-Cl bonds can be homolytic cleaved through direct dissociation pathways. This selective fragmentation can be utilized to identify peptides or proteins of interest. Radicals generated through this process can cause further dissociation of the peptide backbone. Radical directed dissociation (RDD) is useful for identifying the location of modification sites. The selective nature of fragmentation is shown to provide facile identification of PTM sites by greatly simplifying data analysis. Reported herein is the discovery of a

novel gas phase dissociation technique useful for the facile analysis of protein modifications.

Phosphorylation sites are selectively modified through β elimination and Michael addition chemistry, installing photolabile group. Photodissociation yields homolytic cleavage of the C-S bond at the modification site, generating a β radical which is poised to fragment the peptide backbone selectively at the previously phosphorylated residue, thus allowing facile identification. Cysteine residues, uniquely reactive amino acids, are shown to form covalent bonds with quinones. Furthermore, the chromophoric properties can be leveraged for site specific photodissociation. Photodissociation reveals both the presence and location of modified cysteine residues. Selective fragmentation of a single bond in a whole protein is demonstrated. PD can be used to determine both the presence and site of modification generated by naturally occurring molecules, such as dopamine, which can harness quinone chemistry to modify proteins.

Also reported is the discovery of photodissociation at 266 nm to selectively cleave disulfide bonds in the gas phase, while leaving all other bonds intact. This methodology can be used to identify disulfide bonded pairs in complex systems. LC-MS experiments utilizing photodissociation were developed for analysis of protein digests. Peptides containing biomarkers of oxidative stress can be easily

identified by LC-PD-MS. Proteins exposed to oxidative stress can be halogenated at tyrosine residues. Homolytic cleavage of the carbon-halogen bond is a favorable process and allows facile identification of these types of biomarkers. Shown in this dissertation is the selectivity offered by photodissociation; homolytic cleavage allows simplification of data analysis by quickly identifying the peptides of interest in a mixture while subsequent selective backbone fragmentation allows facile analysis of protein modifications.

Table of Contents

LIST OF FIGURES

LIST OF TABLES

LIST OF CHARTS

LIST OF SCHEMES

Chapter 1

IDENTIFICATION OF PROTEIN PTMS BY MASS SPECTROMETRY

1.1 Introduction

Proteins are important in nearly every biological process and play a critical role in the central dogma of biology which is considered to be one of the foundations of all biological processes. In this dogma, DNA (deoxyribonucleic acid) enclosed in the cells of every living organism contains the genetic information needed for life. DNA is transcribed into messenger RNA (ribonucleic acid), which is further used in protein synthesis and includes only the small portion of the DNA needed to synthesize a single protein. The messenger RNA is then translated into a linear chain of amino acids by a ribosomal complex. Folding of the protein into the correct three dimensional structure takes place during and after translation and is often assisted by chaperone proteins. Further modifications to the protein can occur post translation. Proteins are comprised of only twenty naturally occurring amino acids and post translational modifications (PTMs) not only provide increased protein heterogeneity but can modify the functionality of a protein population. These modifications can vary in both type and location. There are many known

protein modifications but the most common ones include methylation, acetylation, ubiquitination, phosphorylation, glycosylation and disulfide bond formation. The amino acid sequence of proteins can be determined from genetic information, however what is not directly obvious from genetic information are the post translational modifications. Thus in order to accurately determine PTM information, they must be identified directly from the protein. Described herein is the development of novel mass spectrometric techniques for use in identifying PTM sites in a facile and accurate manner.

Mass spectrometry has played an important role in the determination of protein sequence and structure. Mass spectrometry is a technique where by analytes of interest can have their mass determined by measuring mass to charge ratio of an ion. Because the mass is measured in the gas phase as a charged species the analyte must be introduced into the gas phase and charged to be of use. Small molecules were primarily the focus of mass spectrometry until the invention of electrospray (ESI) and matrix assisted laser desorption ionization (MALDI). These two gentle ionization techniques made the analysis of biomolecules possible, and as such the study of proteins, peptides, and other biomolecules has grown at an astonishing speed in the last few decades. Mass spectrometry can be utilized to obtain the full mass of a protein or peptide of

interest, but perhaps more useful is sequence information obtained through dissociation methods known generically as tandem mass spectrometry.

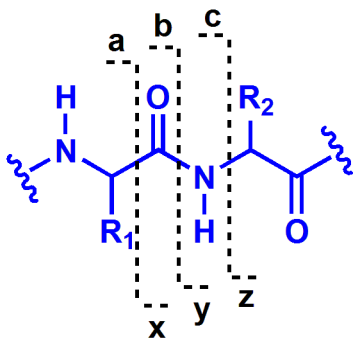

Scheme 1.1 Peptide fragmentation nomenclature.

Dissociation of biomolecules can be accomplished through the use of collisions, photons or electrons. Methods involving use of collisions with an inert gas (collision induced/activated dissociation, CID/CAD) are among the most common fragmentation techniques. Collision based methods primarily cleave the amide bond to produce b and y type fragments (as depicted in Scheme 1.1). a, b, and c fragments are observed if the charge is retained on the N-terminal portion while charge retention in the C-terminal portion allows detection of x, y, and z fragments. Electron based methods such as electron capture dissociation and electron transfer dissociation (ECD and ETD) commonly produce c and z ions (by cleavage of the N-C_α bond). These techniques are less commonly used but are

advantageous due to higher sequence coverage and retention of labile PTMs. Photon based methods (such as IRMPD) can produce a variety of fragment ion types generated by absorption of multiple photons. A variety of photon based methods exist utilizing various wavelengths and chromophores. Additionally multiple dissociation methods have been utilized to yield complementary fragmentation. However fragmentation by all of these methods is largely uncontrollable and unpredictable. The amount of fragmentation can frequently be constrained but the location of fragmentation is often based on a variety of factors and is not something which can be controlled or even accurately predicted a priori.

In contrast, a recently developed dissociation technique is capable of predictable and selective fragmentation. Radical directed dissociation (RDD) is a dissociation technique that is primarily dependent on kinetic and thermodynamically favorable pathways. These two key factors are controlled by structure and bond dissociation energies. It has been previously shown that structure will affect accessibility of the radical to a given site (based on distance constraints) and fragmentation or transfer to that site is dependent on bond dissociation energies. As shown in Figure 1.1 previous work in a peptide based system (where structure effects can largely be ignored) fragmentation follows a

trend based on carbon hydrogen bond dissociation energies.[1] Lower C_β-H dissociation energy correlates with increased fragmentation. As such, fragmentation by RDD is selective and predictable.

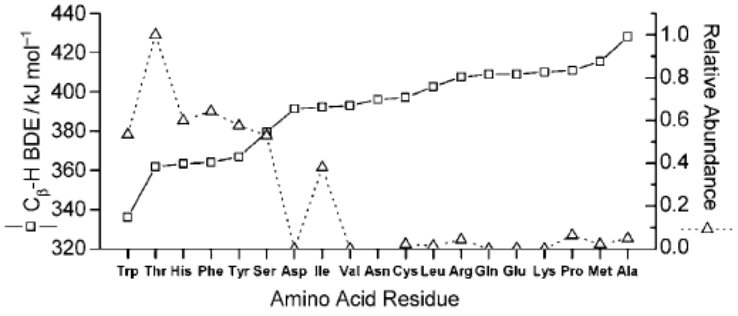

Figure 1.1 Bond dissociation energies vs. fragmentation observed by RDD. [1]

1.2 PD-LCMS

Liquid chromatography when coupled to mass spectrometry allows the analysis of complex mixtures in a straight forward fashion. As separation techniques advance, the ability to analyze increasingly complex mixtures is becoming routine. However as sample complexity increases the analysis of mass spectrometry data also increases greatly. Thus a bioinformatics approach is often needed to deal with large datasets. An alternative approach to identifying all species present in a complex sample would be to focus only on species of interest. This approach has been utilized widely with samples that have been previously analyzed and have a known fragmentation pattern that can be

monitored, either by generation of a fragment of interest (loss of a mass tag or immonium ions) or by a neutral mass loss (such as loss of H_3PO_4 in a phosphorylated peptide). However this approach only monitors for a fragmentation that may or may not occur and previous knowledge of the analyte is needed. What if the same approach could be used but instead by selectively identifying a fragmentation which is created by selective bond dissociation? Photodissociation is an approach which allows this to be done. The specificity of photodissociation is important because it will always be able to distinguish if the species of interest is present. For example the photodissociation of iodinated tyrosine will always produce a loss of iodine. By selectively creating the fragmentation that we are monitoring we get a clear yes or no answer if that species is present. Furthermore the selectivity of photodissociation is advantageous in that we can leverage this selectivity to search large datasets for the species that are of interest. This concept is presented in Figure 1.2. Shown is a chromatogram generated by LCMS of a protein mixture. In order to identify the peptides that are of interest in this sample, analysis of each peak would have to take place. This could mean analysis of hundreds to thousands of spectra, a daunting task without the use of automated analysis. However by using

photodissociation the spectra of interest are easily identified (signified by the red bars). This approach is presented in further detail in chapter 5.

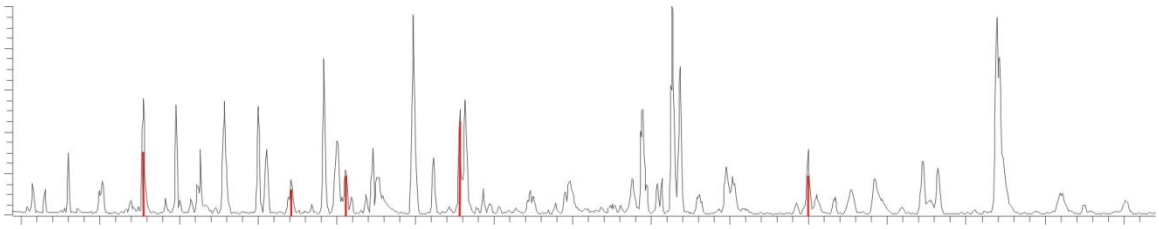

Figure 1.2 LC-MS chromatogram, red bars indicate peaks of interest.

1.3 PTM site Identification

A variety of PTMs can occur on proteins, each imparting a specific functional change to the protein. These modifications occur at site specific locations, which need to be identified directly from the protein to ensure accuracy. With current dissociation techniques this is straight forward for some modifications that are stable and remain intact during protein or peptide backbone dissociation. These modifications, stable under CID, include acetylation, methylation, and ubiquitination. For these modifications the data analysis is increased (to account for the possibility of variable modifications) but can be accurately assigned given sufficient sequence coverage. Coverage is dependent on both the sequence and the dissociation technique utilized and may not always be sufficient. This is

demonstrated in the left panel of Figure 1.3; theoretical fragmentation of a peptide with a PTM at T* is shown. Fragmentation must occur between each amino acid to accurately assign the modification site. A more challenging case occurs with modifications that are labile to common dissociation techniques. These modifications include phosphorylation, and O-linked glycosylation which are labile under CID. Simple loss of the PTM is depicted in the center of Figure 1.3. These types of modifications are often cleaved from the peptide backbone by collision based methods but remain intact with electron based methods. Therefore the presence of these modifications is often easy to distinguish during collision based processes (large loss of H_3PO_4) however the site assignment is a more challenging task. Electron based methods can be used, but as described earlier, success is dependent on adequate sequence coverage. An alternative approach to this dilemma is to generate fragmentation only at the site of interest, as shown in the right panel of Figure 1.3. Utilizing a selective fragmentation method would allow the PTM site to be determined both easily and unambiguously. It is this approach that is the focus of this thesis.

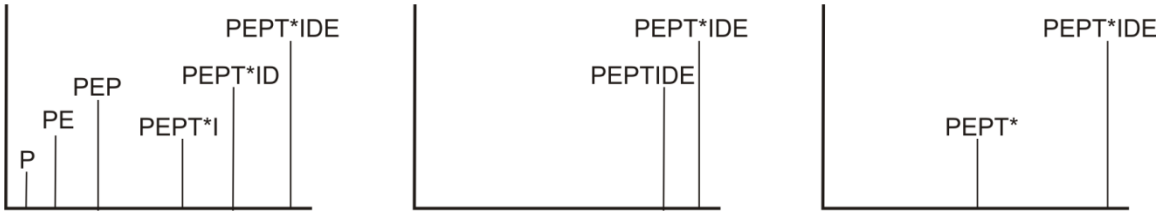

Figure 1.3 Fragmentation of a peptide containing a PTM signified by *. Peak spacing and height are arbitrary.

Identification of phosphorylation sites is of interest due to their importance in protein regulation. However assignment of the exact sites of this type modification is not always easily obtained due to the dynamic nature of phosphorylation and the challenges faced by mass spectrometry analysis. Described in Chapter 2 is a novel technique for assignment of phosphorylation sites in a selective and facile manner. Phosphorylation sites are selectively modified through beta elimination and Michael addition chemistry and utilization of photodissociation yields radical fragmentation at the modification site. Fragmentation primarily occurs at the phosphorylated residue allowing facile identification. Radical directed fragmentation also occurs in smaller abundances at neighboring residues. The mechanisms behind this selective radical fragmentation are presented and the utility is discussed. Fragmentation is shown to be independent of charge state allowing analysis of a wide variety of peptide sequences including peptides with multiple phosphorylation sites. A

comparison of this technique is made to CID and ECD for representative peptides.

O-linked glycosylation sites were also investigated. O-linked glycosylation occurs at serine and threonine side chains and is often present in protein sequences that are rich in serine, threonine, and proline. Similarly O-linked glycosylation is labile to collision induced dissociation and as such suffers some of the same challenges as phosphorylation site identification by mass spectrometry. Fortunately due to the similarity of these two PTMs, the same approach can be utilized for site identification, based on beta elimination and Michael addition chemistry with subsequent photodissociation.

Cysteine is a unique amino acid and can be present in many forms in proteins. The uniqueness of cysteine among the 20 amino acids is due to the thiol functionality of the side chain. The free form of the thiol has been found to be present in the active site of many proteins, and is often vital to the protein's function. The reactivity of this side chain is not only important to protein activity but it can also post translationally form disulfide bonds with a second cysteine residue. This intramolecular or intermolecular bond serves as a structural constraint and as such will stabilize protein structure in a given conformation.

Described in Chapter 3 are several unique analytical applications utilizing mass spectrometry and the selective modification of the free thiol form of cysteine in both peptides and proteins by various quinones. This simple modification can be used to quantify the number of free or disulfide bound cysteines in a protein. In addition, quinone modification can also be used to easily probe the solvent accessibility of cysteine residues, which provides information about protein structure or folding state. Furthermore, the chromophoric properties of the quinone moiety can be leveraged for site specific photodissociation of the backbone. The photodissociation reveals both the presence and location of modified cysteine residues. For example, cleavage of the protein backbone of alpha Hemoglobin is observed selectively at a single cysteine out of 140 residues in the whole protein. This selective backbone fragmentation is accompanied by a parent ion mass loss which is unique to the modifying quinone. When combined, this information can be used to determine both the presence and site of modification generated by naturally occurring molecules, such as dopamine, which can harness quinone chemistry to modify proteins.

Not only can quinone modified cysteine be analyzed through photodissociation but it was discovered that disulfide bonds could be analyzed

directly. Previous chapters focused on photodissociation of carbon- sulfur bonds to yield desired fragmentation. Presented in chapter 4 is the direct analysis of disulfide bound peptides through the photodissociation of sulfur- sulfur bonds. Disulfide bonds stabilize the tertiary and quaternary structure of proteins. Identifying the correct disulfide bond pairs can be extremely useful to understand the nature of a protein. However identifying correct linkages remains a challenge for many proteins. The quinone chemistry presented in chapter 3 can identify linkages in simple systems but it does have limitations. Shown in chapter 4 is the use of UV photodissociation at 266 nm to selectively cleave disulfide bonds in the gas phase, while leaving all other bonds intact. This methodology can be used to identify disulfide bonded pairs in complex systems with multiple disulfide bond partners. Model peptides were used to evaluate the importance of various sequence and structural effects to PD. Subsequently, online LCMS experiments were performed on whole protein digests is shown to correctly identify all disulfide bonded pairs.

Chapter 5 demonstrates the usefulness of PD-LCMS in the analysis of metabolites bound to cysteine residues. Similar to the chemistry described in chapter 3, photodissociation can selectively identify cysteine bound quinones. Quinones or quinone type molecules are present in a variety of drugs and

metabolites. This functionality will be reactive towards cysteine and can be identified by photodissociation. Chapter 5 presents PD-LCMS as a novel method for identifying these metabolites. Chapter 5 focuses on the application of this PD-LCMS technique for biomarkers of oxidative stress. Halogenated tyrosine has been previously shown to be a biomarker of oxidative stress. Iodinated tyrosine was previously studied by RDD. Shown in chapter 5 is the photodissociation of brominated and chlorinated peptides. These halogenated species were shown to be photo cleavable and methodology utilizing PD-LCMS is presented as a viable technique for biomarker studies.

---

[1] Ly, T.; Julian, R. R. *Angew. Chem. Int. Ed.* **2009**, *48*, 7130-7137.

Chapter 2

FACILE IDENTIFICATION OF PHOSPHORYLATION SITES IN PEPTIDES BY RADICAL DIRECTED DISSOCIATION

2.1 Introduction

Many cellular processes are controlled through protein signaling pathways which are mediated by reversible phosphorylation,[1,2] one of the most common post translational modifications in proteins. Phosphorylation occurs most commonly at serine and threonine.[3] Attachment of phosphate to these residues is enzymatically controlled by kinases with rigorous sequence specificity.[4,5] Removal is also an enzymatic process controlled by phosphatases which are generally less site-specific in nature.[6] This dynamic interplay between attachment and removal of phosphate groups creates a way for protein signaling pathways to be manipulated without complete synthesis or degradation of the protein, greatly increasing efficiency. Furthermore, a single protein can be involved in different signaling pathways by possessing multiple reversible phosphorylation sites which each encode a different signal.[7] The importance of phosphorylation in biological systems is evident by the portion of the genome devoted to reversible phosphorylation machinery. Over 5% of the Arabidopsis genome, considered a

simple model system, encodes over 1000 known kinases and several hundred phosphatases.[8] Improper phosphorylation, in terms of the sites or relative abundance of modifications, has been implicated in various diseases states.[9]

The biological importance of phosphorylation dictates that methods capable of site-specific characterization are needed; however, site identification is challenging. Although protein kinases recognize specific sequences as targets for modification, and putative phosphorylation sites can therefore be predicted based on sequence alone, such programs are not able to accurately predict all phosphorylation sites. In one such analysis, 40% of actual phosphorylation sites in plants were missed.[10] Therefore, the only way to accurately determine phosphorylation sites is to identify them in an actual biological sample.

There are several difficulties that hinder assignment of phosphorylation sites. Due to the dynamic nature of phosphorylation, modified proteins are often present in low abundance compared to unphosphorylated proteins.[11] A further complication arises due to the presence of the negatively charged phosphate group, which results in phosphorylated peptides typically being observed with reduced relative abundance and lower overall charge states compared to unmodified peptides.[12] In addition, if successfully observed in the gas phase, phosphates are labile when subjected to collisional activation.[13] Often loss of the

phosphate group is the almost exclusive product in collision induced dissociation (CID) experiments, giving no sequence information and complicating site determination. Several strategies have been developed to overcome these difficulties. Affinity based techniques may be implemented to selectively enrich phosphorylated proteins or peptides.[14-19] Electron based dissociation methods sidestep phosphate instability because backbone dissociation occurs without loss of the phosphate.[20-22] Unfortunately, in order to use these methods the peptides must have two or preferably more charges, which is the opposite of the trend noted above. Replacing the phosphate group with a neutral or positively charged group can increase the charge state and allow use of CID for identification, at the cost of added experimental complexity.[23-26]

Radical chemistry is becoming increasingly important in the analytical interrogation of biological molecules. Numerous methods have been developed for creating radicals on peptides with collisional activation.[27-31] Even more powerful are photodissociation based methods where radicals can be created on peptides[32] or proteins,[33] via either covalent or noncovalent[34] modification. In these experiments, UV photons are used to access dissociative excited states which lead to homolytic cleavage of either carbon-iodine or carbon-sulfur

bonds.[35] We have previously reported in a communication[36] that this type of chemistry can be leveraged to facilitate phosphorylation site identification. Modification of phosphorylated serine or threonine according the Michael addition chemistry outlined in Scheme 2.1 allows for creation of a radical at the β-position. This radical is predisposed to fracture the peptide backbone site-specifically as will be detailed further below.

Scheme 2.1

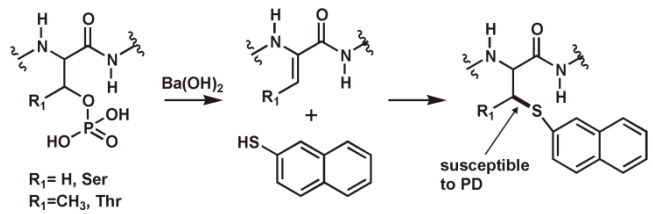

This chapter elaborates on a previously published communication which is not included (Diedrich, J. K.; Julian, R. R. *J. Am. Chem. Soc.* **2008**, *130*, 12212–12213). It is demonstrated that photodissociation can be used to specifically cleave peptides at sites of phosphorylation, directly identifying the site of modification. This chemistry is found to be insensitive to the charge state of the peptide, working for both singly and multiply charged peptides whether positively or negatively charged. These results are consistent with a mechanistic understanding of the dissociation, which involves a competition between

spontaneous site-specific backbone fragmentation and nonproductive radical migration. In certain cases, side chain dissociations are observed which also provide useful supporting information. Peptides with multiple sites of phosphorylation are amenable for analysis, and the site specific identification of numerous sites simultaneously is demonstrated. The specificity of the information which is obtained by this method is a significant advantage in terms of bioinformatics. A straightforward approach for data analysis is described and compared with competitive methods in terms of both accuracy and efficiency.

2.2 Materials and Methods

2.2.1 Materials

Peptides KRtIRR-NH2, Ac-CTTSsFKK-NH2, Ac-SKRFtRSDHLSC-NH2, Ac-CGSMQsRRSsQS-NH2, and Ac-CLKKLsGK- NH2, were purchased from Quality Controlled Biochemicals (Hopkinton, MA), KEAPPAPPQsP-NH2, was purchased from American Peptide Company (Sunnyvale, CA) and RRAAEELDsRAGsPQL and KKKKKRFsFKKsFKLSGFsFKKNKK were purchased from AnaSpec (San Jose, CA). RLEAsLADVR was custom synthesized by GenScript (Piscataway, NJ). All peptides and reagents were used without further purification. 2-Naphthalenethiol, hydrogen peroxide, formic acid, and

TFA were purchased from Sigma (St. Louis, MO). Dioxane and acetonitrile were purchased from EMD (Gibbstown, NJ) and Fisher Scientific (Fairlawn, NJ), respectively. Water was purified by Millipore Direct-Q (Millipore, Billerica, MA). A MacroTrap holder and Peptide MacroTrap consisting of a polymeric reversed-phase packing with retention similar to C8 was purchased from Michrom Bioresources, Inc. (Auburn, CA)

2.2.2 Oxidation of Cysteine residues

Peptides containing cysteine were oxidized prior to dephosphorylation with performic acid in order to avoid side reactions during derivatization with naphthalenethiol.[24] Briefly, an oxidation solution of 5:10:85 H2O2: H2O: formic acid was prepared and allowed to sit at room temperature for one hour prior to use. 250µl of the oxidation solution was combined with 25µl of peptide stock (25nmole in H2O) and placed on ice for one hour. Oxidation of cysteine was confirmed by MS. Oxidized residues are indicated by X#, where X=C or M. Oxidized peptides were purified by MacroTrap and lyophilized. Peptides were redissolved in H2O to 1mM for use in dephosphorylation and derivatization procedures.

2.2.3 Dephosphorylation and Derivatization by Naphthalenethiol

Peptides were dephosphorylated[25] by combining 10µl of peptide stock (10nmole in H2O) and 3µl of saturated barium hydroxide and heating to 55°C for 30 minutes. Dephosphorylated peptides were subsequently derivatized by addition of 0.6mg of naphthalenethiol dissolved in 10µl of dioxane[37] at 55°C over 4 hours. The reaction was stopped by acidification with 0.1%TFA in H2O and lyophilized. Lyophilized peptide was redissolved in 0.1%TFA in H2O and purified by MacroTrap, rinsing with 0.1%TFA in H2O and eluting with 50%ACN and 1% formic acid. Peptide eluent was diluted with 50:50 ACN:H2O to 2-10µM for analysis by MS. During the derivatization procedure the side chain of glutamine in the KEAPPAPPQsP-NH2 peptide was oxidized to glutamic acid modifying the sequence to KEAPPAPPEsP-NH2. However, oxidation of glutamine in RRAAEELADsRAGsPQL was not observed. Deamidation can be induce by high temperature conditions[38] and was observed to occur in a single instance. It is well know that the use of alkaline conditions can result in other side reactions. O-linked glycans will be eliminated in a similar manner, and could result in difficulties distinguishing between O-linked phosphate and O-linked glycans. It has been reported that O-glycans are more facile to beta elimination and thus by altering solution conditions the O-glycans and

phosphate sites can be differentiated.[39] This is a subject that is being investigated further. Dehydration of unmodified serine and threonine has been observed during some modification procedures;[40,41] however, this was tested for but not observed in our experiments.

2.2.4 Photodissociation of Naphthalenethiol Derivatized Peptides

Derivatized peptide solutions were analyzed in positive and negative ion modes by an LTQ linear ion trap mass spectrometer (Thermo Fisher Scientific, Waltham, MA) with a standard electrospray source. The posterior plate of the LTQ was modified with a quartz window to transmit fourth harmonic (266 nm) laser pulses from a flashlamp-pumped Nd:YAG laser (Continuum, Santa Clara, CA). Pulses were synchronized to the end of the isolation step of a typical MS2 experiment by feeding a TTL trigger signal from the mass spectrometer to the laser via a digital delay generator (Berkeley Nucleonics, San Rafael, CA). This allowed photodissociation (PD) to be carried out analogous to collision induced dissociation (CID).

2.2.5 Phosphorylation Site Prediction by CID and Data Analysis

Phosphorylated peptides Ac-CTTSsFKK-NH2 and Ac-SKRFtRSDHLSC-NH2 were subjected to CID for all charge states observed. All peaks and corresponding intensities from CID data were exported from Xcalibur Qual

Browser, version 2.0 (Thermo Electron Co.) to Molecular Weight Calculator42 for analysis. Peptide Sequence Fragmentation Modeling in Molecular Weight Calculator models fragmentation of a given peptide sequence and identifies matches in CID data. Scores are calculated based on an algorithm similar to that used by SEQUEST.[43] Within a single charge state, a larger score signifies a greater possibility that the proposed sequence matches the experimental data. Similar scoring of RDD data was calculated for comparison. RDD score = $(\Sigma\ i_m) \times n_i$ where i_m are the relative intensities and n_i is the number of matching ions. Due to the specific cleavage of RDD only the following ions are used for RDD scoring: d fragments N and C terminal and a fragments N terminal to potentially phosphorylated serines or threonines. Phosphorylation site prediction based on CID and RDD with scoring is compared in Table 2.2.

2.3 Results and Discussion

2.3.1 Underlying Chemistry

In Figure 2.1, PD spectra for three peptides are shown. This data illustrates all of the major and minor dissociation channels which are typically observed following PD which retain elements of site specificity that can be utilized to identify the original site of phosphorylation. Each peptide was modified with naphthalenethiol prior to PD. A peak corresponding to loss of 159Da from the

precursor is abundant in all three spectra. This mass loss is atypical for peptide fragmentation and is due to loss of radical naphthalenethiol following homolytic cleavage of the carbon sulfur bond. This unique loss is ubiquitous in these experiments and may be used as a marker for identifying the presence of a phosphorylation site. In addition to the loss of naphthalenethiol, the most intense backbone fragment results from dissociation via the same pathway for all three peptides in Figure 2.1. In each case, the dominant backbone fragment corresponds to a d ion, generated by the mechanism described previously and highlighted in the center of Scheme 2.2.[36] Importantly, this dominant dissociation channel is observed in all PD experiments on comparably modified peptides. The complement x fragment which is generated is less stable, and will frequently decompose into a z ion via loss of OCNH as shown in Scheme 2.2. In certain cases this z ion will further decompose into a w ion, depending on the nature of the side chain. This is the origin of the relatively abundant w_5 ion in Figure 2.1c.

In addition, several minor dissociation channels are frequently observed. For example, migration of the initial radical to the adjacent N-terminal β-position, followed by dissociation to yield an $a_{(n-1)}$ ion is observed in all three spectra in Figure 2.1. The mechanism is shown in the lower portion of Scheme 2.2. This fragmentation pathway frequently yields the second most abundant backbone

dissociation product. When this type of bracketing fragmentation occurs (see Figure 2.1a), the mass difference between the two fragments allows differentiation of phosphorylated serine or threonine without any prior sequence information. Phosphorylated serine will yield a mass difference of 70Da between the bracketing peaks while phosphorylated threonine will yield a mass difference of 84Da. A complement w+1 type fragment is also formed by the pathway in the lower portion of Scheme 2.2 and is observed in some cases. An entirely analogous pathway to that shown in the lower part of Scheme 2.2 is less frequently observed to yield fragments via migration to the β-position C-terminal to the modification site (not shown in Scheme 2.2).

The radical initially formed following PD typically cleaves the C_β-CO bond as discussed above; however, it is also possible for this radical to cleave the C_β-NH bond as shown in the upper portion of Scheme 2.2. Backbone cleavage in this case initially creates complementary c and w ions (w rather than z due to the absent side chain). For example, the w_6 ion in Figure 2.1c is created via this mechanism. The complement c ion is not typically observed because this radical spontaneously loses OCNH to yield a radical a+1 ion. Depending on the nature of the side chain, the a+1 radical may further decompose to yield a d ion. Importantly, even though multiple minor pathways leading to dissociation are

frequently observed, all of the resulting dissociations are specifically indicative of the location of the phosphorylation site.

Scheme 2.2

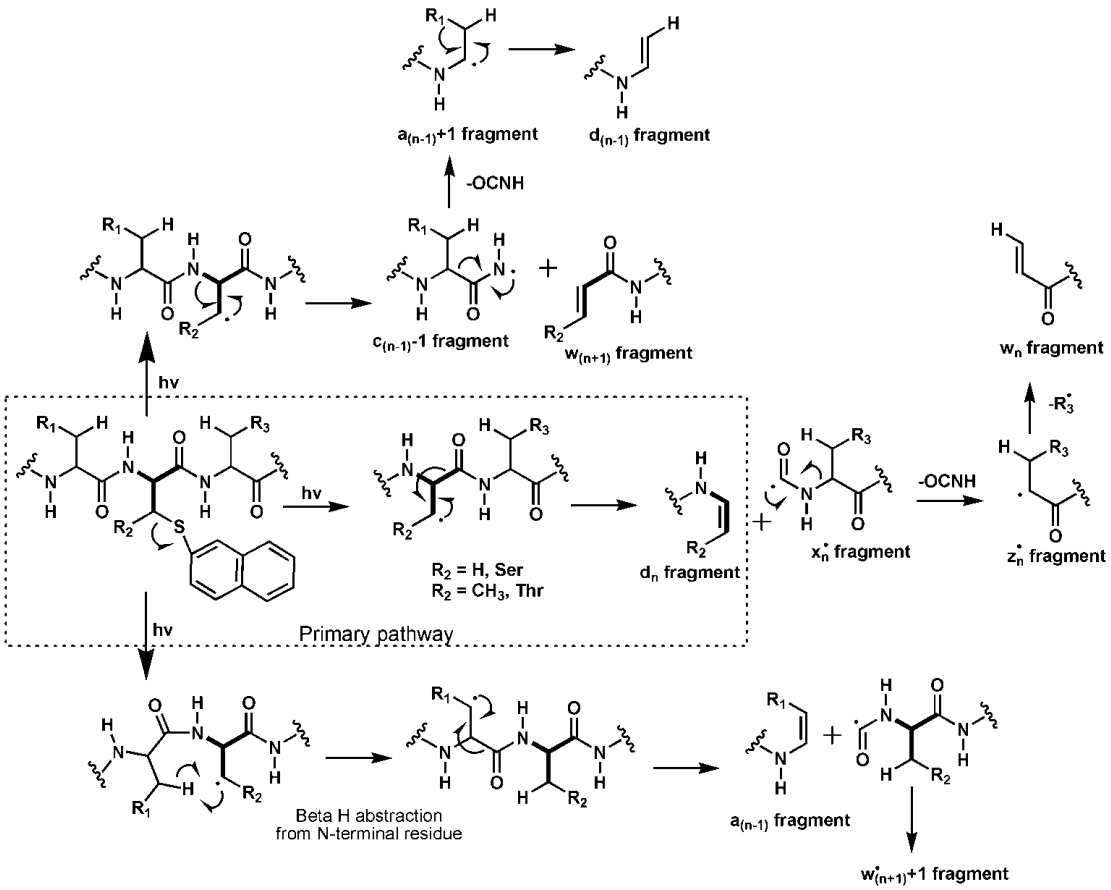

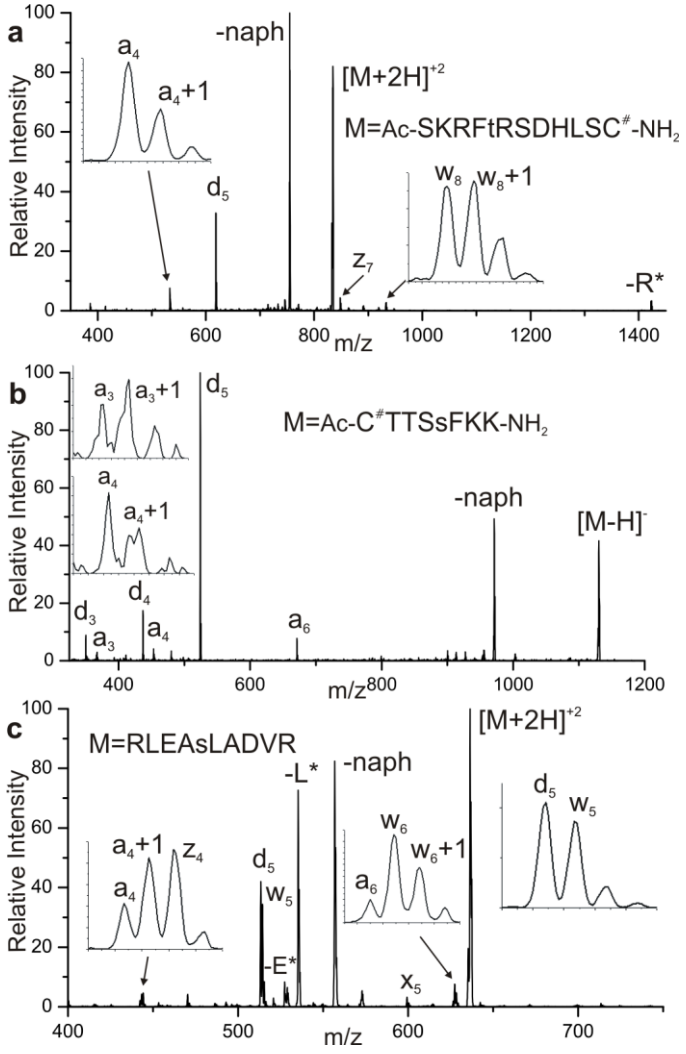

Figure 2.1 a) PD of +2 charge state of naphthalenethiol derivative of Ac-SKRFtRSDHLSC#-NH_2. Loss of naphthalenethiol due to C_β-S cleavage is observed (labeled –naph). d_5, a_4 and z_7 fragments are observed at the modified pThr. Side chain loss of arginine is labeled –R*. b) PD of -1 charge state of naphthalenethiol derivative of Ac-C#TTSsFKK-NH_2. Backbone fragmentation at d_5, a_4 and d_4 brackets the modified residue. c) PD of +2 charge state of RLEAsLADVR naphthalenethiol derivative. Fragmentation is primarily observed at the modified serine residue (d_5, x_5, and w_5) as well as abundant loss of leucine side chain (-L*).

2.3.2 Charge State Independence

Unlike other common fragmentation pathways, direct photodissociation of bonds in excited electronic states is largely independent of precursor charge state. Shown in Figure 2.2 is photodissociation of KRtIRR-NH_2 in the +2 and +3 charge states. The base peak observed in both spectra corresponds to loss of the naphthalenethiol. Two other large fragments are observed at 30 to 40% relative abundance. One of these peaks represents loss of 29Da from the precursor ion and is due to side chain loss from isoleucine. The most abundant product formed due to backbone fragmentation is a d_3 ion, which is present in both spectra at approximately 35% relative intensity and serves to identify the site of modification as described above. The strong similarity between Figures 2.2a and 2b, including the yields of fragmentation occurring through the different pathways, strongly suggests that charges do not significantly influence dissociation. This is in agreement with the mechanisms outlined in Scheme 2.2, which similarly do not involve charge carrying groups.

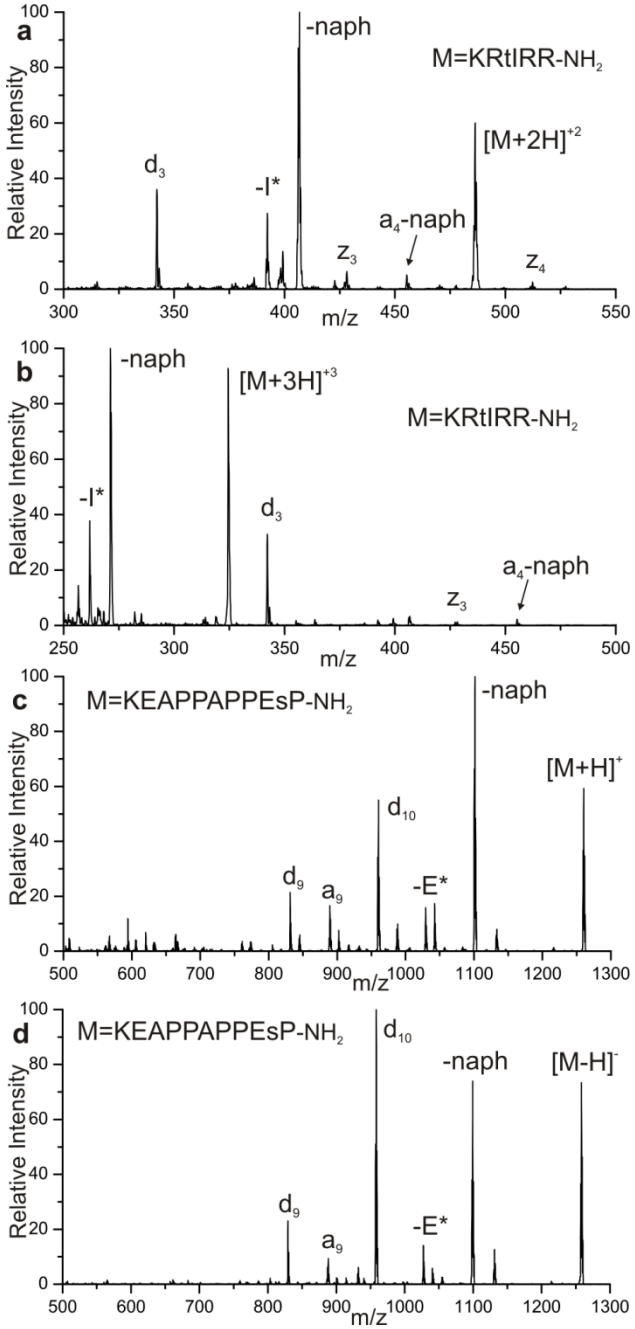

Figure 2.2 a) PD of +2 charge state of naphthalenethiol derivative of KRtIRR-NH_2. Loss of isoleucine side chain is labeled –I*. b) PD of +3 charge state of naphthalenethiol derivative of KRtIRR-NH_2. c) PD of +1 charge state of KEAPPAPPEsP naphthalenethiol derivative. d) PD of -1 charge state of KEAPPAPPEsP naphthalenethiol derivative. Similar fragmentation is observed for both polarities.

In order to examine the potential role of charge polarity, the phosphorylated peptide KEAPPAPPEsP-NH_2 was modified by naphthalenethiol and subjected to photodissociation. Figures 2.2c and 2.2d are the resulting spectra for the +1 and -1 charges states after photodissociation. Loss of the naphthalenethiol is present in both spectra as a major peak. Thus homolytic fragmentation of the carbon sulfur bond by PD is possible with both positively and negatively charged ions. The largest backbone fragmentation observed in the two spectra corresponds to a d_{10} ion (note the structure of a d-fragment is typically defined[44] as being positively charged therefore the d fragments in anion mode are technically d-2H fragments by mass. For the sake of simplicity all ions are herein referred to according to site of dissociation only, regardless of their charge state). The d_{10} fragment occurs just C-terminal to the phosphorylated residue as expected, correctly identifying the side of phosphorylation. Again the fragmentation types and even relative abundances are very similar between the two spectra. The ability of this method to yield the desired information regardless of peptide charge state is a significant advantage relative to most other approaches.

2.3.3 Radical Byproducts

The loss of naphthalenethiol following photodissociation is frequently one of the most intense product ions observed (as seen in both Figures 2.1 and 2.2). Subsequent activation of this product is shown in Figure 2.3a for KEAPPAPPEsP-NH_2. The most abundant fragment is produced by loss of the side chain of glutamic acid. Site specific fragmentation at the serine residue (d_{10} or a_9) is notably absent. The dissimilarity between Figure 2.3a and Figure 2.2c can be rationalized in terms of radical migration. The initially formed β-radical either undergoes rearrangement to yield backbone dissociation as outlined in Scheme 2.2, or migrates to a stable position which does not result in fragmentation. Subsequent activation is then required to observe further dissociation, which is not similar to that observed by PD. A second example of activation of the radical after migration is shown in Figure 2.3b. The radical peptide Ac-SKRFtRSDHLSC$^{\#}$-NH_2 was reisolated (the –naph peak from Figure 2.1a) and collisionally activated. A variety of peaks are generated, some correspond to radical directed dissociation pathways which have been discussed previously,[32,33,35,36] and others result from proton catalyzed dissociation.[45] Thus the results in Figure 2.3 indicate that additional collisional activation of the radical peptide, created by loss of naphthalenethiol, does not generate the

desired site specific fragmentation which is only observed during photodissociation.

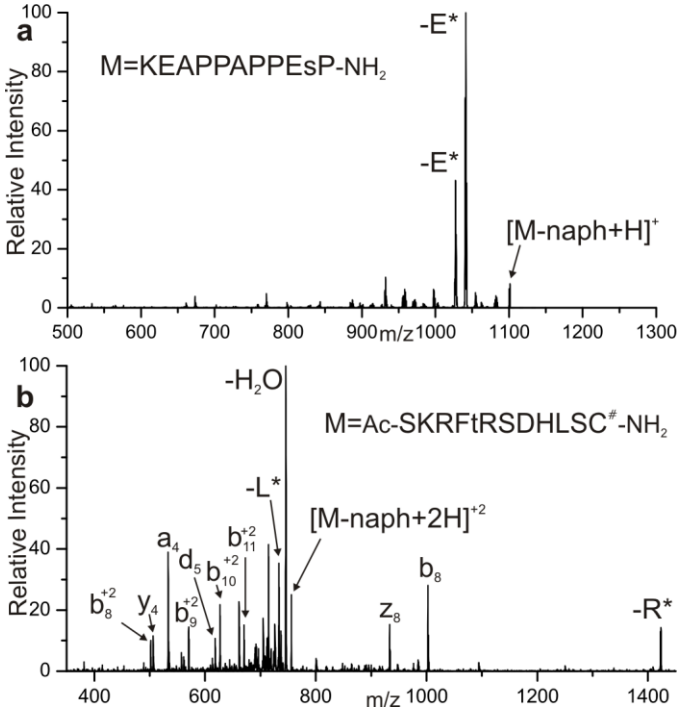

Figure 2.3 a) CID of re-isolated radical peptide KEAPPAPPEsP-NH_2 formed by cleavage of the carbon-sulfur bond by PD. b) CID of radical peptide Ac-SKRFtRSDHLSC#-NH_2 formed by PD. Fragmentation lacks the selectivity observed by PD.

Side chain losses are also frequently observed with photoactivation alone. In Figure 2.1c there is an abundant loss of 43Da corresponding to loss of leucine side chain from RLEAsLADVR. Isoleucine side chain loss was also observed during PD of KRtIRR-NH_2 in Figures 2.2a and b. Note that leucine and isoleucine are adjacent to the initial radical site in both cases. Is this coincidental, or is side chain loss observed during photodissociation also informative in terms of

identifying sites of modification? Summarized in Table 2.1 are the side chain losses recorded following photoactivation of seven peptides. It can be seen from this summary that the observed side chain loss is often located only one residue away from the phosphorylated site. The radical initially generated by PD has the ability to migrate to neighboring residues and cause fragmentation of the side chains, but without further activation the radical is only observed to actually yield fragmentation in local proximity to the site of phosphorylation. Thus this side chain loss data provides another level of information about the location of phosphorylation. Not only can the site of phosphorylation be identified by specific backbone fragmentation but the identification can be further supported by examining the side chain losses occurring at neighboring residues.

Table 2.1: Side Chain Losses Observed During Photodissociation

Peptide	*Side Chain Loss Observed*
Ac-C#GS**M**#**Q**sRRSs**Q**S-NH_2	M# and Q side chains
Ac-C#LKK**L**sGK	L side chain
Ac-C#TT**S**sF**KK**-NH_2	S and K side chains
KEAPPAPP**E**sP	E side chain
KRt**I**RR-NH_2	I side chain
R**L**EAs**L**ADVR	L side chain
RRAA**EE**L**D**s**R**AGsPQL	D, E and R side chains

2.3.4 Multiple modification sites

Phosphorylation can often occur at multiple residues within a single peptide, as is the case with RRAAEELDsRAGsPQL. Figure 2.4a shows the PD spectrum of the peptide which has both sites dephosphorylated and a single naphthalenethiol modification incorporated. Loss of the naphthalenethiol is observed as usual. Backbone dissociation is most abundantly observed at two locations yielding d_9 and d_{13} fragment ions. Other fragments similar to those detailed in discussion above are also observed. Importantly, fragmentation at both serine residues results from the single naphthalenethiol modification, suggesting little preference in terms of sequence for the modification chemistry with this peptide. The addition of two naphthalenethiol groups to RRAAEELDsRAGsPGL was also explored. Figure 2.4b shows the spectrum resulting from PD of the doubly modified peptide. A significant fraction of both naphthalenethiol modifications are cleaved off of the peptide during PD. Backbone fragmentation is similar to that observed with a single naphthalenethiol modification; however, the incomplete loss of the modification leads to an additional set of peaks corresponding fragmentation with retention of naphthalenethiol. Thus it can be seen from comparison of Figures 2.4a and 2.4b that the presence of multiple phosphorylation sites is not problematic and that the location information can be

determined by either complete modification of all sites (Figure 2.4b) or a single modification which is distributed between sites (as demonstrated in 2.4a). The case of a single modification at multiple sites does simplify data analysis though as only a single set of peaks are generated per cleavage site and there is not also a population of fragmentation retaining the additional modification.

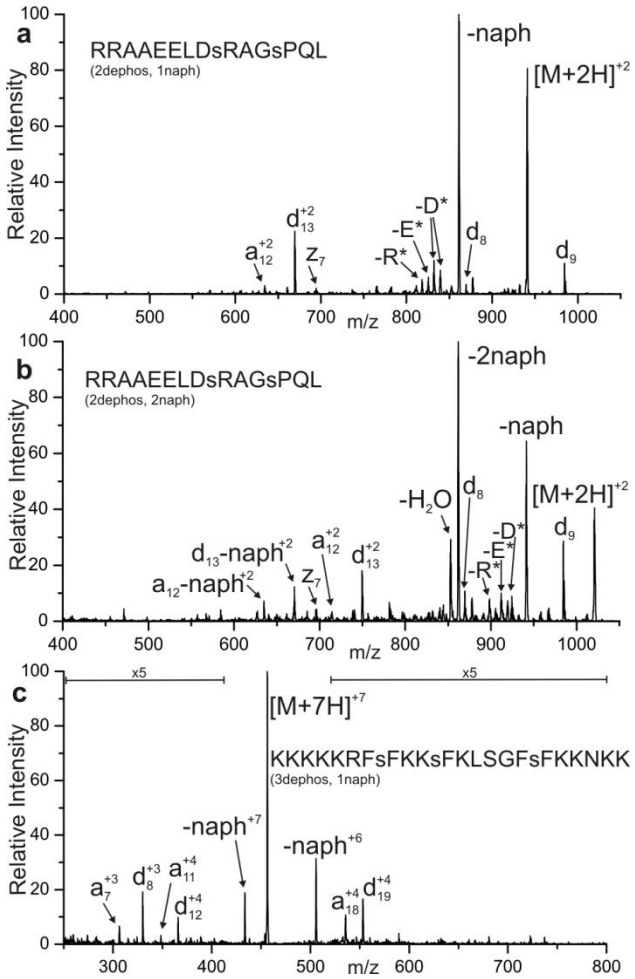

Figure 2.4 a) PD of $[RRAAEELDsRAGsPQL]^{2+}$ with single naphthalenethiol modification at either phosphorylation site. b) PD of $[RRAAEELDsRAGsPQL]^{2+}$ with naphthalenethiol modification at both phosphorylation sites. c) PD of

KKKKKRFsFKKsFKLSGFsFKKNKK peptide with a single naphthalenethiol modification. Unambiguous assignment is facile in each case.

A more complicated situation is demonstrated in Figure 2.4c with the peptide KKKKKRFsFKKsFKLSGFsFKKNKK. This peptide contains both multiple phosphorylation sites as well as a site that is not phosphorylated. All three sites were dephosphorylated by addition of base and a single naphthalenethiol was incorporated into the peptide. Photodissociation of the singly modified peptide is shown in Figure 2.4c. Loss of naphthalenethiol is observed as the two major peaks in the spectrum (at two different charge states). Three clusters of backbone fragmentation are observed; a_7 and d_8 bracket the first serine, Ser8, a second set of fragments bracket Ser12 (a_{11} and d_{12}) and a third set of backbone fragments (a_{18} and d_{19}) cluster around Ser19; however, there is no backbone fragmentation observed to occur at Ser16. Thus it can be easily determined that Ser8, Ser12 and Ser19 are sites of phosphorylation while Ser16 is not. This follows the selective nature of the technique where fragmentation is observed only to occur at the sites of phosphorylation and assignment of these few peaks in the spectrum allows facile identification of the sites of phosphorylation. Furthermore, the incorporation of a single naphthalenethiol was adequate to identify all three sites of phosphorylation as the modification

was incorporated at all three sites without any indication of preference for one site over another.

2.3.5 PD vs. ECD or CID

Collision induced dissociation is a commonly used fragmentation technique. Although not an ideal method of fragmentation for use in identification of phosphorylation sites, studies still show that it results in the largest number of phosphopeptide identifications.[46] The phosphate group is labile under CID and loss of H_3PO_4 is a primary fragmentation pathway observed for phosphorylated peptides. As shown in Figures 2.5a and 2.5b collision induced dissociation of the phosphorylated peptides Ac-SKRFtRSDHLSC-NH_2 and Ac-CTTSsFKK-NH_2 (respectively) yields primarily loss of phosphoric acid (-98Da) and very little backbone fragmentation of the peptide. Loss of 98Da is a useful indicator that a phosphorylated peptide is present; however, there is little to no information gained about the location of the phosphorylation site. In contrast, these same two peptides were modified by naphthalenethiol at the phosphorylation site and analyzed by photodissociation (shown in Figures 2.1a and 2.1b).

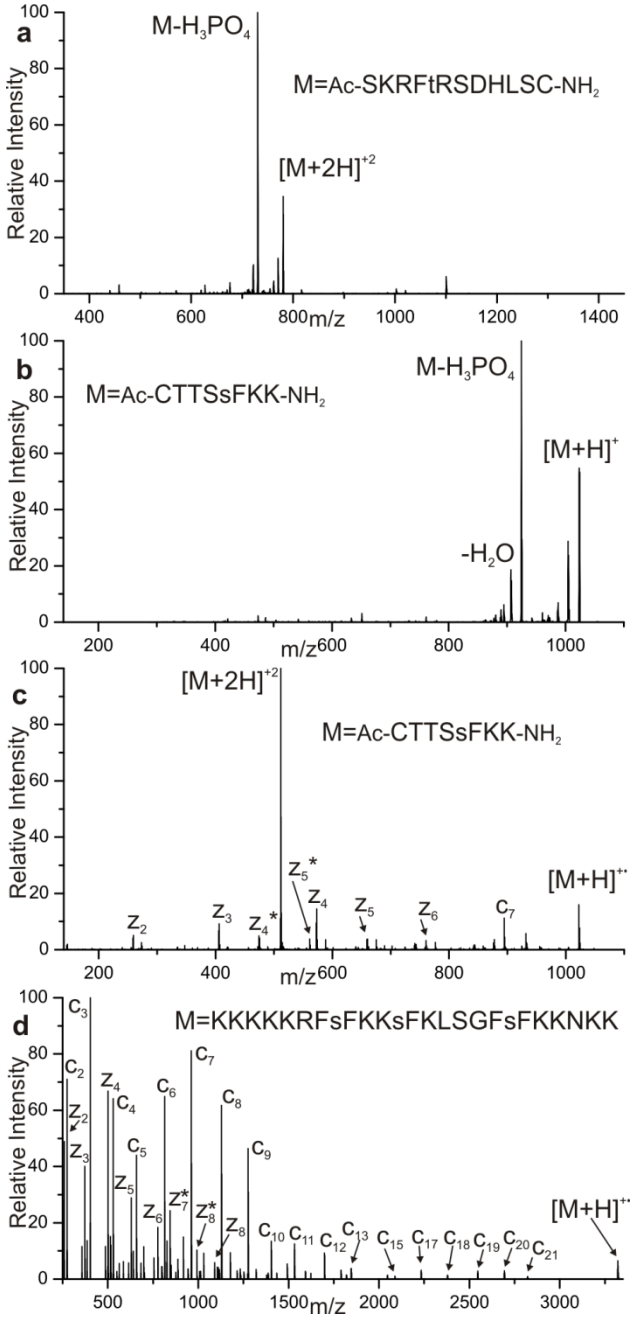

Figure 2.5 a) CID of phosphorylated Ac-SKRFtRSDHLSC-NH_2. b) CID of phosphorylated Ac-CTTSsFKK-NH_2. Primarily loss of phosphate is observed. c) ECD of phosphorylated Ac-CTTSsFKK-NH_2. d) ECD of phosphorylated KKKKKRFsFKKsFKLSGFsFKKNKK

To give a more quantitative comparison of the two fragmentation techniques, the two peptides were scored for proper phosphorylation site identification. Scoring of the CID data was performed through the use of an algorithm similar to that used by Sequest.[39] The resulting scores and site assignments are shown in Table 2.2. A higher score indicates that the observed spectrum better matches the phosphorylation site being at the given position. Scoring of CID data of the phosphorylated peptide Ac-SKRFtRSDHLSC-NH_2 was calculated for all the observed charge states (+3, +2, and -1). Fairly similar scores were obtained for each possible site of phosphorylation, giving not only ambiguous results but in each charge state the highest matching score is obtained for the incorrect sites. In contrast the scoring for the PD data of the +2 charge state results in a clear cut assignment of the site of phosphorylation at Thr5.

In the case of the peptide Ac-CTTSsFKK-NH_2 CID and scoring is able to correctly identify the site of phosphorylation in the +2 charge state, although it only received a slightly higher score than for the other sites. However, CID performed on the +1 and -1 charge states resulted in incorrect assignment of Thr2 and Ser4 respectively. Scoring of the PD data in this instance did result in small scores for the sites that are not phosphorylated, but the difference between the scores for the correct and incorrect sites differ by an order of magnitude. In both

of these instances, it can be seen that the site specificity inherent in the PD data greatly facilitates the correct assignment of the site of phosphorylation.

Table 2.2: Phosphorylation Site Prediction of Ac-SKRFtRSDHLSC-NH$_2$

		Possible Sites of Phosphorylation				Predicted Site
Charge State		pSer1	pThr5	pSer7	pSer11	
	# peak matches	103	101	**103**	88	
CID +3	Score	684.1	658.3	**696.1**	525.2	pSer7
	# peak matches	**80**	78	78	69	
CID +2	Score	**607.0**	566.1	561.0	436.9	pSer1
	# peak matches	26	26	**29**	25	
CID -1	Score	56.9	55.0	**66.2**	51.9	pSer7
PD +2	Score	0.0	**86.0**	0.0	0.0	**pThr5**

Phosphorylation Site Prediction of Ac-CTTSsFKK-NH$_2$

		Possible Sites of Phosphorylation				Predicted Site
Charge State		pThr2	pThr3	pSer4	pSer5	
	# peak matches	53	57	60	**62**	
CID +2	Score	432.5	518.4	587.2	**638.9**	**pSer5**
	# peak matches	**42**	40	40	39	
CID +1	Score	**318.6**	274.5	287.2	276.9	pThr2
	# peak matches	28	31	**32**	31	
CID -1	Score	130.0	161.1	**172.6**	150.0	pSer4
PD -1	Score	0.0	2.9	37.3	**359.2**	**pSer5**

Phosphorylation site prediction based on CID data and analysis by Molecular Weight Calculator. Higher score indicates better match of CID fragmentation to given sequence.

Electron capture dissociation (ECD) is an alternative fragmentation technique that is amenable to peptides which contain labile modifications such as phosphorylation. Unlike the radical directed dissociation presented herein, ECD is not selective and often generates high sequence coverage. ECD of the phosphorylated peptide Ac-CTTSsFKK-NH_2 is shown in Figure 2.5c. A series of z fragments is observed (although in low intensities) along most of the peptide backbone. The combination of fragments z_4, z_5, and z_6 are all necessary to determine the phosphorylation site. ECD of the multiply phosphorylated peptide KKKKKRFsFKKsFKLSGFsFKKNKK is shown in Figure 2.5d. A nearly completely series of c fragments is observed as well as a short series of z fragments is obtained by ECD. Therefore sufficient information is obtained to correctly assign the three sites of phosphorylation. However, upon close inspection of the Figure 2.5d it can be seen that the differentiation between Ser 16 and pSer19 is dependent on 4 of the smaller peaks in the spectrum. Assuming that ECD generates only c and z fragments at each residue, there will be 2n-2 peaks (where n is the peptide length) to be assigned in order to determine the phosphorylation site(s). In contrast PD generates only a few peaks that need to be assigned to determine the site of phosphorylation, and these are often the

most abundant peaks in the spectrum. Not only is the data analysis reduced (fewer peaks to be assigned) but splitting ion intensity into only a few fragments will be advantageous in the situation of low abundance phosphorylated species. Generating fragmentation only at the sites of phosphorylation as opposed to at every residue affords better sensitivity.

Table 2.3 shows the comparison of the relative efficiency of ECD and PD for the peptides KKKKKRFsFKKsFKLSGFsFKKNKK and Ac-CTTSsFKK-NH_2 using the data shown in Figures 2.1b, 2.4c, 2.5c, and 2.5d. The efficiency, or the percent of the fragmentation, that is useful for identifying the sites of phosphorylation was calculated relative to the sum of all fragmentation. The precursor and loss of naphthalenethiol peaks were not included in the calculations. The selectivity of fragmentation by PD is evident, and it is this selectivity that would result in increased sensitivity.

Table 2.3: Efficiency of ECD vs. PD for Phosphorylation Site Identification

	KKKKKRFsFKKsFKLSGFsFKKNKK		**Ac-CTTSsFKK-NH_2**	
	ECD	**PD**	**ECD**	**PD**
% of informative fragmentation	1.45%	51.15%	16.11%	54.85%

% of informative fragmentation only includes fragments which identify phosphorylation site and does not include precursor or loss of naph in calculations.

2.3.6 PD and CID provide complementary information

One advantage of ECD is that sequence information can be determined in cases where it is unknown. Although PD alone does not provide substantial sequence information for an unknown peptide, CID can be utilized to provide this information. Shown in Figure 2.6a is CID of the peptide Ac-SKRFtRSDHLSC#-NH_2 that has been modified with naphthalenethiol at the phosphorylation site. A series of b fragments and a few y fragments are observed yielding almost complete sequence coverage of the peptide. Figure 2.6b is CID of the peptide KEAPPAPPEsP-NH_2 that was modified with naphthalenethiol. Only a few b and y fragments are observed and are due to proline and glutamic acid effects. Thus it can be seen from these two spectra that the modification at the phosphorylated residue does not significantly affect CID. The naphthalenethiol replaces the phosphate group with a neutral substituent that is stable under CID and allows sequence information to be obtained. Therefore PD and CID of the modified peptide can be utilized to produce orthogonal and complementary information. PD provides phosphorylation site assignment and subsequently CID can be used to provide sequence information that can be utilized in denovo sequencing or database matching to determine the sequence of the peptide of interest.

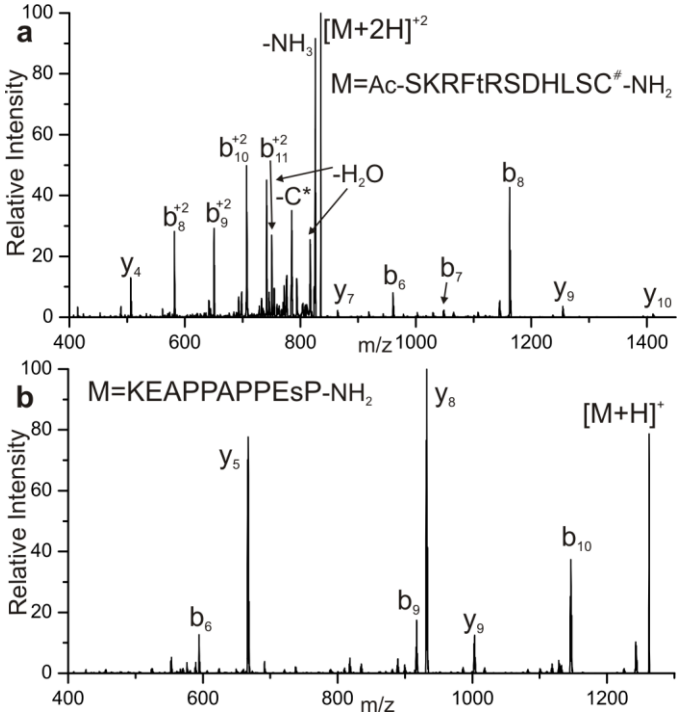

Figure 2.6 a) CID of naphthalenethiol modified $[Ac\text{-}SKRFtRSDHLSC^{\#}\text{-}NH_2]^{2+}$. b) CID of naphthalenethiol derivative of $[KEAPPAPPEsP\text{-}NH_2]^{+}$ Fragmentation is essentially unaffected by modification.

2.4 Conclusions

The ability to direct fragmentation to a particular site is useful for several reasons. For one, dissociation at the desired location is assured, which in this case guarantees that the site of phosphorylation will be identified. This contrasts with methods that rely on stochastic dissociation, where the desired fragmentations may simply not occur. Another advantage is that fragmentation at other sites is suppressed, which leads to enhanced sensitivity by channeling most of the ion

intensity into productive channels. A third advantage is greatly simplified data analysis, which originates from the ability to easily predict how a given peptide should fragment.

Photodissociation of naphthalenethiol peptides was shown to homolytically cleave the C_β-S bond to generate a radical. Pathways by which this radical can direct further backbone and side chain fragmentation were shown. Several pathways are accessible, but all are localized to the radical origination site. This localized fragmentation allows simple and unambiguous identification of phosphorylation sites. Selective fragmentation occurs due to immediate dissociation and is not observed upon subsequent activation. The radical fragmentation was shown to be independent of charge state and peptides with multiple phosphorylation sites can easily be assigned. A comparison of the efficiency and accuracy of this technique to CID and ECD demonstrates that PD is a viable dissociation technique for phosphorylation site identification.

---

[1] Mukherji, M. *Expert Rev. Proteomics* **2005**, 2, 117-128.

[2] Rodriguez, M. C. S.; Petersen, M.; Mundy, J. *Annu. Rev. Plant Biol.* **2010**, 61, 621-649.

[3] Hunter, T. *Cell*. **1995**, 80, 225-36.

[4] Pinna, L. A.; Ruzzene, M. *Biochim. Biophys. Acta, Molecular Cell Research.* **1996**, 1314, 191-225.

[5] Kreegipuu, A.; Blom, N.; Brunak, S.; Jarv, J. *FEBS Lett.* **1998**, 430, 45-50.

[6] Sparks, J. W.; Brautigan, D.L. *Int. J. Biochem.* **1986**, 18, 497-504.

[7] Summers, J.; Yu, M.; *J Virol.* **1994**, 4341-4348

[8] The Arabidopsis Genome Initiative. *Nature* **2000**, 408, 796–815.

[9] Harsha, H. C.; Pandey, Akhilesh. *Mol. Oncol.* **2010**, 4, 482-495.

[10] Kersten, B.; Agrawal, G. K.; Iwahashi, H.; Rakwal, R. *Proteomics* **2006**, 6, 5517-5528.

[11] Thingholm, T. E.; Jensen, O. N.; Larsen, M. R. *Proteomics* **2009**, 9, 1451-1468.

[12] Kim, S.; Choi, H.; Park, Z. *Mol. Cells* **2007**, 23, 340-348.

[13] Boersema, P. J.; Mohammed, S.; Heck, A. J. R. *J. Mass Spectrom.* **2009**, 44, 861-878.

[14] Holmes, L. D.; Schiller, M. R. *J. Liq. Chromatogr. Relat. Technol.* **1997**, 20, 123-142.

[15] Kweon, H. K.; Hakansson, K. *Anal. Chem*. **2006**, 78, 1743-1749.

[16] Eyrich, B.; Sickmann, A.; Zahedi, R. P. *Proteomics.* **2011**, 11, 554-570.

[17] Salih, E. *Mass Spectrom. Rev.* **2005**, 24, 828-846.

[18] Tseng, H.; Ovaa, H.; Wei, N. J. C.; Ploegh, H.; Tsai, L. *Chem. Biol.* **2005**, 12, 769-777.

[19] Oda, Y.; Nagasu, T.; Chait, B. T. *Nat. Biotechnol.* **2001**, 19, 379-382.

[20] Stensballe, A.; Jensen, O. N.; Olsen, J. V.; Haselmann, K. F.; Zubarev, R. A. *Rapid Commun. Mass Spectrom.* **2000**, *14*, 1793−1800

[21] Chi, A.; Huttenhower, C.; Geer, L. Y.; Coon, J. J.; Syka, J. E. P.; Bai, D. L.; Shabanowitz, J.; Burke, D. J.; Troyanskaya, O. G.; Hunt, D. F. *Proc. Natl. Acad. Sci. U.S.A.* **2007**, *104*, 2193–2198.

[22] Molina, H.; Horn, D. M.; Tang, N.; Mathivanan, S.; Pandey, A. *Proc. Natl. Acad. Sci. U.S.A.* **2007**, *104*, 2199–2204.

[23] Kati, M.; Jaana, S.; Lajos, B.; Mikko, O.; Harri, L. *Org. Biomol. Chem.* **2005**, 3, 3039-3044.

[24] Vosseller, K.; Hansen, K.; Chalkley, R.; Trinidad, J.; Wells, L.; Hart, G.; Burlingame, A. *Proteomics* **2005**, 5, 388-398.

[25]Klemm, C.; Schroder, S.; Gluckmann, M.; Beyermann, M.; Krause, E. *Rapid Commun. Mass Spectro.* **2004**, 18, 2697-2705.

[26] Ahn, Y. H.; Ji, E. S.; Kwon, K. H.; Lee, J. Y.; Cho, K.; Kim, J. Y.; Kang, H. J.; Kim, H. G.; Yoo, J. S. *Anal. Biochem.* **2007**, 370, 77-86.

[27] Hodyss, R.; Cox, H. A.; Beauchamp, J. L. *J. Am. Chem. Soc.* **2005**, *127*, 12436–12437.

[28] Laskin, J.; Yang, Z.; Lam, C.; Chu, I. K. *Anal. Chem.* **2007**, *79*, 6607–6614.

[29] Masterson, D. S.; Yin, H.; Chacon, A.; Hachey, D. L.; Norris, J. L.; Porter, N. A. *J. Am. Soc. Mass Spectrom.* **2004**, *126*, 720–721.

[30] Chu, I. K.; Rodriguez, C. F.; Hopkinson, A. C.; Siu, K. W. M. *J. Am. Soc. Mass Spectrom.* **2001**, 12, 1114–1119

[31] Barlow, C. K.; Moran, D.; Radom, L.; McFadyen, W. D.; O'Hair, R. A. J. *J. Phys. Chem. A* **2006**, 110, 8304–8315

[32] Sun, Q.; Nelson, H.; Ly, T.; Stoltz, B. M.; Julian, R. R. *J. Proteome Res.* **2009**,*8*, 958–966.

[33] Ly, T.; Julian, R. R. *J. Am. Chem. Soc.* **2008**, *130*, 351–358.

[34] Sun, Q. Y.; Tyler, R. C.; Volkman, B. F.; Julian, R. R. *J. Am. Soc. Mass. Spectrom.* **2011**, *22*, 399-407.

[35] Diedrich, J. K.; Julian, R. R. *Anal.Chem.* **2010**, *82*, 4006-4014

[36] Diedrich, J. K.; Julian, R. R. *J. Am. Chem. Soc.* **2008**, *130*, 12212–12213.

[37] Gold, A; Nam, T.; Jayaraj, K.; Sangaiah, R.; Klapper, D.; Ball, L.; French, J.; Nylander-French, L. *Organic Prep. Proc Int.* **2003**, 35, 375-382.

[38] Scotchler, J. W.; Robinson, A. B. *Anal. Biochem.* **1974**, 59, 319-322.

[39] Vosseller, K.; Hansen, K. C.; Chalkley, R. J.; Trinidad, J. C.; Wells, L.; Hart, G. W.; Burlingame, A. L. *Proteomics*. **2005**, 5, 388-398.

[40] Li, W.; Backlund, P. S.; Boykins, R. A.; Wang, G.; Chen, H. *Anal. Biochem*. **2003,** 323, 94-102.

[41] Byford, M. F., *Biochem. J*. **1991**, 280, 261-265.

[42] Monroe, M. Version 6.45, **2007,** http://ncrr.pnl.gov/software/MWCalculator.stm

[43] Eng, J. K.; McCormack, A. L.; Yates, J.R. *J. Am. Soc. Mass Spectrom*. **1994**, 5, 976-989.

[44] Johnson, R.S.; Martin, S. A.; Biemann, K. *Int. J. Mass S*pectrom. **1988**, 86, 137-154.

[45] Wysocki, V. H.; Tsaprailis, G.; Smith, L. L..; Breci, L. A. *J. Am. Soc. Mass Spectrom.* **2000**, 35, 1399-1406.

[46] Sweet, S. M. M.; Bailey, C. M.; Cunningham, D. L.; Heath, J. K.; Cooper, H. J. *Mol Cell Proteomics.* **2009**, 8, 904–912.

Chapter 3

SITE SELECTIVE FRAGMENTATION OF PEPTIDES AND PROTEINS AT QUINONE MODIFIED CYSTEINE RESIDUES INVESTIGATED BY ESI-MS

3.1 Introduction

Cysteine is unique among the canonical amino acids for several reasons. For one, cysteine is the only residue which routinely defines protein structure with covalent bonds coupled through the side chain.[1,2] The typical arrangement requires two cysteine side chains, which are oxidized and linked together to form a cystine disulfide bridge. Cysteine also plays an important role in metal ion coordination, serving as a metal ligand in numerous metalloproteins.[3-6] Cysteine is also among the most reactive amino acids,[7,8] which facilitates post translational modifications and leads to active participation in redox chemistry within cells.[9-12] These unique chemical properties of cysteine make it an important analytical target. Mass spectrometry (MS) is well suited for the analysis of biological molecules, including peptides and proteins; however, cysteine frequently interferes with mass spectral analysis. Disulfide bridges form undesirable cross links which prevent linear dissociation of the molecule and are therefore frequently reduced and capped to avoid interference.[13] Additionally, the

oxidation of cysteine is a common post translational modification which is not always of biological origin, but can complicate the analysis of spectra and must be given due consideration.[14,15]

Another approach which can be employed to avoid these problems is to directly target cysteine or disulfide bonds in proteins with site specific chemistry. For example, disulfide bonds can be targeted with some degree of selectivity in the gas phase via electron capture dissociation[16,17] or the use of 157nm light.[18] In solution, there are various strategies which can be employed to selectively modify cysteine.[19-26] Of particular relevance presently, it has been shown previously that thiol functional groups will react with quinones via a Michael type addition in aqueous solution.[27] This modification can be implemented to yield selective modification of free cysteine residues in peptides and proteins. Due to the selectivity of this modification, only cysteine residues are modified to any significant extent.[28] An example of this type of modification is shown in Scheme 3.1 below. The semiquinone formed from the Michael addition can revert back to the quinone form depending on the redox potential of the solution. The quinone form is primarily observed in the experiments described below. The mass shift after reaction with quinone can effortlessly be used to quantify the number of cysteines present in a peptide or protein. This easily attainable

information has been used previously to improve protein identification through database searching.[29]

Scheme 3.1 Modification of cysteine by quinone

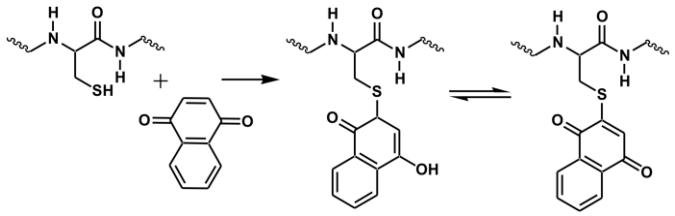

In addition to causing a mass shift, quinone modification of cysteine introduces a chromophore which is adjacent to the C_β-S bond. Recent experiments on modified phosphopeptides have demonstrated that chromophores adjacent to a C_β-S bonds can be used to selectively fragment the peptide backbone following photoactivation with ultraviolet (UV) light.[30] Photodissociation (PD) occurs due to dissociative excited state chemistry which allows bonds to be broken homolytically prior to significant energy redistribution.[31-33] This contrasts with the situation which occurs with radicals generated by collisional activation which tend to yield less selective fragmentation.[34-39] When beta radicals are generated by PD, specific backbone fragmentation at the modified residue is highly favored. Similar chemistry should be accessible by photoexcitation of quinone modified cysteine residues, which is the subject of the present manuscript.

It is demonstrated herein that quinone modified cysteine residues undergo direct dissociation following excitation by 266nm light. The dissociation yields a radical on the remaining peptide or protein at the beta position of cysteine. This beta radical facilitates selective backbone dissociation, typically yielding d-type ions at the modified cysteine residues for both peptides and whole proteins. In addition, quinone modification can be harnessed to monitor protein structure via solvent accessibility moderated differential reactivity. Site selective backbone dissociation can be used to identify the sites of modification in these structure probing experiments, if desired. Finally, PD can be also be used to characterize biologically relevant post translational modification of cysteine by quinones. For example, dopamine can adopt a quinone intermediate structure capable of reacting with free cysteine residues. It is demonstrated that site specific PD can be utilized to identify both the presence and location of dopamine modifications. Interestingly, a novel double modification state is identified for dopamine which can crosslink backbone strands in a manner similar to a disulfide bond.

3.2 Materials and Methods

3.2.1 Materials

Peptides SKGKSKRKKDLRISCNSK, SLRRSSCFGGR, RLCRIVVIRVCR, DYMGWMDF, MEHFRWG, KWDNQ, IARRHPFL, and KKRAARATS-NH_2 were purchased from American Peptide Company. AEAEYEK and Ac-CLKKLsGK were purchased from QCB. Beta lactoglobulin, and lysozyme were purchased from MP Biomedicals. DRVYIHPF, human Hemoglobin, Alpha Lactalbumin, the oxidized beta chain of insulin, dopamine, Benzoquinone (BQ), 1,2 Naphthoquinone (1,2NQ), 1,4 Naphthoquinone (1,4NQ), dithiothreitol (DTT), Guanidine HCl, and Trifluoroacetic acid (TFA) were purchased from Sigma-Aldrich. Tris(2-carboxyethyl)phosphine (TCEP), and acetonitrile (ACN) were purchased from Fisher Scientific. Urea and acetic acid were from EMD and 1,4 Anthraquinone (AQ) was from Alfa Aesar. All were used as received without further purification. Water was purified by Millipore Direct-Q (Millipore, Billerica, MA). A protein MacroTrap and trap holder consisting of a polymeric reversed-phase packing with retention similar to C4 was purchased from Michrom Bioresources, Inc. (Auburn, CA)

3.2.2 Quinone modification (under non-reducing conditions)

Quinone stocks were prepared in ACN at mM concentrations and stored in the dark to reduce degradation and prepared fresh daily. Quinone stock was added to peptide solutions in 0.5 to 4 times excess of peptide concentration. Solutions were diluted with 50:50 ACN: water to peptide concentrations of 10μM for analysis.

Hemoglobin was diluted to concentrations of 5μM protein and 40μM of 1,4NQ in 50:50 ACN: water. Acid was not added to samples in order to favor the formation of lower charge states which facilitates charge state assignments of the fragments generated.

Modification of the free cysteine of Beta lactoglobulin was performed in non reducing conditions as follows: 5μl of 20mM NQ stock in ACN was added to 10ul of 87uM protein stock along with an additional 5μl of ACN to give 50:50 water: ACN solution. The reaction was allowed to sit at room temperature for 4 hours before excess NQ was removed with a protein MacroTrap according to manufacturer's instructions. Final protein concentration after cleanup was ~4μM for analysis by MS.

3.2.3 Modification of disulfide containing proteins

Disulfide bonds were reduced prior to addition of quinone with either DTT or TCEP. Alpha Lactalbumin (7μM) was combined with 100μM DTT and allowed to sit at RT for 15min prior to addition of Naphthoquinone (40μM). Lysozyme (0.732mM, 2μl of 1.83mM) was reduced with TCEP (50mM, 1μl of 250umM) for 2 hours at RT. Guanidine (~2M, 2μl of ~5M stock) was added to the sample to denature the protein. NQ (10μl of 1mM stock in ACN) was added to the reduced protein solution. Excess reactants were removed by desalting with a protein MacroTrap and diluted to ~7μM protein prior to analysis by MS.

3.2.4 Probing solvent accessibility of cysteines in Hemoglobin

Hemoglobin stock solution was diluted into each of the three following solutions with a final protein concentration of 8.6μM: 20mM PBS (phosphate buffered saline), 8M urea, and 50% ACN. 20mM Ammonium bicarbonate was added to each sample to maintain a constant pH. To each sample 1μl of 5mM BQ or AQ stock was added (50uM final conc). The samples were allowed to react at room temperature for 15min at which point the reaction was stopped by addition of TFA to reach a pH of 3-4. Protein samples were desalted by protein Macrotrap, eluding the protein from the trap in 200μl of 90% ACN and 0.1%TFA. Stopping

the reactions by addition of acid allows cleanup of the samples to be performed, and all solutions were electrosprayed directly from the trap eluent.

3.2.5 Dopamine modification

Peptide SKGKSKRKKDLRISCNSK (10μM) was mixed with dopamine (50μM) and 0.0033% hydrogen peroxide to promote the formation of dopamine quinone. The solution was diluted to the listed peptide concentration in 50:50 water: ACN and electrosprayed. Hemoglobin (4μM) was mixed with dopamine (100μM) alone, then diluted and electrosprayed in 50:50 water: ACN.

3.2.6 Photodissociation of quinone modified peptides and proteins:

Solutions were analyzed in cation mode by an LTQ linear ion trap mass spectrometer (Thermo Fisher Scientific, Waltham, MA) with a standard electrospray source. The posterior plate of the LTQ was modified with a quartz window to transmit fourth harmonic (266 nm) laser pulses from a flashlamp-pumped Nd:YAG laser (Continuum, Santa Clara, CA). Pulses were synchronized to the end of the isolation step of a typical MS^2 experiment by feeding a TTL trigger signal from the mass spectrometer to the laser via a digital delay generator (Berkeley Nucleonics, San Rafael, CA). This allowed photodissociation (PD) to be carried out analogous to collision induced dissociation (CID). Multi shot experiments were carried out with a burst pulse sequence where each of the

pulses were separated by 100msec and the activation time was adjusted in the instrument software to accommodate adequate time for multiple pluses prior to scanning.

3.3 Results and Discussion

3.3.1 Selective cysteine modification by quinones.

The following peptides were treated with either 1,4-naphthoquinone (NQ) or anthraquinone (AQ): KWDNQ, IARRHPFL, MEHFRWG, DRVYIHPF, KKRAARATS, AEAEYEK, DYMGWMDF, SKGKSKRKKDLRISCNSK, SLRRSSCFGGR, RLCIVVIRVCR (containing a disulfide bond), and the beta chain of insulin with oxidized cysteines. These peptides were chosen because they contain collectively all 20 natural amino acids and three common forms of cysteine (free, oxidized, and disulfide bound). The full mass spectrum of peptide SLRRSSCFGGR is shown in Figure 3.1a after reaction with NQ. Abundant addition of a single quinone to the peptide is observed in all three charge states. No unmodified peptide is observed to remain after the reaction. Modification at the cysteine side chain was confirmed by MS/MS (shown below in Figure 3.3b). SKGKSKRKKDLRISCNSK was the only other peptide to mass shift due to attachment of NQ or AQ. A single modification at cysteine was also observed for

this peptide (data not shown). These results demonstrate the selectivity for quinone addition to free cysteine and suggest that in the absence of structural interference or steric hindrance, modification can easily be driven to completion. In Figure 3.1b the mass spectrum of Hemoglobin treated with NQ is shown. Hemoglobin consists of four protein chains, two alpha and two beta. In the human variant, the alpha chain contains a single cysteine residue and the beta chain contains two, none of which are involved in disulfide bonds and are expected to exist in the free thiol form. A single distribution of peaks is observed in Figure 3.1b for the alpha chain of Hemoglobin (labeled as #). Deconvolution of the data yields a single molecular weight corresponding to loss of the noncovalently bound heme and addition of a single quinone. The beta chain yields two distributions of peaks, both of which result from loss of heme and addition of either one (labeled with *) or two (**) NQ. Little or no unmodified protein was observed in any of the charge states for either protein chain. Nevertheless, structural interference likely prevents complete modification of the beta chain. As was observed for the peptide in Figure 3.1a, the maximum number of quinones attached to the protein is consistent with the number of free cysteines in both systems.

Chart 3.1 Quinones examined herein.

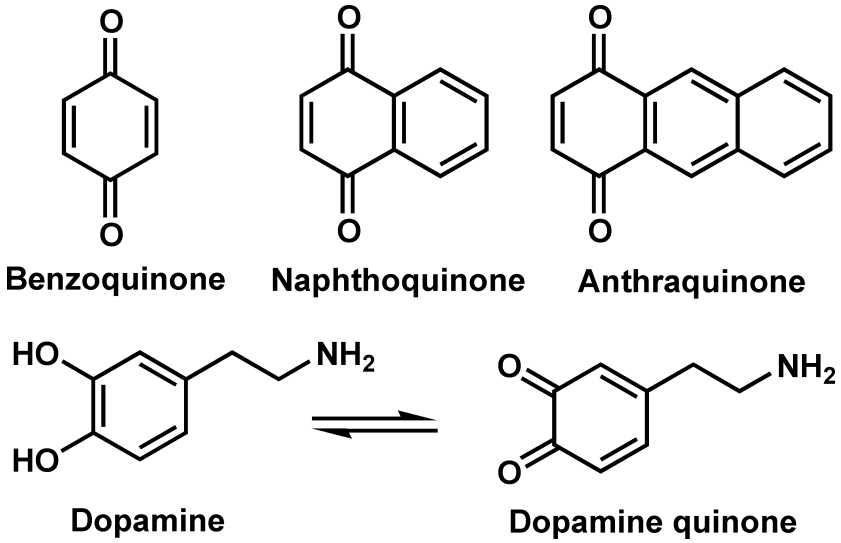

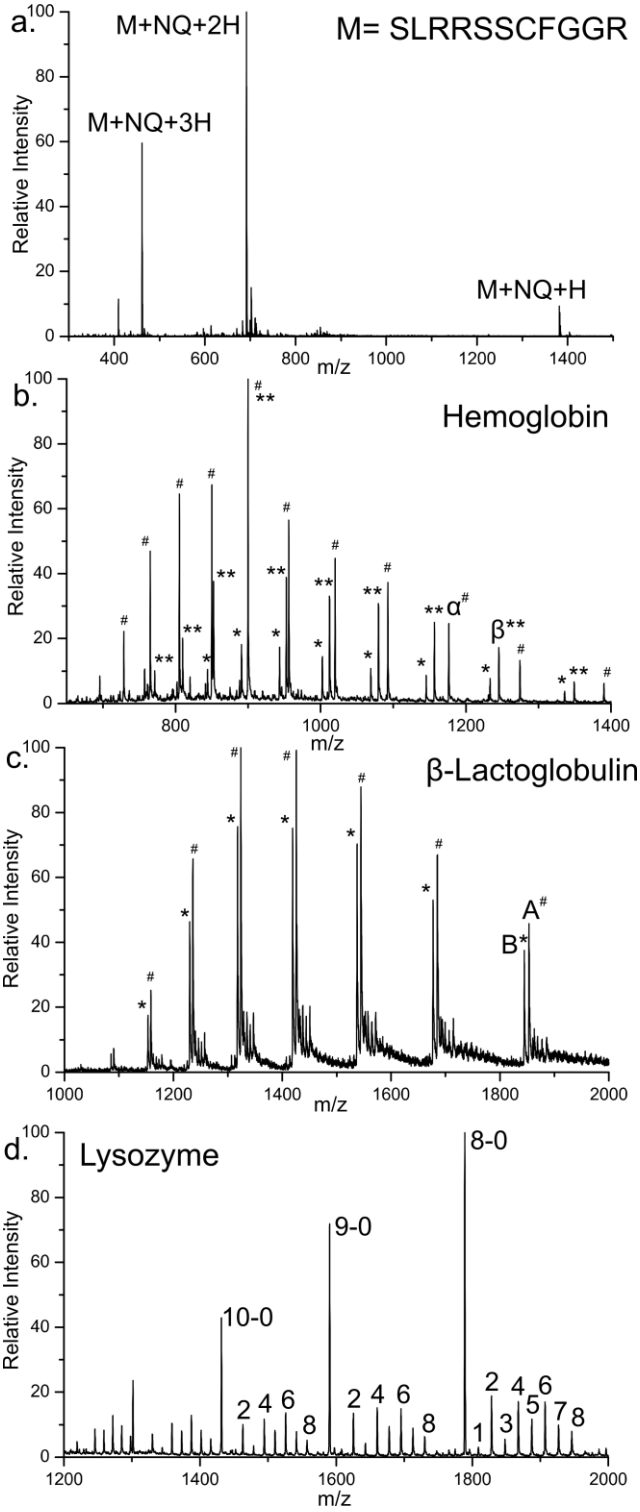

Figure 3.1 a) Full mass spectrum of SLRRSSCFGGR after reaction with NQ. b) Full mass spectrum of Hemoglobin modified with NQ. Alpha chain (#) modified by one NQ. Beta

chain single (*) and double (**) NQ modifications. c) Beta Lactoglobulin after NQ modification. Two natural variants A and B (both containing five cysteines and two disulfide bonds) are observed each with a single NQ modification. d) NQ modification of lysozyme after partial reduction of all four disulfide bonds.

Modification of beta lactoglobulin with disulfide bonds intact is shown in Figure 3.1c. Beta lactoglobulin contains five cysteine residues, four of which are bound by two disulfide bonds. Two variants of beta lactoglobulin are observed in the full mass spectrum. These two common variants, A (labeled #) and B (labeled *) differ in sequence by two amino acids D64G and V118A. Beta lactoglobulin contains a disulfide bond between cysteines 66 and 160 and a second disulfide bond between cysteine 106 and either cysteine 119 or 122 (both have been cited in literature).[40,41] Both variants A and B are observed to have shifted mass due to modification with a single quinone. This mass shift relative to the unmodified protein allows easy determination of the number of free cysteines present in beta lactoglobulin.

Cysteines are often used to stabilize protein structure through the formation of disulfide bridges. Determining the presence of a disulfide bond by mass alone can be difficult, especially in large proteins where it can be difficult to detect a two dalton mass difference. Modification of free cysteines yields a much larger mass difference which is easily distinguishable. Cysteine modification before and

after disulfide reduction can be utilized to determine the number of disulfide bonds present in a protein. For example, lysozyme contains eight cysteine residues that are all involved in disulfide bonds. Addition of quinone to the native protein results in no change in mass because there are no free cysteines to react with the quinone. After treatment with TCEP to partially reduce disulfide bonds, attachment of quinone is evident as shown in Figure 3.1d. (TCEP is used in place of DTT because of its ability to reduce disulfide bonds without reacting with NQ.) A distribution of zero to eight NQ modifications of lysozyme is observed, indicative that some fraction of all four disulfide bonds was reduced. It is also interesting to note that modification peaks follow a statistical pattern favoring an even number of modifications. It is likely that once a disulfide bond is reduced, attaching quinone to both cysteines is favored over attaching quinone to only one site. These observations are in agreement with the known high reactivity of the cysteine side chain.[42] It is also clear in Figure 3.1d that the protein observed without modification decreases in relative intensity as the charge state of the protein increases. It is well known that unfolded proteins in ESI spectra are present in the higher charge states.[43,44] A protein with larger surface area, due to unfolding, is able to accommodate a larger number of charges than a more compact form of the same protein. It follows that the protein

observed at higher charge states originated from a more open conformation. It is also likely that protein with a disulfide bond reduced would take on a more open conformation since the structure is no longer rigidly held in place. The increased amount of quinone modification at higher charge states is consistent with a change in the protein structure to a more open conformation.

3.3.2 Probing Protein Structure

The possibility for probing protein structure as a function of the accessibility of cysteine residues was examined in greater detail by modification of Hemoglobin with benzoquinone (BQ) and anthraquinone (AQ) under different solvent conditions. BQ and AQ were chosen for the comparison as they encompass the two extremes of the quinone sizes utilized. Three different solvent conditions were employed to produce different structural states of Hemoglobin: 20mM phosphate buffered saline (PBS), 8M urea, and 50% ACN. The PBS solution should maintain the native protein conformation while the 8M urea and 50% ACN solution are likely to yield denatured states. A representative full mass spectrum is shown in Figure 3.2a for modification with BQ in 50% ACN. In order to facilitate comparison of the results, the relative amount of modification observed for each protein chain summed over all charge states is shown in Figures 3.2b and c.

As seen in Figure 3.2b, the alpha chain of Hemoglobin is only ~40% modified with BQ in PBS, but almost completely modified in urea and 50%ACN. These results suggest that denaturing of the protein structure enables more complete quinone attachment. Similar results are obtained for the beta chain, which has two cysteine residues. In PBS a single modification is dominant, whereas two modifications are favored in the urea and ACN denaturing environments. Interestingly, for the beta chain the extent of reactivity is not identical in the two denaturing environments, suggesting that different structures or structural ensembles are present. In Figure 3.2c, modification with the larger AQ is shown. The alpha chain is not completely modified under any solvent condition for AQ, which contrasts the results obtained with BQ. The most straightforward explanation for this observation is that the larger size of AQ reduces the accessibility of cysteine and the amount of modification observed. With AQ, the extent of modification is different for both the alpha and beta chains in all solvent environments, suggesting that AQ is a more sensitive probe of protein structure.

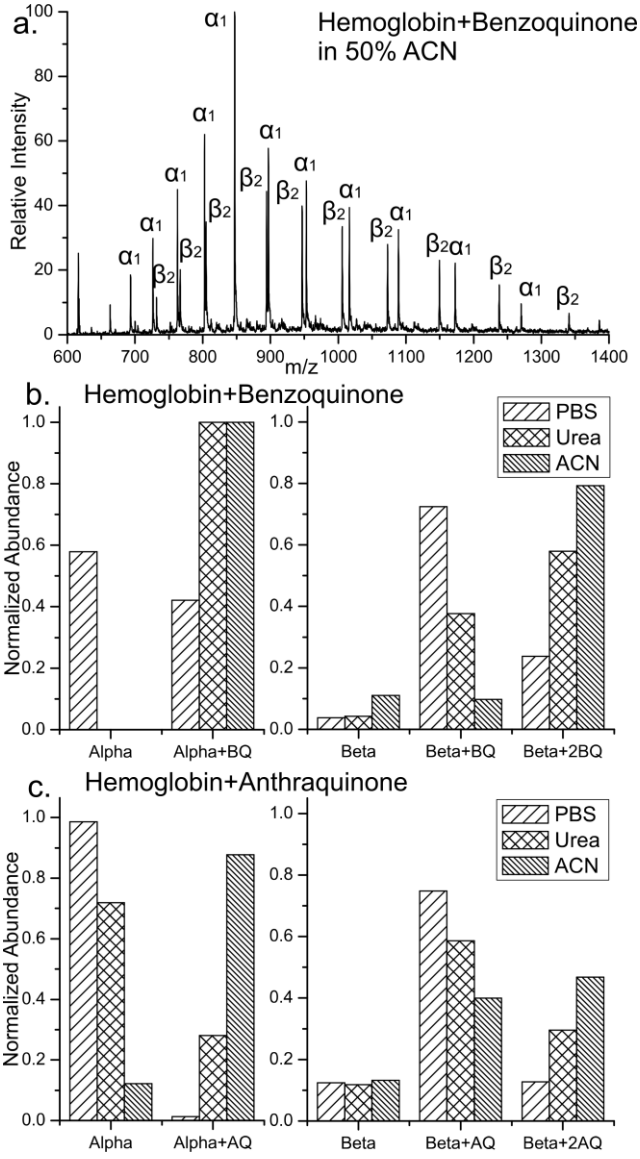

Figure 3.2 a) Full mass spectrum for Hemoglobin modified by BQ in 50%ACN, subscripts indicate number of modifications. b) The relative extent of BQ modification of Hemoglobin over all charge states is summarized for three solvent systems: phosphate buffered saline (PBS), 8M urea, and 50% ACN. The x-axis labels indicate the chain and corresponding number of modifications. c) Anthraquinone modifications are shown in plots analogous to those in b).

3.3.3 Fragmentation at modified cysteine residues

Photodissociation of the +3 charge state of the SLRRSSCFGGR peptide modified with a single NQ is shown in Figure 3.3a. Two major fragment peaks are observed. The first (labeled C-S) is due to homolytic cleavage of the C_β-S bond of cysteine. This characteristic loss of 190Da is a unique indicator that the selected ion contains a cysteine residue modified by NQ. The second most abundant peak observed is the d_7 fragment. Generic fragment structures are shown in Scheme 3.2. This ion results from selective backbone fragmentation at the modified cysteine. Also observed, although in smaller abundance, is fragmentation of the peptide backbone on the N terminal side of the modified cysteine to yield an a_6 fragment. The mechanism of fragment formation will be discussed below. PD of the unmodified peptide was also performed (data not shown). No fragmentation was observed from PD of the unmodified peptide, indicating that the fragments in Figure 3.3a are generated due to absorption at the quinone.

Scheme 3.2 Structures of fragments formed by photodissociation

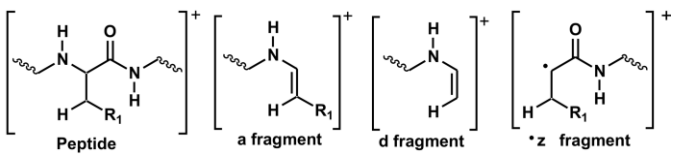

Collision induced dissociation (CID) of the +3 charge state of NQ modified peptide SLRRSSCFGGR is shown in Figure 3.3b. For comparison, CID of the +3 charge state of the unmodified peptide is shown in Figure 3.3c. Fragmentation by CID of the modified and unmodified peptides is very similar. Nearly all fragmentation pathways are analogous between the two, and nearly identical relative abundances are observed as well. Fragments including the modified cysteine are shifted in mass due to the retained quinone modification. The primary difference between the two CID spectra is the loss of modified cysteine side chain (labeled M-C*). This fragment is generated by cleavage of the carbon sulfur bond. However, fragmentation does not occur homolytically as in PD, thus a radical is not generated. Overall, the modification does not seem to significantly affect the fragmentation behavior of the peptide by CID. Comparison of Figures 3.3a and b, which are PD and CID of the modified peptide, reveals the selectivity afforded by photodissociation. The site of modification can be determined with either CID or PD. However this process is simpler by PD due to the selectivity and simplicity of the fragmentation. While the value of this fragmentation may not be apparent in determining the site of cysteine in peptides, the utility becomes more apparent in larger systems.

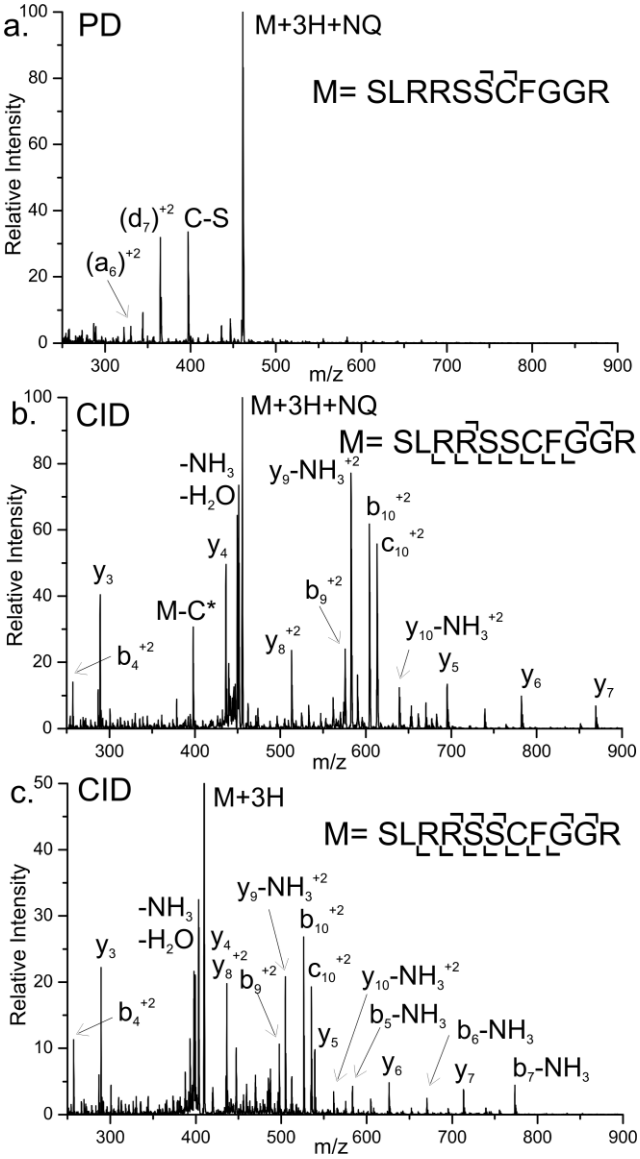

Figure 3.3 a) Photodissociation of the peptide SLRRSSCFGGR modified with NQ. Homolytic cleavage of the C_β-S bond of the modified cysteine side chain is labeled C-S. b) CID of the NQ modified peptide. c) CID of the unmodified peptide for comparison.

3.3.4 Fragmentation at cysteine residues in whole proteins

This methodology can also be extended to whole proteins. In Figure 3.4a, the PD spectrum for the +20 charge state of alpha Hemoglobin modified with NQ is shown. Homolytic cleavage of the C_β-S bond is clearly present. The characteristic loss of the quinone-thiol at M-190Da is labeled as C-S. A single backbone fragment is observed at Cys104 yielding the +15 and +16 d_{104} ions. The complementary z fragment (z_{37}) is also observed, although with smaller intensity compared to d_{104}. The z_{37} fragment is also present in two charge states (+4 and +5). The charge states of the two complementary fragments equal the parent ion charge state of +20, also indicating that the d and z fragments are formed from a single initial backbone fragmentation. The single cysteine in alpha Hemoglobin is located at residue 104, the only site at which backbone fragmentation is observed. This demonstrates the ability of RDD to selectively cleave a single bond in a whole protein. This level of selectivity has not been achieved in any previous experiments and even supersedes previous PD experiments with whole proteins where iodination at tyrosine was observed to yield semi-selective fragmentation.[32]

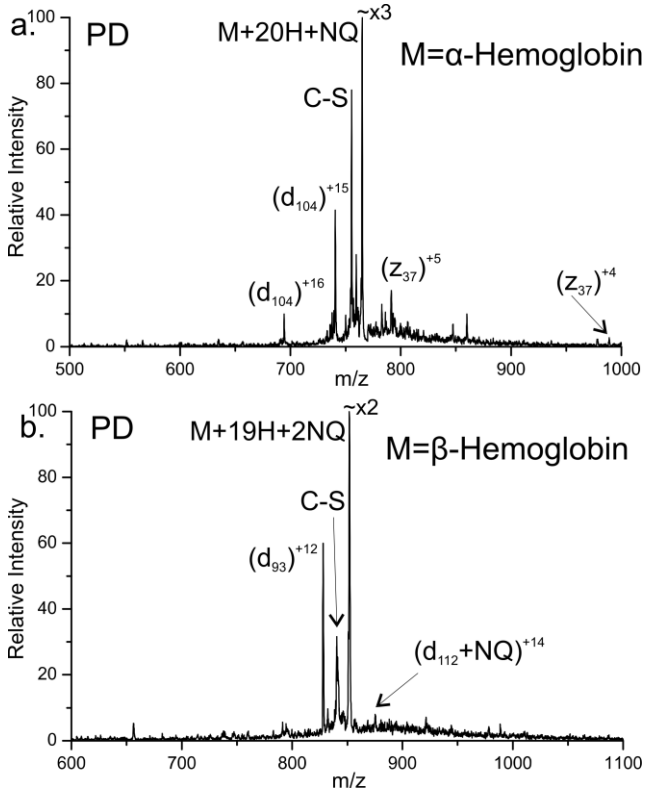

Figure 3.4 a) Photodissociation of the alpha chain of Hemoglobin modified with a single NQ. The NQ modification is lost due to homolytic cleavage of the C_β-S bond of cysteine (labeled as C-S). Backbone fragmentation at cysteine is observed generating d_{104} and z_{37}. b) Photodissociation of the beta chain of Hemoglobin with two NQ modifications.

Photodissociation of the beta chain with two NQ was also performed as shown in Figure 3.4b. Loss of a single naphthoquinone-thiol is primarily observed although a very small amount of the second quinone is also lost. Fragmentation at the two cysteine residues, positions 93 and 112, is observed. Fragments d_{93} and d_{112} are generated just C terminal to the two cysteines although the amount of fragmentation at cysteine 93 is significantly larger in

abundance. Three laser pulses were used in the spectrum shown, thus it is possible that absorption and fragmentation will occur at a single cysteine or at both sites. The d_{112} fragment can only be observed if absorption does not occur or result in fragmentation at cysteine 93. However d_{93} can be observed regardless of what occurs at cysteine 112. Therefore the fragmentation observed at d_{112} is smaller in abundance than at d_{93}. If absorption and fragmentation occurred at both positions simultaneously, an internal fragment could theoretically be observed. No such fragment was identified.

3.3.5 Probing protein structural changes

Alpha Lactalbumin (ALA) is a 123 residue protein containing eight cysteines involved in four disulfide bonds. Partial reduction by DTT and subsequent addition of NQ yields the full mass spectrum shown in Figure 3.5a. Peaks are labeled with the charge state and the number of quinone modifications determined by mass (11-1 denotes the +11 charge state with a single quinone). The majority of the protein either has one or two NQ modifications. The number and relative abundance of NQ varies depending on the charge state, with higher charge states having a larger number of NQ modifications. Again, this observation is likely correlated with a difference in protein structure.

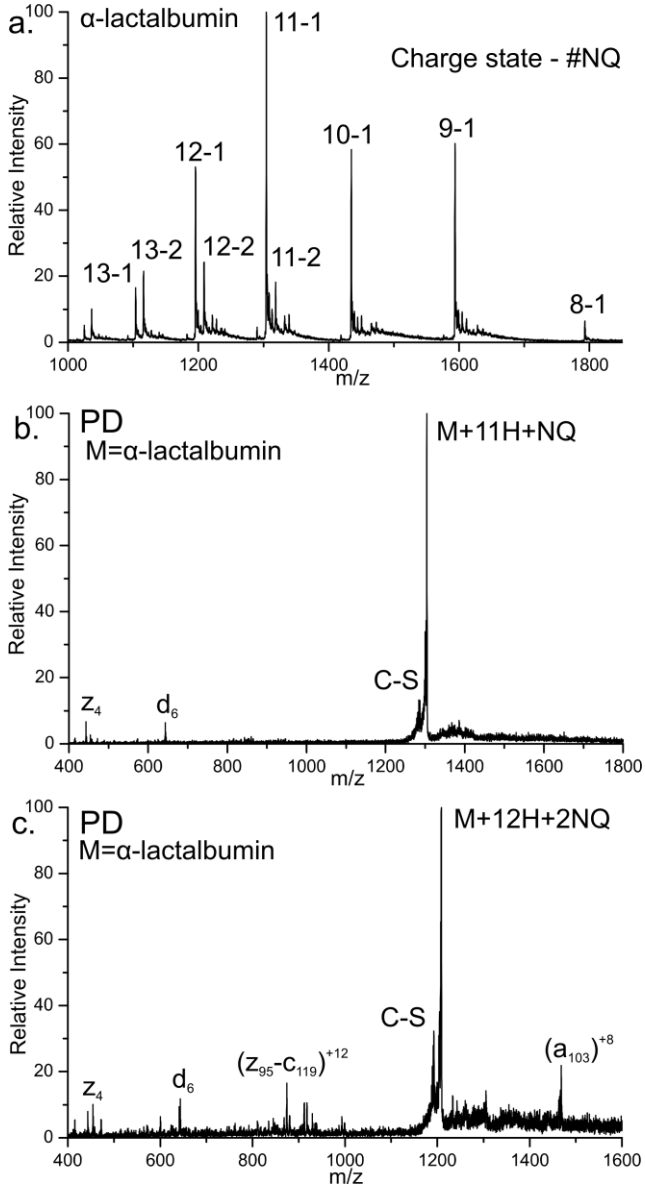

Figure 3.5 a) Full mass spectrum of Alpha Lactalbumin (ALA) following modification with NQ. Peaks are labeled with the charge state and the number of NQ modifications. b) Photodissociation of the +11 charge state of ALA with a single NQ modification. C_β-S bond cleavage is labeled (C-S). Two backbone fragments are observed, z_4 and d_6, at the N and C terminal cysteines. c) Photodissociation of the +12 charge state of ALA with two NQ modifications.

Photodissociation of the 11-1 peak is shown in Figure 3.5b. Fragmentation of the C_β-S bond of cysteine (labeled C-S) is noted. Two peaks are observed due to backbone fragmentation, z_4 and d_6. These fragments occur at the two cysteines (Cys6 and Cys120) located near the N and C termini of the protein. These two cysteines have previously been shown to be linked through a disulfide bond. Thus the protein in the 11-1 peak most likely has a single disulfide bond reduced between Cys6 and Cys120. Photodissociation of the higher charge state (+12) of protein with two quinones attached is shown in Figure 3.5c. Fragments z_4 and d_6 are observed as before. Additional backbone fragmentation is observed in comparison to Figure 3.5b. One of these new fragments (z_{95}-c_{119}) corresponds to an internal fragment between residues 28 and 119. More specifically, the internal fragment is due to a z-type fragmentation at Cys28 and a c-type fragmentation at Cys120. Additional nonselective dissociation is observed at Tyr103, which is known to be a favorable radical dissociation pathway.[32] These results illustrate that site specific identification of cysteine will probably be limited to the two or three most reactive sites in proteins containing multiple disulfide bonds.

3.3.6 Dopamine modified protein

Dopamine is a biologically relevant small molecule neurotransmitter involved in several processes in the brain. Dopamine can also adopt a quinone form and modify cysteine residues.[45,46] The PD method described herein was explored as a method for characterizing peptides and proteins modified by dopamine. To confirm that cysteine residues react with dopamine, the cysteine containing peptide SKGKRKKDLRISCNSK was mixed with dopamine and a small amount of H_2O_2 (also present in cells) to promote formation of dopamine quinone. Subsequent MS of the sample determined that a small amount of the dopamine adduct had formed with the peptide. CID confirmed that a covalent bond had formed between the peptide and dopamine (data not shown). PD of this protein-dopamine adduct is shown in Figure 3.6a. The largest fragment generated due to PD is a mass loss of 184Da. This unique loss corresponds to the loss of dopamine and the sulfur of cysteine by homolytic cleavage of the C_β-S bond. The primary backbone fragment observed, although small, is d15 at cysteine. These two fragments yield all the necessary information to determine both the presence and location of the dopamine modification. The peak corresponding to a loss of 184 Da is unique to dopamine and the presence of this peak alone indicates that a dopamine modification is present. Furthermore the

additional d-fragment selectively identifies the location of the dopamine modified cysteine residue.

Figure 3.6b is the full mass spectrum observed upon spraying a solution containing Hemoglobin incubated with dopamine without the addition of any H_2O_2. The alpha chain is observed in a single distribution of unmodified apo-protein. The beta chain is observed in two distributions. The larger of the two is the unmodified apo-protein. The second distribution corresponds to apo-protein with addition of a single dopamine modification by mass. Figure 3.6c is PD performed on the peak at m/z 1068 selected from the spectrum in Figure 3.6b. By deconvolution of charge states it was determined that the peak corresponded to the +15 charge state of the beta chain of Hemoglobin with a single dopamine modification. PD of the unmodified +15 charge state of the beta chain of Hemoglobin (from a solution without dopamine) is shown in Figure 3.6d for comparison. PD of both the modified and unmodified protein generates peaks corresponding to fragments y_{131} and b_{15} which occur at W15. The side chain of tyrosine is also observed to be lost in both spectra. This fragmentation at tryptophan is atypical and is not observed in CID, thus it is likely due to electronic excitation at tryptophan. [47] However this behavior is not due to the quinone modification as it is also present in the unmodified protein. Three peaks

observed are unique to PD of the modified protein. The first of these is a loss of 184Da, the same loss observed with the dopamine modified peptide due to homolytic cleavage of the C_β-S bond of cysteine. The presence of this peak alone confirms that the isolated species contains a dopamine modification at a cysteine residue. The other two unique peaks correspond to selective fragmentation at the modified site to yield z_{34} and d_{112}+dopamine. These complementary d and z fragments occur due to radical directed fragmentation at cysteine 112; however, beta Hemoglobin contains another cysteine residue at position 93. Based on the mechanism in Scheme 3.3, fragmentation at the modified residue should be accompanied by loss of the modification. Thus the d_{112}+dopamine fragment is unexpected. Further experiments were performed to understand this unique instance. A subsequent step of CID on the d_{112}+dopamine fragment was performed to determine if the dopamine was covalently or non-covalently attached to the protein fragment. Dopamine was not lost upon CID (data not shown), suggesting it is covalently bound.

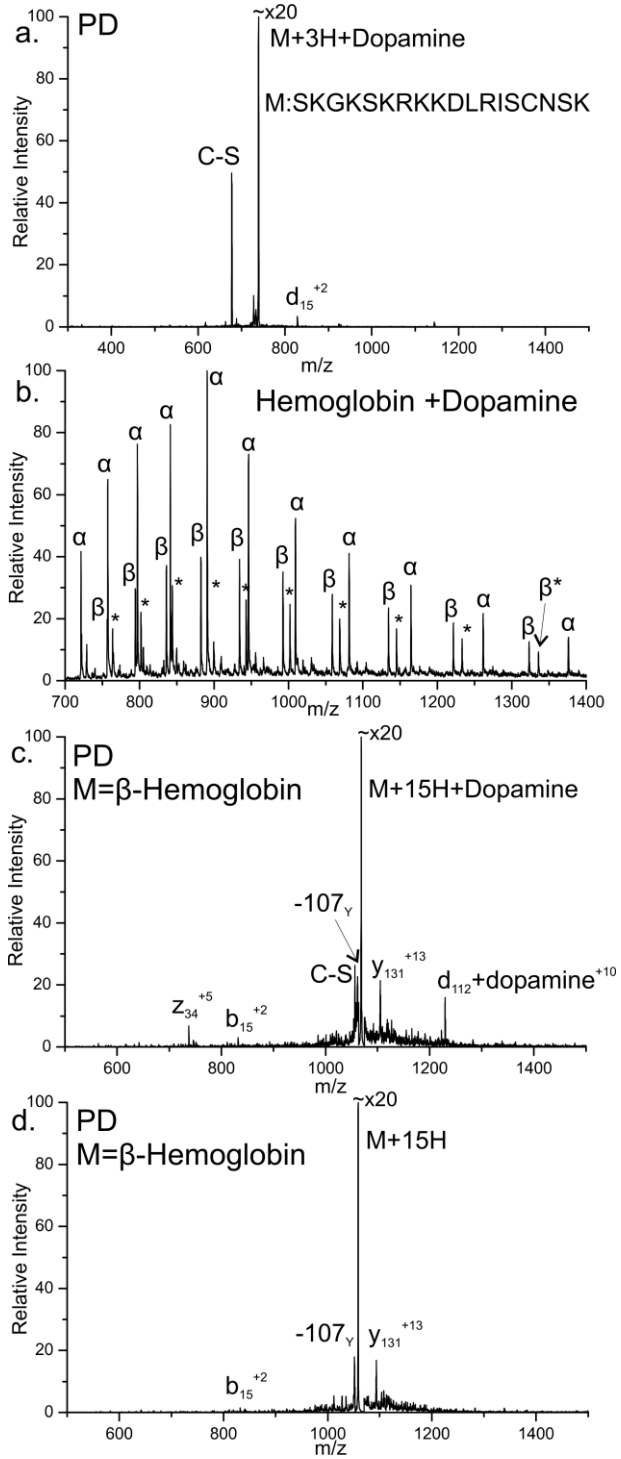

Figure 3.6 a) Photodissociation of the peptide SKGKSKRKKDLRISCNSK modified with dopamine. Homolytic cleavage of the C_β-S bond is observed (C-S). Backbone fragmentation (d_{15}) at cysteine identifies the site of modification. b) Full MS observed

after dopamine addition to Hemoglobin. Only the β chain is modified (labeled *). c) PD of the +15 charge state of β chain of Hemoglobin with a single dopamine modification. d) PD of the +15 charge state of β chain of Hemoglobin without modification for comparison.

Figure 3.7 shows CID spectra for the unmodified and modified beta chain of Hemoglobin, respectively. As seen in Figure 3.7a, CID of the unmodified protein yields abundant y_{111}, y_{96}, and y_{47} fragments, which form due to fragmentation at proline residues 36, 51, and 100 respectively.[48,49] In comparison, CID of the modified protein shown in Figure 3.7b only yields abundant y_{111} and y_{96} fragments which are mass shifted by the addition of dopamine. Fragmentation at proline 100, yielding fragment y_{47} is observed in the modified protein with and without dopamine modification, however the fragmentation at proline 100 is greatly reduced in the modified protein. This indicates that there is something preventing fragmentation from occurring or being observed at proline 100. Due to the structure of dopamine, it is possible for two Michael type additions to occur on a single dopamine. The beta chain of Hemoglobin contains two cysteine residues. Attachment of both cysteines to a single dopamine would cyclize part of the protein and explain this fragmentation behavior. If proline fragmentation at P100 occurs during collisional activation, it will not be observed because both fragments are still held together by dopamine. This is consistent with the large

decease in intensity of y_{47} in the modified protein. The small amount of y_{47} that is observed can be rationalized by a small amount of uncylcilzed protein with dopamine attached to only one cysteine. Even in this special case of double modification, PD is capable of identifying one of the sites of attachment with ease and the existence of the other is revealed by retention of the dopamine modification.

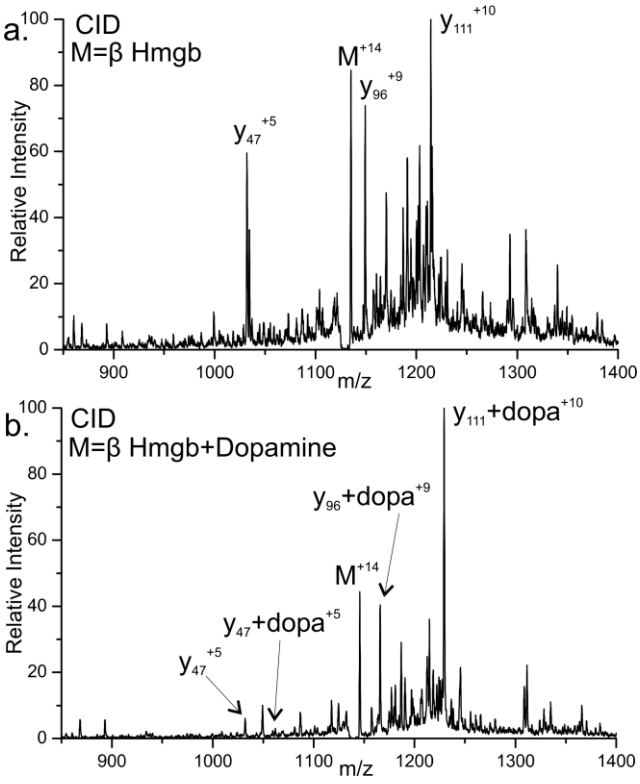

Figure 3.7 a) CID of the +14 charge state of the unmodified beta chain of Hemoglobin. The primary fragments observed are y_{111}, y_{96} and y_{47} occurring due to proline fragmentation at residues 36, 51, and 100 b) CID of the +14 charge state of beta Hemoglobin with a single dopamine modification.

3.4 Conclusions

Modification by quinones is selective to the free thiol form of cysteine and was shown to easily quantify the reactive cysteines in both peptides and proteins. Photodissociation of the quinone modified species was utilized to determine the location of modified residues through selective backbone fragmentation. Photo-excitation of the quinone homolytically cleaves the C_β-S bond of cysteine. This homolytic cleavage results in a radical located at the beta position of cysteine, which facilitates electronic rearrangement to cleave the peptide or protein backbone at the modified cysteine. Photodissociation of modified alpha Hemoglobin was shown to selectively cleave a single bond in the protein backbone at the modified cysteine. This selective modification and fragmentation can be used to probe protein structure. Finally, the technique is amenable for identifying protein modification by naturally occurring quinones such as dopamine.

---

[1] Freedman, R. B. *Curr. Opin. Struct. Biol.* **1995,** *5*, 85-91.

[2] Darby, N.; Creighton, T. E. *Method. Mol. Biol.* **1995,** *40*, 219-252.

[3] Henehan, C. J.; Pountney, D. L.; Zerbe, O.; Vasak, M. *Protein Sci.* **1993,** *2*, 1756-1764.

[4] Ngu, T. T.; Stillman, M. J. *Dalton Trans.* **2009,** *28*, 5425-5433.

[5] Duncan, K. E. R.; Ngu, T. T.; Chan, J.; Salgado, M. T.; Merrifield, M. E.; Stillman, M. J. *Exp. Biol. M.* **2006,** *231*, 1488-1499.

[6] Przybyla, A. E.; Robbins, J.; Menon, N.; Peck, H. D. J. *FEMS Microbiol. Rev.* **1992,** *8*, 109-135.

[7] Herring, P. A.; Jackson, J. H. *Microb. Comp. Genomics* **2000,** *5*, 75-87.

[8] Rauk, A.; Yu, D.; Taylor, J.; Shustov, G. V.; Block, D. A.; Armstrong, D. A. *Biochemistry* **1999,** *38*, 9089-9096.

[9] Ghezzi, P.; Bonetto, V.; Fratelli, M. *Antioxid. Redox Sign.* **2005,** *7*, 7-8.

[10] Barnes, S.; Shonsey, E. M.; Eliuk, S. M.; Stella, D.; Barrett, K.; Srivastava, O. P.; Kim, H.; Renfrow, M. B. *Biochem. Soc. Trans.* **2008,** *36*, 1037-1044.

[11] Ronsein, G. E.; Miyamoto, S.; Bechara, E.; Di Mascio, P.; Martinez, G. R. *Quim. Nova* **2006,** *29*, 563-568.

[12] Grimsrud, P. A.; Xie, H.; Griffin, T. J.; Bernlohr, D. A. *J. Biol. Chem.* **2008,** *283*, 21837-21841.

[13] Witze, E. S.; Old, W. M.; Resing, K. A.; Ahn, N. G. *Nat. Methods* **2007,** *4*, 798-806.

[14] Thornalley, P. J. *Protein Oxidation and Disease* **2006**, 143-178.

[15] Steen, H.; Mann, M. *Adv. Mass Spectrom.* **2001,** *15*, 527-528.

[16] Chalkley, R. J.; Brinkworth, C. S.; Burlingame, A. L. *J. Am. Soc. Mass Spectrom.* **2006,** *17*, 1271-1274.

[17] Zubarev, R. A.; Kruger, N. A.; Fridriksson, E. K.; Lewis, M. A.; Horn, D. M.; Carpenter, B. K.; McLafferty, F. W. *J. Am. Chem. Soc.* **1999,** *121*, 2857-2862.

[18] Fung, Y. M. E.; Kjeldsen, F.; Silivra, O. A.; Chan, T. W. D.; Zubarev, R. A. *Angew. Chem. Int. Ed.* **2005,** *44*, 6399-6403.

[19] Chowdhury, S. M.; Munske, G. R.; Ronald, R. C.; Bruce, J. E. *J. Am. Soc. Mass Spectrom.* **2007,** *18*, 493-501.

[20] Cui, H.; Leon, J.; Reusaet, E.; Bult, A. *J. Chromatogr. A* **1995,** *704*, 27-36.

[21] Goodlett, D. R.; Bruce, J. E.; Anderson, G. A.; Rist, B.; Pasa-Tolic, L.; Fiehn, O.; Smith, R. D.; Aebersold, R. *Anal. Chem.* **2000,** *72*, 1112-1118.

[22] Kondo, T. *Seikagaku* **2004,** *76*, 385-390.

[23] Kostic, N. M. *Comments Inorg. Chem.* **1988,** *8*, 137-162.

[24] Thevis, M.; Loo, R. R. O.; Loo, J. A. *J. Proteome Res.* **2003,** *2*, 163-172.

[25] Wang, Y.; Vivekananda, S.; Men, L.; Zhang, Q. *J. Am. Soc. Mass Spectrom.* **2004,** *15*, 697-702.

[26] Zhou, H.; Boyle, R.; Aebersold, R. *Method. Mol. Biol.* **2004,** *261*, 511-518.

[27] Dayon, L.; Roussel, C.; Girault, H. H. *Chimia* **2004,** *58*, 204-207.

[28] Mason, D. E.; Liebler, D. C. *Chem. Res. Toxicol.* **2000,** *13*, 976-982.

[29] Roussel, C.; Dayon, L.; Lion, N.; Rohner, T. C.; Josserand, J.; Rossier, J. S.; Jensen, H.; Girault, H. H. *J. Am. Soc. Mass Spectrom.* **2004,** *15*, 1767-1779.

[30] Diedrich, J. K.; Julian, R. R. *J. Am. Chem. Soc.* **2008,** *130*, 12212-12213.

[31] Izquierdo, J. G.; Amaral, G. A.; Ausfelder, F.; Aoiz, F. J.; Banares, L. *ChemPhysChem* **2006,** *7*, 1682-1686.

[32] Ly, T.; Julian, R. R. *J. Am. Chem. Soc.* **2008,** *130*, 351-358.

[33] Sun, Q.; Nelson, H.; Ly, T.; Stoltz, B. M.; Julian, R. R. *J. Proteome Res* **2009,** *8*, 958-966.

[34] Bagheri-Majdi, E.; Ke, Y.; Orlova, G.; Chu, I. K.; Hopkinson, A. C.; Siu, K. W. M. *J. Phys. Chem. B* **2004,** *108*, 11170-11181.

[35] Hodyss, R.; Cox, H. A.; Beauchamp, J. L. *J. Am. Chem. Soc.* **2005,** *127*, 12436-12437.

[36] Laskin, J.; Yang, Z.; Lam, C.; Chu, I. K. *Anal. Chem.* **2007,** *79*, 6607-6614.

[37] Masterson, D. S.; Yin, H.; Chacon, A.; Hachey, D. L.; Norris, J. L.; Porter, N. A. *J. Am. Soc. Mass Spectrom.* **2004,** *126*, 720-721.

[38] O'Hair, R. A. J.; Styles, M. L.; Reid, G. E. *J. Am. Soc. Mass Spectrom.* **1998,** *9*, 1275-1284.

[39] Ryzhov, V.; Lam, A. K. Y.; O'Hair, R. A. J. *J. Am. Soc. Mass Spectrom.* **2009,** *20*, 985-995.

[40] Kuwata, K.; Hoshino, M.; Forge, V.; Era, S.; Batt, C. A.; Goto, Y. *Protein Sci.* **1999,** *8*, 2541-2545.

[41] McKenzie, H. A.; Ralston, G. B.; Shaw, D. C. *Biochemistry* **1972,** *11*, 4539-4547.

[42] Roussel, C.; Rohner, T. C.; Jensen, H.; Girault, H. H. *ChemPhysChem* **2003,** *4*, 200-206.

[43] Ferguson, P. L.; Kuprowski, M. C.; Boys, B. L.; Wilson, D. J.; Pan, J.; Konermann, L. *Curr. Anal. Chem.* **2009,** *5*, 186-204.

[44] Kaltashov, I. A.; Abzalimov, R. R. *J. Am. Soc. Mass Spectrom.* **2008,** *19*, 1239-1246.

[45] LaVoie, M. J.; Hastings, T. G. *J. Neurosci.* **1999,** *19*, 1484-1491.

[46] Nicolis, S.; Zucchelli, M.; Monzani, E.; Casella, L. *Chem. Eur. J* **2008,** *14*, 8661-8673.

[47] Perot, M.; Lucas, B.; Barat, M.; Fayeton, J. A.; Jouvet, C. *J. Phys. Chem. A* **2009,** *ASAP*.

[48] Loo, J. A.; Edmonds, C. G.; Smith, R. D. *Anal. Chem.* **1993,** *65*, 425-438.

[49] Vaisar, T.; Urban, J. *J. Mass Spectrom.* **1996,** *31*, 1185-1187.

Chapter 4

DIRECT ELUCIDATION OF DISULFIDE BOND PARTNERS USING ULTRAVIOLET PHOTODISSOCIATION MASS SPECTROMETRY

4.1 Introduction

Disulfide bonds in proteins are formed between highly reactive thiol groups, and help to define both the tertiary and quaternary structure of proteins.[1] Identifying the correct disulfide bond pairs formed between cysteine residues can therefore be critical for understanding the structure of a protein or protein complex.[2] Unfortunately, identifying correct disulfide bond linkages is frequently a complicated task due to the complex chemical environment that proteins present. Chemical transformations and/or deconvolution of highly complex sequence information are typically employed to yield information about disulfide connectivity.[3-13] The presence of post-translational modifications (PTMs) or sequence mutations arising from single nucleotide polymorphisms or other sources can significantly complicate such analyses. Herein, we describe a simple, selective and extremely efficient way of both identifying and characterizing disulfide bond pairs within proteins which is insensitive to post-translational modifications, sequence variations, or other sources of unexpected pairings.

Direct ultraviolet photodissociation (UVPD) of disulfide bonds at 248 nm and 193 nm has been demonstrated previously in the gas phase for very small molecules.[14] Dissociation occurs in the excited state, enabling prompt, homolytic cleavage of the S-S bond. This photochemistry has never been implemented with larger molecules such as peptides or proteins, although linear (i.e. non-disulfide bound) peptides have been subjected to UVPD. At 266nm, absorption in peptides typically occurs at tyrosine and tryptophan and is followed by internal conversion of the excited state energy into vibrational excitation.[15] Therefore, there are no significant direct dissociation channels which compete with disulfide bond cleavage in peptides at 266nm. (Note: the same is not true in the vacuum ultraviolet, as observed previously.[8]).

4.2 Materials and Methods

4.2.1 Materials

Peptides VCYDKSFPISHVR, EAGDDIVPCSMSYTWTGK, CGYGPKKKRKVGG, and CQDSETRTFY were purchased from American Peptide Company (Sunnyvale, CA), Ac-CTTSsFKK-NH_2 was purchased from Quality Controlled Biochemicals (Hopkinton, MA), and Ac-RRWWCR-NH_2 was purchased from AnaSpec (San Jose, CA). All reagents were used as received unless specified. Dimethyl sulfoxide (for molecular biology, >99.9%), Tris

(hydroxymethyl)-aminomethane, Alpha lactalbumin (bovine) and Guanidine hydrochloride were purchased from Sigma Aldrich (St. Louis, MO). Acetonitrile was purchased from Fisher Scientific (Waltham, MA). LysC was purchased from Wako Chemicals USA, Inc. (Richmond, VA). Water was purified to 18.2-MΩ resistivity using a Millipore Direct-Q (Millipore, Billerica, MA).

4.2.2 Formation of Disulfide Bound Peptides:

50 μL of 1mM peptide solutions were added to 25 μL DMSO and mixed thoroughly. This mixture was placed in a water-bath at 37° C for 12 hours. The resulting solution was then lyophilized to remove any excess DMSO and redissolved in 50 μL Q-H_2O. 10 μL of this solution was diluted to 1 mL with 50:50:1 (by volume) Methanol: H_2O: Acetic Acid.

4.2.3 Digestion of Alpha-lactalbumin (ALA from bovine):

100 μL of 250 μM ALA stock solution was taken in an Eppendorf tube. 20 μL of Acetonitrile, 5 μL of 1M Tris.HCl buffer (pH = 6.8), 20 μL of 5M Guanidine HCl, 5 μL of LysC stock (enzyme) and 50 μL of Q-H_2O were all added to make the total volume 200 μL. This solution was placed in a water bath at 37° C overnight. Performing digestion under slightly acidic condition was found to be critical to avoid any disulfide bond scrambling.

4.2.4 Liquid Chromatography (LC):

Protein digests were separated on an Agilent 1100 HPLC system using a BetaBasic-18 column (particle size of 5 μm, pore size of 150Å, length of 150 mm and inside diameter of 2.1 mm) purchased from Thermo Fisher Scientific (Waltham, MA). Peptides were separated using 0.1% Trifluoroacetic Acid in water (v/v, solvent A) and 0.1% Trifluoroacetic Acid in acetonitrile (v/v, solvent B) with the total flow rate of 0.2 mL/ min. The following gradient was used: 5% to 25% B over 15 minutes, 25% to 50% B over the next 45 minutes followed by a column wash.

4.2.5 Photodissociation Mass Spectrometry:

Samples were directly infused into a standard electrospray source of an LTQ linear ion trap mass spectrometer (Thermo-Fisher, Waltham, MA) or coupled via the LC column outlet in the case of Alpha lactalbumin. A quartz window was installed on the back plate of the LTQ vacuum housing to transmit fourth-harmonic (266 nm) laser pulses from a flash lamp-pumped Nd:YAG "MiniLite" laser (Continuum, Santa Clara, CA) directly into the linear ion trap. Pulses were synchronized to the activation step of a typical MS*n* experiment by feeding a TTL trigger signal from the mass spectrometer to the laser via a digital delay generator (Berkeley Nucleonics, San Rafael, CA).

4.3 Results and Discussion

The effect of 266 nm light on the +6 charge state of a disulfide linked peptide pair (CGYGPKKKRKVGG and VCYDKSFPISHVR) is shown in Figure 4.1a. Selective photodissociation of the disulfide bond, as shown in Scheme 4.1, yields only two abundant product ions which correspond to the two constituent peptides, each observed in the +3 charge state. Inspection of the remainder of the spectrum reveals virtually no other products. Residual excitation energy leads to small secondary fragments (see inset spectrum) which correspond to losses of NH_3 and CH_2S from CGYGPKKKRKVGG. Results similar to those shown in Figure 4.1a are not unusual and have been obtained for a variety of peptide pairs. In almost all cases, UVPD does not produce any other peaks apart from minor secondary losses of NH_3, H_2O, CO_2, and CH_2S (i.e. <6% relative intensity compared to peptide fragment peaks). In contrast, collision induced dissociation (CID) is not expected to and does not yield selective dissociation of disulfide bonds. In Figure 4.1b the CID spectrum for the same peptide pair from Figure 4.1a is shown. No comparable cleavage of the disulfide bond is observed as highlighted in the inset spectra.

Scheme 4.1 Selective homolytic cleavage of disulfide bond with 266 nm light in cysteine containing disulfide linked peptides

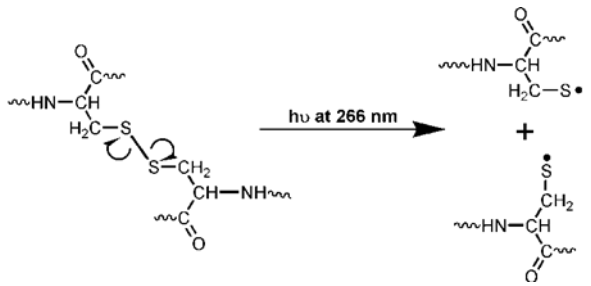

It should also be noted that the specificity demonstrated herein is substantially different from that discussed previously in relation to electron capture dissociation or previous photodissociation experiments.[8,16] In previous work, selectivity referred to an enhancement of disulfide bond cleavage among numerous other fragmentations, many of which yielded products that were comparable or larger in intensity to those produced by the desired disulfide bond dissociation. Selective dissociation in the present manuscript refers to the almost exclusive cleavage of a single bond, generating primarily two fragments. Importantly, this selectivity is not lost even when highly labile groups are present. Shown in Figure 4.1c is the UVPD spectrum for disulfide linked Ac-CTTSsFKK-NH_2 (small cap s indicates phosphorylated serine) and CGYGPKKKRKVGG in the +5 charge state. UVPD yields selective fragmentation of the disulfide, which is exclusively cleaved without the loss of phosphate

group. The uniquely selective fragmentation illustrated in Figure 4.1 reveals two critical aspects about precursor ions immediately: (1) dissociation into two primary products indicates the presence of a disulfide bond and (2) the product ion masses correspond to the masses of peptides which were connected by a disulfide bond. This should allow for easy identification and characterization of disulfide bound peptides in complex mixtures, which will be discussed now.

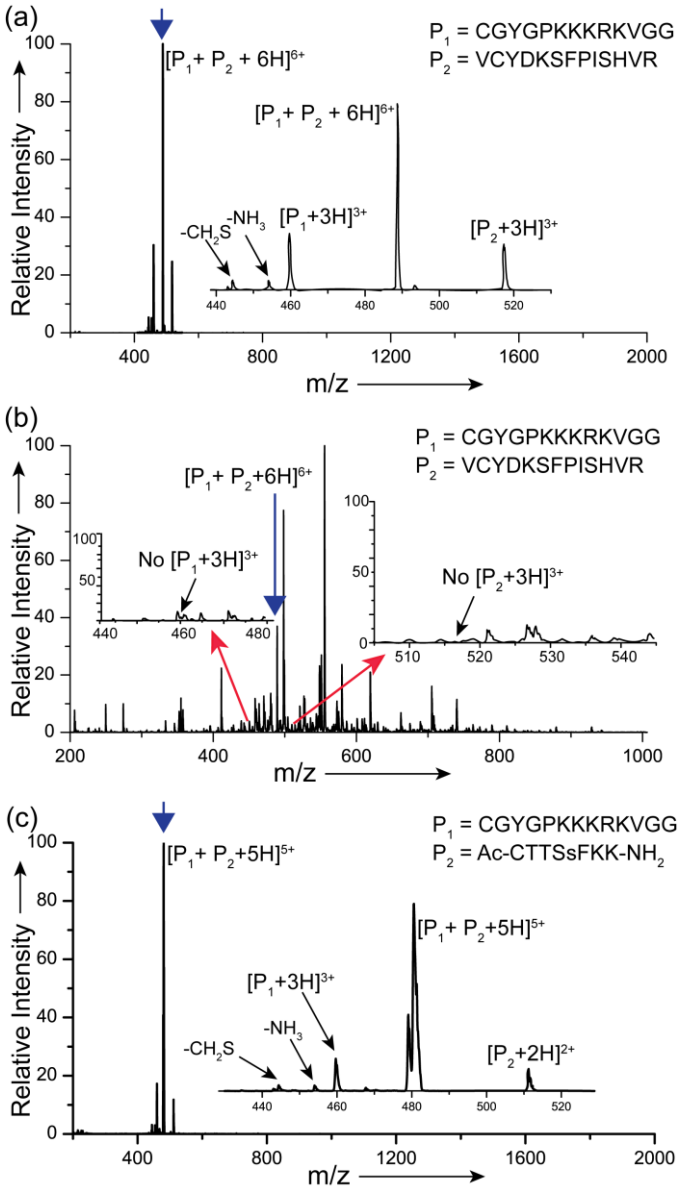

Figure 4.1 a) UVPD symmetrically cleaves a disulfide bound peptide pair. b) CID spectrum of the same peptide pair, absence of disulfide bond dissociation is highlighted in insets. c) UVPD spectrum of a disulfide bound peptide pair with a phosphorylated serine residue (represented by small s). Bold downward arrows indicate precursor ions.

UVPD is compatible with liquid chromatography (LC) and can be used in an online fashion to investigate complex mixtures such as whole protein digests. To

demonstrate this, bovine alpha lactalbumin (ALA) was digested with LysC. ALA is a 14.9 kDa protein with 123 amino acids including eight cysteine residues which form four disulfide bonds. Full mass, ultrazoom, UVPD, and CID spectra were acquired for each eluting peak following separation by LC. Disulfide containing ions were identified by the characteristic dissociation of the precursor into two peaks in the PD step, and characterized with UVPD and CID data. The results are summarized in Figure 4.2a, where the relative abundance and sequences for each identified peptide pair are shown. The abundance is qualitatively approximated by ion count. The three largest bars (blue) correspond to the expected disulfide bond partners. Only three groups are observed because two peptides are linked to the same partner (2^{nd} largest bar in the figure). The UVPD spectrum for this peptide trimer is shown in Figure 4.2b. Selective dissociation of both disulfides individually (yielding the P_1+P_2 and P_2+P_3 peaks) and simultaneously (yielding P_2 alone) is observed. The peptide which serves to bridge the other two peptides can be immediately identified (P_2, revealed by absence of P_1+P_3); however the overall connectivity cannot be established without further experiments.

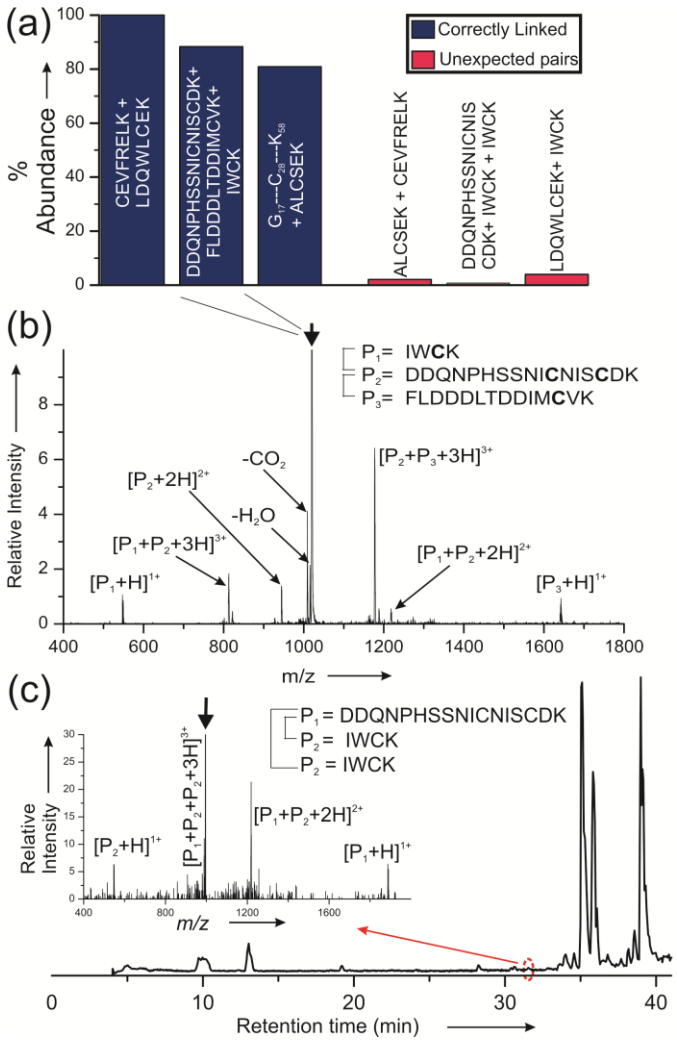

Figure 4.2 a) Cumulative results from LCMS-UVPD on ALA. Abundance is approximated by ion count. b) UVPD spectrum for the indicated peptide trimer from a). c) UVPD spectrum of the least abundant LC peak. Bold downward arrows indicate precursor ions.

Interestingly, small amounts of non-native disulfide pairs were also detected, as shown on the right side of Figure 4.2a (red bars). Selective UVPD is evident even for these low intensity ions as illustrated in Figure 4.2c where the

LC chromatogram is shown along with the UVPD spectrum (inset) for one of the minor peaks corresponding to a mismatched double disulfide bound trimer. There are several potential sources for non-native disulfide bonds including: misfolding of the protein, aggregation of multiple proteins, and scrambling during or following protein digestion. A control experiment was conducted to evaluate the level of scrambling which might occur under our protein digestion conditions. Pairs of model peptides were disulfide bonded separately, and then combined and digested together using the exact same procedure implemented with ALA at similar concentrations. After digesting the two model dipeptides, LC-UVPD-MS revealed a small amount of one mismatched pair. The ion intensity relative to correctly matched pairs was ~0.067%. This illustrates both that our digestion conditions do not lead to a significant amount of disulfide scrambling, and that the method is capable of detecting very minor components within mixtures. The relative intensities of the non-native pairings for ALA in Figure 4.2a are ten times higher than those expected from scrambling, which suggests that something else is the cause of the unexpected pairings. The mismatch highlighted in Figure 4.2c most likely results from protein aggregation as there are no sequence repeats in ALA and yet peptides with identical sequences (IWCK) are connected together. It is well known that ALA aggregates

over time.[17] The other two peptide pairs could in theory be the result of misfolding or aggregation.

One potential complication for this type of experiment could occur when tryptophan or tyrosine is present. For disulfide bound peptides, this could lead to observation of additional peaks that result from vibrational excitation following internal conversion. In theory, such spectra might be difficult to distinguish from single peptides containing tyrosine or tryptophan which would also yield product ions similar to those observed by CID. In practice, this is rarely the case. For example, tyrosine is present in the peptides in both Figures 4.1a and 4.1c, yet dissociation is observed to be highly selective. Tyrosine or tryptophan residues are also present in several of the peptides examined in Figure 4.2, but selective dissociation is dominant for these peptides as well.

The UVPD spectrum for a +4 peptide pair containing collectively 3 Trp and 1 Tyr residues is shown in Figure 4.3a. Nonselective fragmentation is evident as numerous peaks are present in addition to those corresponding to disulfide dissociation. The origin of the additional peaks in Figure 4.3a can be ascribed to two sources. Some of the peaks correspond to fragments observed in CID (Figure 4.3b for comparison) and likely result from vibrational excitation of the precursor ion. The remaining peaks likely originate from secondary dissociation of the

radical peptides generated by disulfide bond dissociation. This was confirmed by repeating the experiment with reduced laser intensity, which led to significant reduction in the number and intensity of peaks between 200 and 600 m/z. It should be noted that comparison of Figures 4.3a and 4.3b immediately reveals obvious differences, suggesting direct dissociation as the origin for some of the products. Comparison of CID and UVPD spectra dominated by internal conversion are significantly more similar.[18] This suggests that in an online experiment any spectra significantly different by UVPD and CID should be examined more closely. For the data in Figure 4.3, the largest dissimilar peaks correspond to the peptide radicals generated by disulfide bond dissociation. In fact, the extent of disulfide bond dissociation in Figure 4.3a is quite large, accounting for greater cumulative intensity than the precursor ion. This is likely a consequence of energy transfer from the electronically excited chromophoric side chains to the disulfide bond, followed by disulfide dissociation.[19] Such "dissociative quenching" appears to be quite favorable and may explain why the presence of aromatic chromophores is not typically problematic.

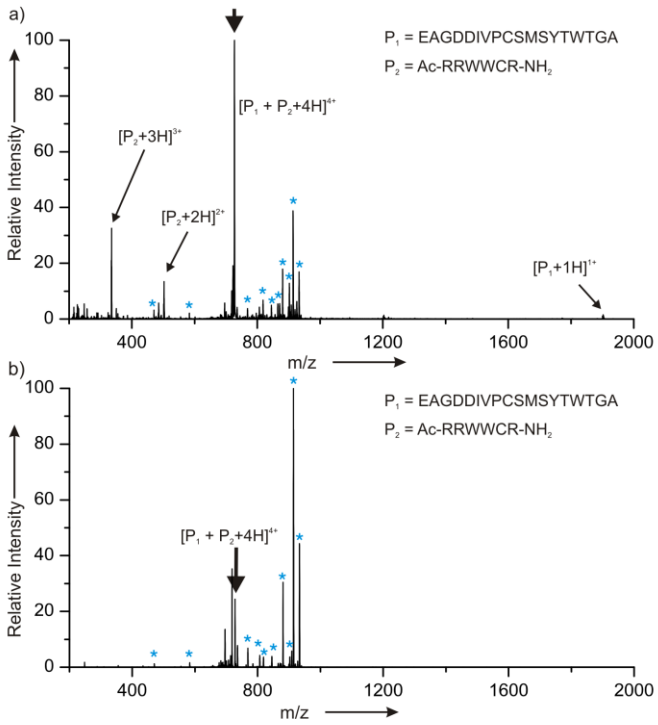

Figure 4.3 a) UVPD spectrum of peptides with multiple chromophores, where selectivity is partially compromised. b) CID spectrum for the same peptide pair reveals significant differences, enabling identification of likely disulfide bond. Bold downward arrows indicate precursor ions. * indicate identical peaks in both spectra.

Table 4.1: Precursor and Product Ions of Disulfide Linked Peptides

Peptide	Theoretical Mass	Observed m/z	Observed Charge State	Retention time (min)
CGYGPKKKRKVGG ●	1375.7	459.67	+3	
VCYDKSFPISHVR ●	1548.8	517.33	+3	
CGYGPKKKRKVGG ‖ VCYDKSFPISHVR	2926.5†	488.67	+6	
AcCTTSsFKKNH$_2$ ●	1020.4	511.25	+2	
CGYGPKKKRKVGG ‖ AcCTTSsFKKNH$_2$	2397.8†	480.58	+5	
CEVFRELK●	1021.5	1023.42	+1	
LDQWLCEK●	1032.5	1034.17	+1	

CEVFRELK | LDQWLCEK	2055.4†	1028.42	+2	34.9
DDQNPHSSNICNISCDK ●●	1886.7	944.17	+2	
FLDDDLTDDIMCVK ●	1640.7	1642.42	+1	
IWCK●	547.3	547.30	+1	
IWCK | DDQNPHSSNICNISCDK | FLDDDLTDDIMCVK	4077.6†	1020.33	+4	39.1
IWCK | ● | DDQNPHSSNICNISCDK	2434.0	813.0 and 1218.25	+3 and +2 respectively	
DDQNPHSSNICNISCDK ● | FLDDDLTDDIMCVK	3527.4	1177.08	+3	
GYGGVSLPEWVCTTFHTSGYDTQAIVQN NDSTEYGLFQINNK (G_{17}---C_{28}---K_{58}) ●	4652.1	1552.08	+3	
ALCSEK●	648.3	650.33	+1	
G_{17}---C_{28}---K_{58} | ALCSEK	5303.8†	1326.7	+4	45.3
ALCSEK | CEVFRELK	1670.9†	836.2	+2	28.3
IWCK IWCK | | | DDQNPHSSNICNISCDK	2983.42†	995.1	+3	31.4
LDQWLCEK | IWCK	1580.91†	791.25	+2	33.8
AcRRWWCRNH_2●	1001.5	334.6, 502.4	+2 and +3	
EAGDDIVPCSMSYTWTGA ●	1900.8	1901.6	+1	
EAGDDIVPCSMSYTWTGA | AcRRWWCRNH_2	2904.3†	727.0	+4	

LC retention time for the disulfide bound peptides of Alpha-lactalbumin is indicated

4.4 Conclusions

In conclusion, UVPD can be utilized to specifically identify and characterize disulfide bound peptide pairs. This method can be implemented in conjunction with LC-MS for the analysis of complex mixtures. The specificity of the dissociation chemistry greatly simplifies ultimate data analysis and allows the facile identification of trace components.

---

[1]Thornton J. M. *J. Mol. Biol.* **1981,** *151*, 261-287.

[2] Wedemeyer W. J.; Welker E.; Narayan M.; Scheraga H. A. *Biochemistry* **2000,** *39*, 4207-4216.

[3]Bean M.; Carr S. *Anal. Biochem.* **1992,** *201*, 216-226.

[4]Tsuji T.; Nakagawa R.; Sugimoto N.; Fukuhara K. *Biochemistry* **1987,** *26*, 3129-3134.

[5]Gorman J.; Wallis T.; Pitt J. *Mass Spec. Review* **2002,** *21*, 183-216.

[6]Wells J.; Stephenson Jr. J.; McLuckey S. A. *Int. J. Mass Spectrom.* **2000,** *203*, A1–A9.

[7]Chrisman P. A.; McLuckey S. A. *J. Proteome Res.* **2002,** *1*, 549-557.

[8]Fung Y. M. E.; Kjeldsen F.; Silivra O. A.; Chan T. W. D.; Zubarev R. A. *Angew. Chem. Int. Ed.* **2005,** *44*, 6399 –6403.

[9]Gunawardena H. P.; O'Hair R. A. J.; McLuckey S. A. *J. Proteome Res.* **2006,** *5*, 2087-2092.

[10] Zhang M. X.; Kaltashov I. A. *Anal. Chem.***2006,** *78*, 4820-4829.

[11] Mihalca R.; van der Burgt Y. E. M.; Heck A. J. R.; Heeren R. M. A.; *J. Mass Spectrom.* **2007,** *42*, 450-458.

[12] Kalli A.; Hakansson K. *Int. J. Mass Spectrom.* **2007,** *263*, 71-81.

[13]Kim H. I.; Beauchamp J.L. *J. Am. Soc. Mass Spectrom.* **2009,** *20*, 157-166.

[14]Bookwalter C. W.; Zoller D. L.; Ross P. L.; Johnston M. V. *J. Am. Soc. Mass Spectrom.* **1995,** *6*, 872-876.

[15]Ly T.; Julian R. R. *Angew. Chem. Int. Ed.* **2009,** *48*, 7130-7137.

[16]Zubarev R. A.; Kruger N. A.; Fridriksson E. K.; Lewis M. A.; Horn D. M.; Carpenter B. K.; McLafferty F. W. *J. Am. Chem. Soc.***1999**, *121*, 2857-2862.

[17] Li J.; Zhang S.; Wang C. C. *J. Biochem.***2001,** *129*, 821-826.

[18]Yeh G. K.; Sun Q.; Meneses C.; Julian R. R. *J. Am. Soc. Mass Spectrom.* **2009,** *20*, 385-393.

[19]Bak M. S.; Kim W.; Cappelli M. A. *Appl. Phys. Lett.* **2011,** *98*, 0115021-011502-3

Chapter 5

DEVELOPMENT OF LC-PD-MS FOR IDENTIFYING REACTIVE METABOLITES AND OXIDATIVE STRESS BIOMARKERS IN PROTEINS

5.1 Introduction

Post translational modifications are important for in biological systems as they have the ability to perturb protein function. PTMs can occur directly after protein synthesis or later on at any point in the lifetime of the protein. There are PTMs which are commonly studied, such as phosphorylation and glycosylation that are known to directly impact protein function.[1] These types of modifications are often controlled by enzymes, such as kinases and phosphatases which control phosphorylation status. There are also protein modifications which are less specific in nature and are often undesirable, such as oxidation[2] or protein halogenation.[3] These are often not directly related to enzymatic activity, and as such may be more challenging to identify.[4]

Two types of approaches can be utilized for identifying modifications. During data analysis and peptide identification the possibility of various modifications can be considered by utilizing a bioinformatics approach.[5] However there are limitations to the number of modifications that can be

considered simultaneously. The alternative approach to this would be to selectively monitor an ion or fragmentation that is related to the modification of interest, such as loss of 98Da for phosphopeptides.[6] In the instances where the unique fragmentation is observed assignment is straightforward. However, it is not guaranteed that the fragment will be generated 100% of the time that the modification is present; i.e. not all phosphorylated peptides will lose 98Da.[7] This is perhaps a more common approach, often utilizing a triple quad. Only predetermined masses will pass through the first quad, collisionally activated in the second quad, and products with predetermined fragment ion or neutral loss of interest are allowed to pass through the third quad for detection.[8] A similar process could be performed with an ion trap; however the ability to quantitate analytes of interest is one of the strengths of the triple quad. In this way an ion of interest can be monitored throughout multiple samples or a neutral loss that is of interest can be used to detect species of interest for further analysis (such as the neutral loss of PTMs that are labile under CID).

Hyphenation of liquid chromatography with MS has allowed for the analysis of increasingly complex samples. Due to the increased complexity of the samples analyzed the amount of data analysis also increases substantially. Therefore it

would be advantageous to simplify data analysis and to focus on the analytes that are of interest. [9]

Photodissociation has the ability to selectively generate an ion of interest by selective fragmentation. Photodissociation has previously been shown to selectively cleave carbon-iodine bonds[10], carbon-sulfur bonds[11], and sulfur-sulfur bonds[12,13]. This fragmentation occurs by accessing direct dissociation pathways and results in the homolytic cleavage of the mentioned bonds. The selectivity of this fragmentation is advantageous due to the fact that little to no other fragmentation is observed. The selectivity of photodissociation can be harnessed to detect PTMs that contain a bond that is susceptible to photodissociation.

The side chain of cysteine is one of the more reactive sites in a protein. Due to the reactivity of this free thiol, it can be modified either by exogenous or endogenous molecules. Quinones and quinone like molecules are frequently present in biological systems and in drug molecules.[14] Previously reported was the use of exogenous quinones to modify and locate cysteine residues.[15] The reaction between the side chain of cysteine and naphthoquinone is shown in Scheme 5.1. As previously demonstrated this chemistry is limited to cysteine residues which are in the free thiol form and solvent accessible. The side chain of cysteine forms a carbon-sulfur bond with the quinone initially forming a

semiquinone which can then return to a quinone or hydroquinone, depending on the solution properties. As previously described, photodissociation can be used to determine the site at which the quinone is attached to a peptide or protein.

Scheme 5.1 Quinone reaction with cysteine side chain

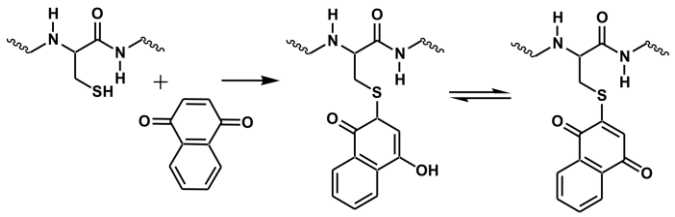

A second type of modification that possesses a bond that could be photolabile is halogenated aromatic residues. Myeloperoxidase is an enzyme present in neutrophils that utilizes H_2O_2 to generate HOCl and HOBr.[16] The hypochlorite and hypobromite are more reactive than hydrogen peroxide and it is through production of these reactive species that neutrophils can destroy invading bacteria.[17] Upon engulfing the foreign organism, MPO is up-regulated, in turn increasing the local concentrations of HOCl and HOBr. Hypochlorite and hypobromite have been shown to be very reactive, and will either oxidize or halogenate proteins in a nonselective manner. The oxidative damage is effective for destroying the invading organism. It has been show through previous studies

that chlorinated tyrosine is an effective biomarker for monitoring the presence of oxidative damage and the extent of bacterial infections.[1819]

Techniques for distinguishing the presence of chlorinate tyrosine include monitoring for immonium ions in MS/MS data[20] of peptides or detection of chlorotyrosine in GC-MS following amino acid hydrolysis.[21] Both of these techniques rely on detection of a species that may or may not be generated. An alternative technique would be to selectively generate fragmentation of the halogenated species.

Described herein is the use of photodissociation to generate fragmentation that is selective to the analyte of interest. Two applications of this methodology are presented. The first application focuses on the selective detection of cysteine bound metabolites. As previously shown quinones are reactive towards free thiols, and in particular, this is of interest in modification of cysteine residues in both peptides and proteins.[22] Reaction of the neucleophilic cysteine side chain and a quinone will generate a carbon- sulfur bond which is susceptible to fragmentation by 266nm photons. It was previously shown how this chemistry could be used to locate cysteine residues within peptides and proteins.[15] Similarly photodissociation has the ability to distinguish and selectively identify quinone modifications. The carbon sulfur bond is homolytically cleaved

regardless of the composition of the molecule and the mass loss due to this cleavage will be distinct for the molecule. This mass loss due to photodissociation is advantageous as this specific neutral loss that can be used to extract data that are of interest. Therefore this same technique could be used to identify cysteine bound metabolites. Quinone functionalities are found in many drug molecules, drug metabolites, and in biologically relevant small molecules. Analysis of three such molecules is demonstrated herein, yet this technique could be easily extended to numerous systems.

The second application described herein is the identification of oxidative stress biomarkers. Iodinated tyrosine has been shown to possess unique photochemistry; excitation with a 266nm photon will result in homolytic fragmentation of the carbon iodine bond through direct dissociation. [10] Thus other halogen could possess similar photodissociation properties. Described herein is the photodissociation of brominated and chlorinated tyrosine. Demonstrated for both of these applications is the simplification of data analysis by use of the selectivity provided by photodissociation.

5.2 Materials and Methods

5.2.1 Materials:

Peptides VCYDKSFPISHVR, EAGDDIVPCSMSYTWTGA, SKGKSKRKKDLRISCNSK, VTCG, SLRRSSCFGGR, RYLPT, and RGYALG were purchased from American Peptide Company (Sunnyvale, CA). RPHERNGFTVLCPKN and Ac-RRWWCR-NH_2 were from AnaSpec (San Jose, CA). Beta lactoglobulin, and Lysozyme were purchased from MP Biomedicals. Cytochrome C (horse heart), Alpha Lactalbumin, Myoglobin, Alpha Casein, Beta Casein, Kappa Casein, Menadione (K3), Acetaminophen, Dopamine, Chloramine T, Sodium hypochlorite solution, Guanidine HCl, and Trifluoroacetic acid (TFA) were purchased from Sigma-Aldrich. Sodium bromide and acetonitrile (ACN) were purchased from Fisher Scientific. LysC was purchased from Wako Chemicals USA, Inc. (Richmond, VA). Water was purified by Millipore Direct-Q (Millipore, Billerica, MA).

5.2.2 Cysteine Modification:

1.5ul of each of the following peptides stocks (1mM) were used to test for modification with quinones: RPHERNGFTVLCPKN, VCYDKSFPISHVR, EAGDDIVPCSMSYTWTGA, SLRRSSCFGGR. SKGKSKRKKDLRISCNSK, Ac-RRWWCR-NH_2, and VTCG (5mM stock). The peptide stock solutions were

mixed with either dopamine, K3, or acetaminophen in a 5:1 (quinone: peptide) ratio in a solution containing 20% acetonitrile and 20mM Ammonium Acetate buffer. These solutions where allowed to sit at room temperature for a few hours prior to LCMS. Addition of acetaminophen alone did not result in peptide modification. Conversion into the reactive metabolite N-acetyl-p-benzoquinonimine (NAPQI) was accomplished by use of a peroxidase.[23] One unit of the peroxidase enzyme was added along with 0.01% H_2O_2 to the peptide mixture.

5.2.3 Bromination Chemistry:

The peptide RGYLG was brominated by the Chloramine T method. 4nmole of peptide was mixed with 400nmole of sodium bromide and 6nmole of Chloramine T. The modified peptide was separated by HPLC after reaction at room temperature for 10min. CytC was brominated by the Chloramine T method; procedure was adapted from the previously used iodination procedure[24] and utilizing 80nmole of CytC, 400nmole of NaBr, and 280nmole of Chloramine T.

The peptide RYLPT was modified by use of hypochlorite to simulate oxidative stress. The peptide RYLPT was mixed with a sodium hypochlorite solution in a 1:2 (peptide: HOCl) ratio. 20mM Ammonium acetate buffer was

used and various reaction time points (from 10 minutes to 17 hours) were tested. The mixed halogenation experiment was carried out in the same fashion but with addition of sodium bromide to give a 1:2:4 ratio (peptide: HOCl: NaBr). Peptide samples were diluted to 10μM for analysis by MS

5.2.4 Protein digest:

Proteins were enzymatically digested by Endoproteinase Lys-C according to the following procedure. Brominated Cytochrome C stock solution was digested in a total volume of 50μl in 10% ACN, 0.5M Guanidine HCl, and 100mM Ammonium bicarbonate buffer, LysC was used in a 1:1000 enzyme to protein ratio. Similar procedure was used for protein mixture, Beta lactoglobulin, Lysozyme, Alpha Lactalbumin, Myoglobin, Alpha Casein, Beta Casein, and Kappa Casein were combined digested with LysC. The protein digest mixture and brominate Cytochrome C were then combined with relatively similar ratios just prior to analysis by PD-LCMS.

5.2.5 Photodissociation of modified peptides:

Solutions were analyzed in cation mode by an LTQ linear ion trap mass spectrometer (Thermo Fisher Scientific, Waltham, MA) with a standard electrospray source. The posterior plate of the LTQ was modified with a quartz window to transmit fourth harmonic (266 nm) laser pulses from a flashlamp-

pumped Nd:YAG laser (Continuum, Santa Clara, CA). Pulses were synchronized to the end of the isolation step of a typical MS^2 experiment by feeding a TTL trigger signal from the mass spectrometer to the laser via a digital delay generator (Berkeley Nucleonics, San Rafael, CA). This allowed photodissociation (PD) to be carried out analogous to collision induced dissociation (CID). Data dependent analysis of LC samples was performed with a four step scan process. This included a full mass scan from which an ion is selected for subsequent ultra zoom, PD and CID scans. Laser pulses were triggered during the MS^2 step. In order to perform both PD and CID as MS^2 within a single run the CID step was performed as a pseudo MS^3 step. An average of 3 scans was collected for PD and CID steps.

5.2.6 LC-MS method and data dependent analysis:

An Agilent 1100 HPLC system was used for LC data with a BetaBasic-18 column (150mm by 2.1mm, 5 μm particles) purchased from Thermo Fisher Scientific (Waltham, MA). Peptides were separated using 0.1% Trifluoroacetic Acid in water (v/v, solvent A) and 0.1% Trifluoroacetic Acid in acetonitrile (v/v, solvent B) at a flow rate of 0.2 mL/ min. Cysteine peptides were separated utilizing the following gradient. 5 to 15%B over the first 10 minutes, 15 to 45%B over the next 45minutes, 45 to 95%B over the final 20minutes, followed by

column re-equilibration. The brominated Cytochrome C digest utilized a slightly longer gradient of: 5 to 15%B over the first 15 minutes, 15 to 40%B over the next 50 minutes, 40 to 95%B over the final 25 minutes, followed by column re-equilibration. The following gradient was used for the protein digest mixture due to increased sample complexity: 5 to 15%B over the first 15 minutes, 15 to 45%B over the next 60 minutes, 45 to 70%B over 25 minutes, and 70 to 95%B during the final 10 minutes, followed by column re-equilibration.

5.3 Results and Discussion

5.3.1 Cysteine Modifications

The three molecules that were used as part of this study are shown in Chart 5.1. Acetaminophen is not initially present as a quinone but during metabolism it is converted into a quinonimine (NAPQI) which possesses similar structure to quinones. Furthermore it has been shown that this reactive metabolite can form adducts with proteins and it is still under debate whether this modification of proteins is responsible for toxicological damage associated with acetaminophen.[25] Dopamine is a biologically relevant small molecule and it is present as a neurotransmitter. Dependent on the oxidative conditions of the solution, dopamine can be converted into dopamine quinone which has been

shown to be reactive with cysteine side chains.[26] The third molecule that was utilized was menadione or also known as vitamin K3. Menadione is a precursor to vitamin K2 and is converted upon modification with a fatty acid.[27] Unlike the other two molecules it is initially present as a quinone. Due to the quinone functionality menadione also could be reactive toward proteins, namely at cysteine residues. These three small molecules were the focus of further experiments detailed here.

Chart 5.1 Quinones examined

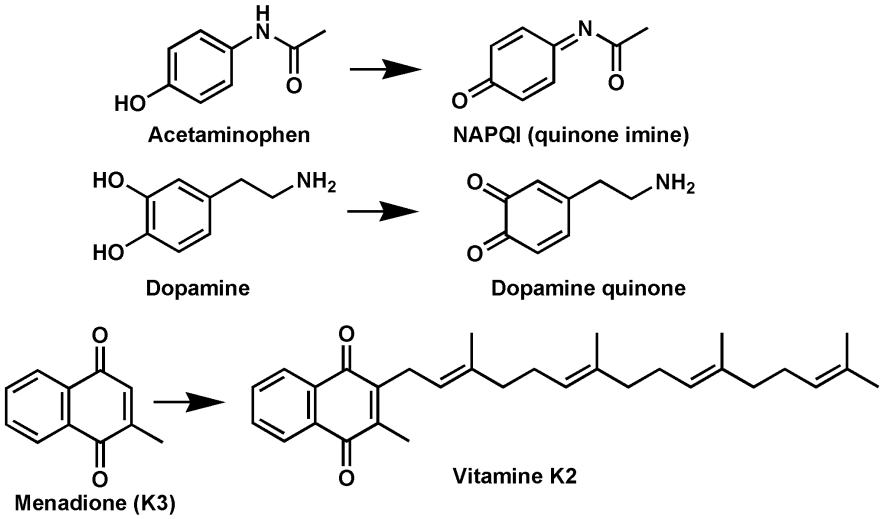

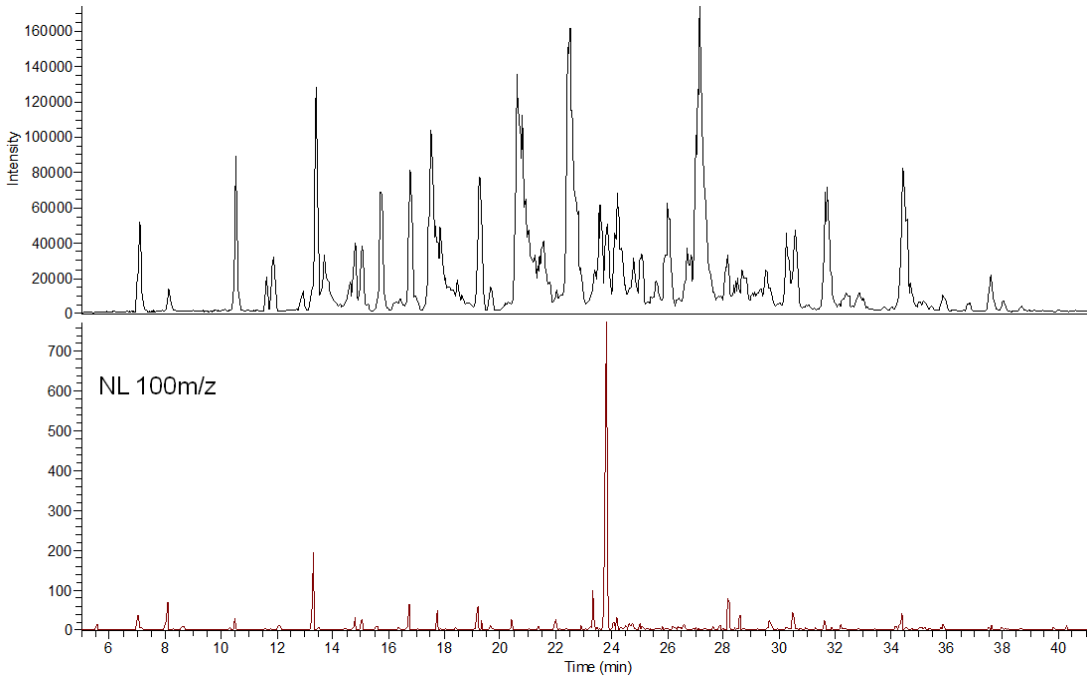

Figure 5.1 LCMS chromatogram of peptide mixture with acetaminophen. TIC is shown in the top panel along with extracted neutral loss (NL) of 100m/z below.

Shown in the top portion of Figure 5.1 is the LC trace resulting from a mixture of peptides was allowed to react with acetaminophen. One photodissociation spectrum from this LCMS data that is of interest is shown in Figure 5.2a. The largest and nearly the only fragment that is observed due to photodissociation is loss of 200Da (+2 charge state). This neutral loss corresponds to cleavage of the C_β-S bond and loss of the thiol quinone. This is consistent with previous results and demonstrates that the direct dissociation pathway is predominant, even with the slightly different structure of the quinonimine. The

unique thing about this quinonimine is that photodissociation mostly produces a non radical species. Observation of this single peak is sufficient to determine that the peptide was modified with the molecule of interest and that it was located at the side chain of cysteine. Furthermore the mass of the peptide can be used to determine peptide identity as VCYDKSFPISHVR. If necessary, CID data can be used to confirm sequence. CID was performed in the subsequent data dependent scan and is shown in Figure 5.2b. CID, in this case, primarily cleaves the modification in the same fashion as was seen in PD, very small amount of backbone fragmentation is observed. CID was also performed on the loss of quinonethiol from the PD scan. This PD-CID data is shown in Figure 5.2c. Several y fragments are observed along the peptide backbone, confirming the peptide sequence. This PD-CID fragmentation matches the low abundance CID in Figure 5.2b, confirming that the peak generated by PD is largely non-radical in composition. There is a w_{12} fragment that would often be indicative of radical fragmentation, but it is present in the CID data (in small abundance). Protein modification by high levels of acetaminophen has previously been reported, however it is still under debate whether these modification lead to the toxicity associated with high levels. Analysis of acetaminophen modification by photodissociation would be facile even in complicated mixtures due to the

selective nature of PD. The selectiveness of the fragmentation by PD can be used to easily determine the species that are of interest. Shown in the bottom panel of Figure 5.1 are the extracted spectra where there is a neutral loss of 100 during MS^2, or loss of quinonimine is present. The large peak at 23.8 minutes corresponds to the spectrum shown in Figure 5.2a. This method for searching for spectra of interest by neutral loss is shown throughout the remaining data.

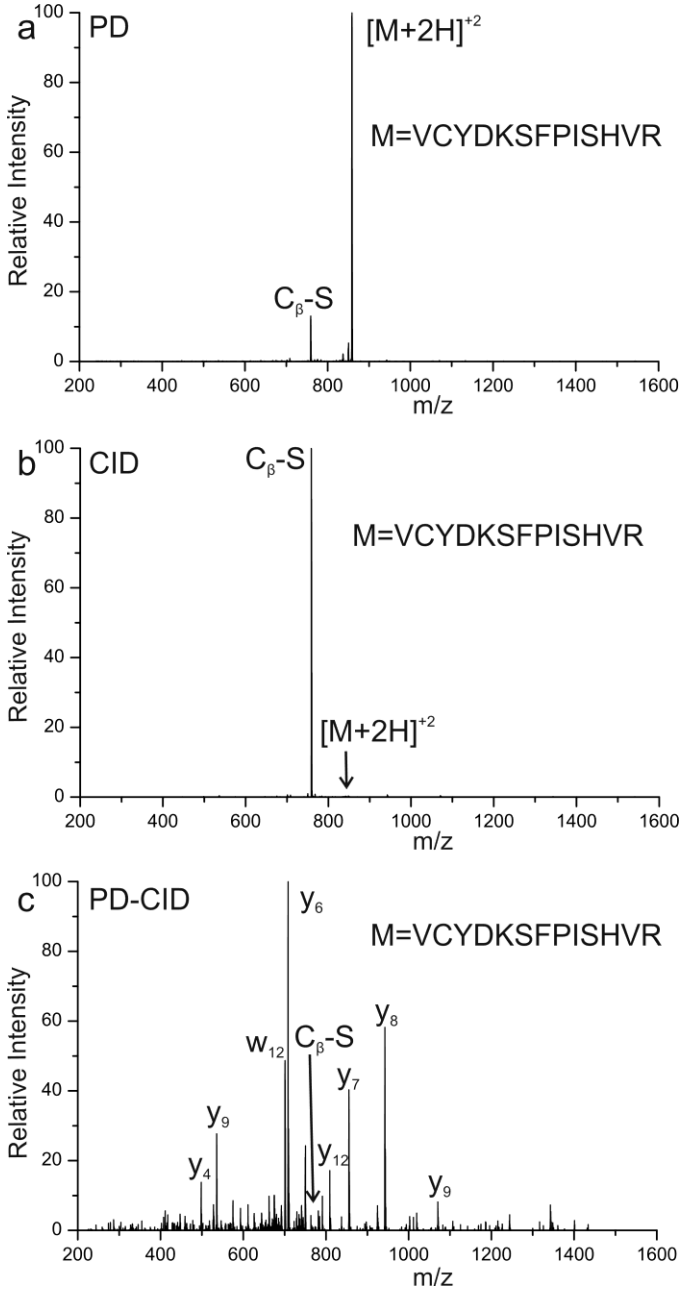

Figure 5.2 a) PD spectrum from Figure 5.1 at 23.8min. Loss of acetaminophen-thiol (200Da loss) is observed. b) CID of the acetaminophen modified peptide. c) PD-CID spectrum of VCYDKSFPISHVR resulting from CID on C_β-S peak from 2a.

Figure 5.3 is the LC-PD-MS data of a peptide mixture after reaction with dopamine. The top panel simply shows the chromatogram of the separation, based on the full MS scan. The lower three panels show the extracted spectra where neutral losses are observed during the PD step. In this case the neutral losses correspond to the loss of dopamine thiol (186Da). Because the neutral losses are on the m/z scale, various peptide charge states need to be accounted for. The first shows loss of 186m/z, which corresponds to the loss of dopamine-thiol from a peptide in a +1 charge state. Neutral loss of 93m/z and 62m/z are also shown for +2 and +3 charge states, respectively. The validity of these identifications can easily be checked by insuring that the charge state of the peptide matches the corresponding loss. Ultra zoom scan is performed just prior to PD for this purpose. An example of one of these PD scans highlighted through the neutral loss search is shown in Figure 5.4. This spectrum is selected from the large peak at 22.1 minutes in the NL93m/z window. The peptide is confirmed to be in the +2 charge state. The loss of dopamine-thiol is a relatively small peak, but it is the largest fragment in the spectrum. This peak alone indicates that the peptide was modified by dopamine at a cysteine residue. The sequence of the peptide can be determined based on this mass alone, and confirmed using CID if necessary.

Scheme 5.2 Photodissociation at cysteine

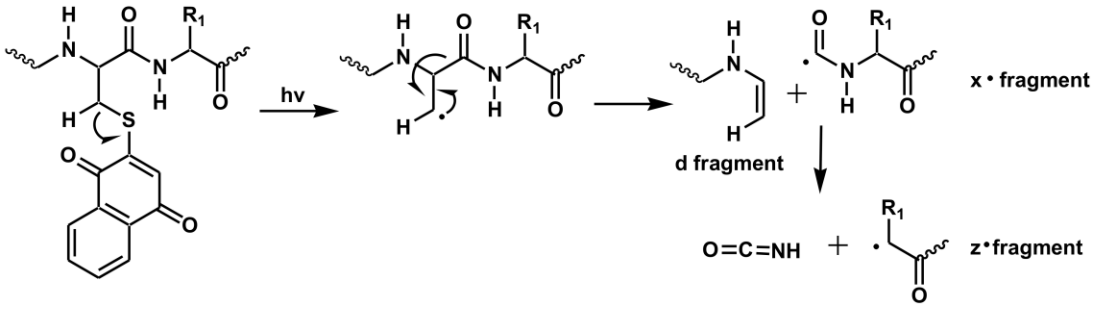

Upon closer inspection of the PD spectrum it can be seen that there is backbone fragmentation of the peptide also occurring, this is shown in the inset. This single backbone fragment (d_{12}) is located at the cysteine residue. The fragmentation observed here is similar to that previously reported for other quinone modifications. The mechanism of fragmentation is shown in Scheme 5.2. Photodissociation of this peptide-dopamine complex leads to homolytic cleavage of the C_β-S bond, producing the loss of dopamine-thiol peak which is observed. The radical produced at the beta position of cysteine can rearrange as shown to fragment the peptide backbone at the cysteine residue, producing the observed d fragment. Although the fragmentation is present in relatively low abundance, neutral loss search easily identifies the spectrum of interest and the identity of the peptide and fragmentation is easily assigned due to the specific nature of photodissociation.

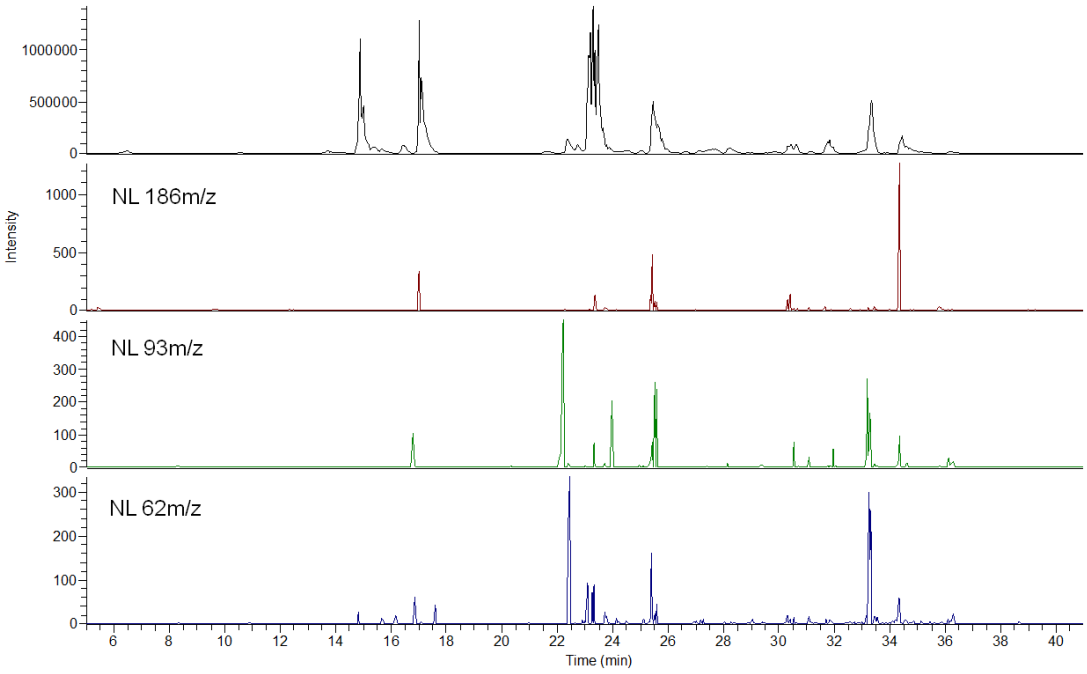

Figure 5.3 LCMS chromatogram of peptide mixture with dopamine. TIC is shown in the top panel. Neutral loss (NL) of 186m/z, 93m/z, and 62m/z from the MS^2 indentify the spectra of interest.

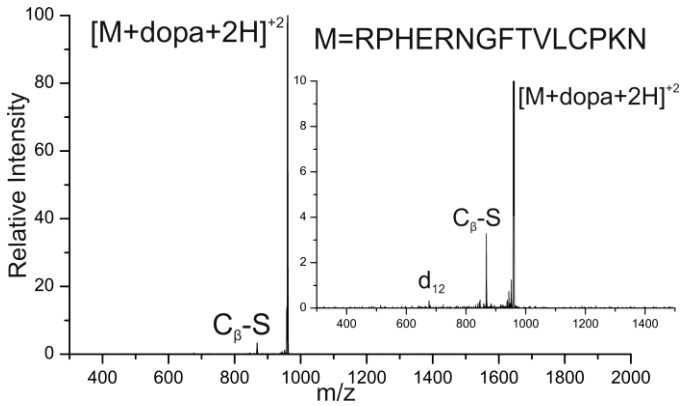

Figure 5.4 PD spectrum from Figure 5.3 at 22.1min. Loss of dopamine-thiol (-186Da) is observed and is labeled C_β-S. Backbone fragmentation is observed as d_{12} identifying the site of modification.

Figure 5.5 demonstrates the same type of experiment with Menadione (K3) as the molecule of interest. The separation of the peptide mixture is shown along with neutral mass loss in the MS^2 step for various charge states. The neutral loss of Menadione along with the sulfur of cysteine is 204Da. Neutral loss in charge states +1 through +3 are shown, 204m/z, 102m/z, and 68m/z respectively. Shown in Figure 5.6 is the PD spectrum at 34.4 min. The neutral loss of the menadione-thiol is labeled and results from homolytic cleavage of the C_β-S bond as shown above. Backbone fragmentation at the cysteine residue is also observed (d_{12}), allowing identification of the modification site

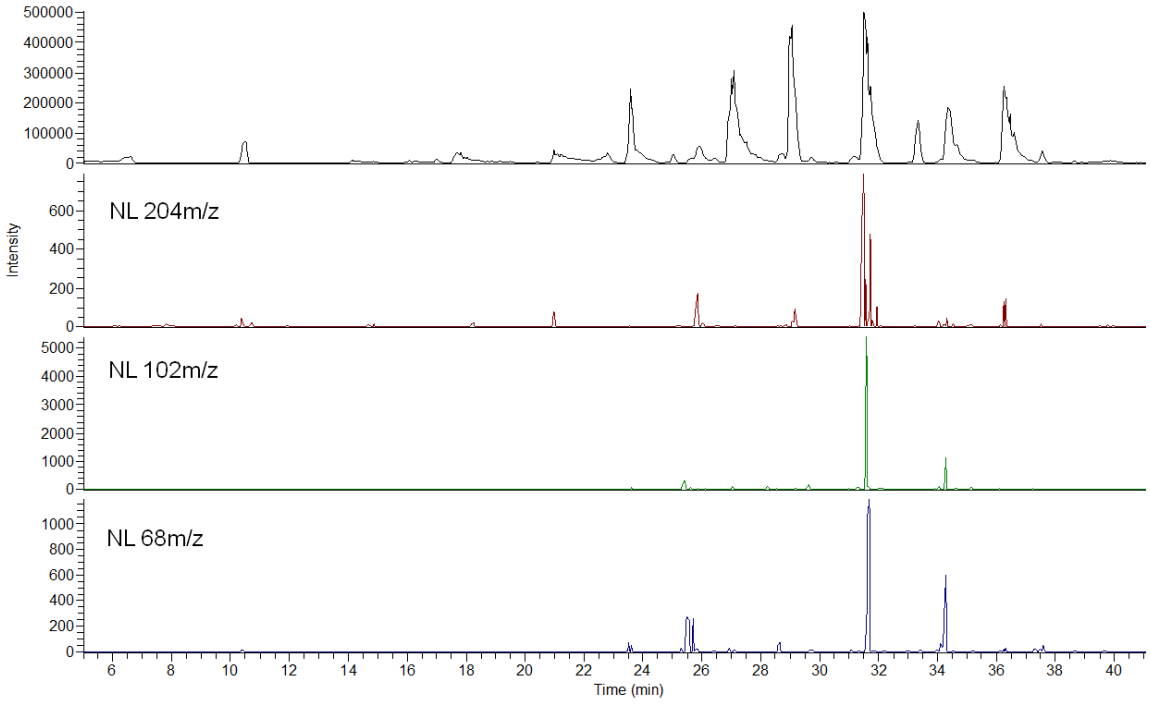

Figure 5.5 LCMS chromatogram of peptide mixture with Menadione (K3). TIC is shown in the top panel. Neutral loss (NL) of 204m/z, 102m/z, and 68m/z from the MS^2 indentify the spectra of interest.

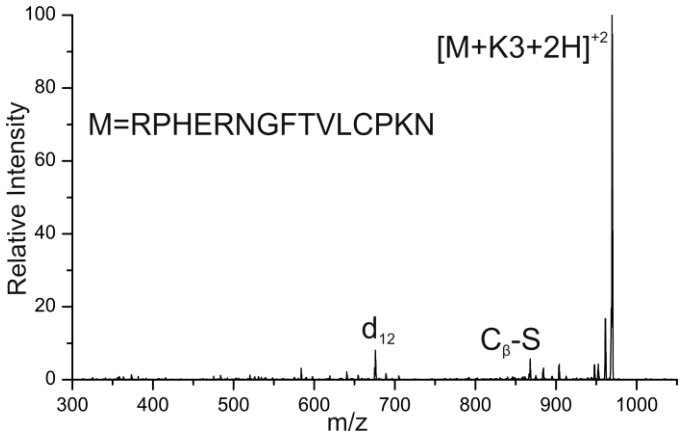

Figure 5.6 PD spectrum from Figure 5.5 at 34.4min. Loss of K3-thiol (-204Da) is observed and is labeled C_β-S. Backbone fragmentation is observed as d_{12} identifying the site of modification.

Table 5.1 summarizes the peptides identified from the dopamine and K3 experiments shown in Figures 5.3 and 5.5. Modified peptides were identified by use of the neutral loss function and values listed in Table 5.1 correspond to the amount of the peptide that was modified relative to the sum of the modified and unmodified peptide. These two experiments were carried out at identical conditions, only varying by the quinone identity. Quantification is based solely on the ion intensity, thus slight variation between peptides within each modification type is likely due to the influence of the modification on ionization. The percent modification of these peptides by dopamine versus K3 is nearly two orders of magnitude different. This can be attributed to the fact that K3 is initially

present in the quinone form while only a small portion of the dopamine exists in the quinone form, and conversion to quinone is dependent on solution conditions. Thus it is not surprising that the amount of modification is greater in the case of K3. Despite the fact that the amount of modified peptide varied greatly between the two experiments, identifying the peptides of interest was simple in both cases because of the specificity offered by photodissociation.

Table 5.1: Relative Abundance of Cysteine Modification

Sequence	% modified by dopamine	% modified by K3
VTCG	4.24%	97.68%
Ac-RRWWCR-NH_2	1.33%	83.0%
SLRRSSCFGGR	0.74%	70.7%
VCYDKSFPISHVR	2.39%	78.6%
RPHERNGFTVLCPKN	1.23%	77.34%
EAGDDIVPCSMSYTWTGA	4.69%	70.95%
SKGKSKRKKDLRISCNSK	1.36%	67.57%

5.3.2 PD of Brominated peptides

Chloramine T has been shown to be a gentle and effective method for Iodination of peptide and proteins, thus this same chemistry was extended to brominate a model peptide for initial experiments. RGYALG was modified at the tyrosine residue with a single and two bromine atoms. The peptide was purified by HPLC and MS experiments were performed on the individual peptides. The

photodissociation spectra of the single and double brominated species are shown in Figure 5.7a and b respectively. Loss of bromine is observed in both cases and results from homolytic cleavage of the carbon-bromine bond. Only a single bromine loss is observed in each spectrum and it is this fragment that serves as an indicator that the peptide contains bromine. Whether the peptide contains a single or two bromines at the tyrosine can be determined by the amount of bromine loss. The relative intensity of the –Br peak is obviously smaller for the double brominated species and this is a trend that is consistent for the experiments detailed within. The intensity of this bromine loss was quantified for approximately 20 peptides; the single Br peptides upon PD give a –Br peak of 36.0 $\pm$7.5% relative to the precursor while peptides containing two bromines yield 15.1 $\pm$6.0% bromine loss. This distinction allows the number of bromines to be determined without any prior sequence knowledge.

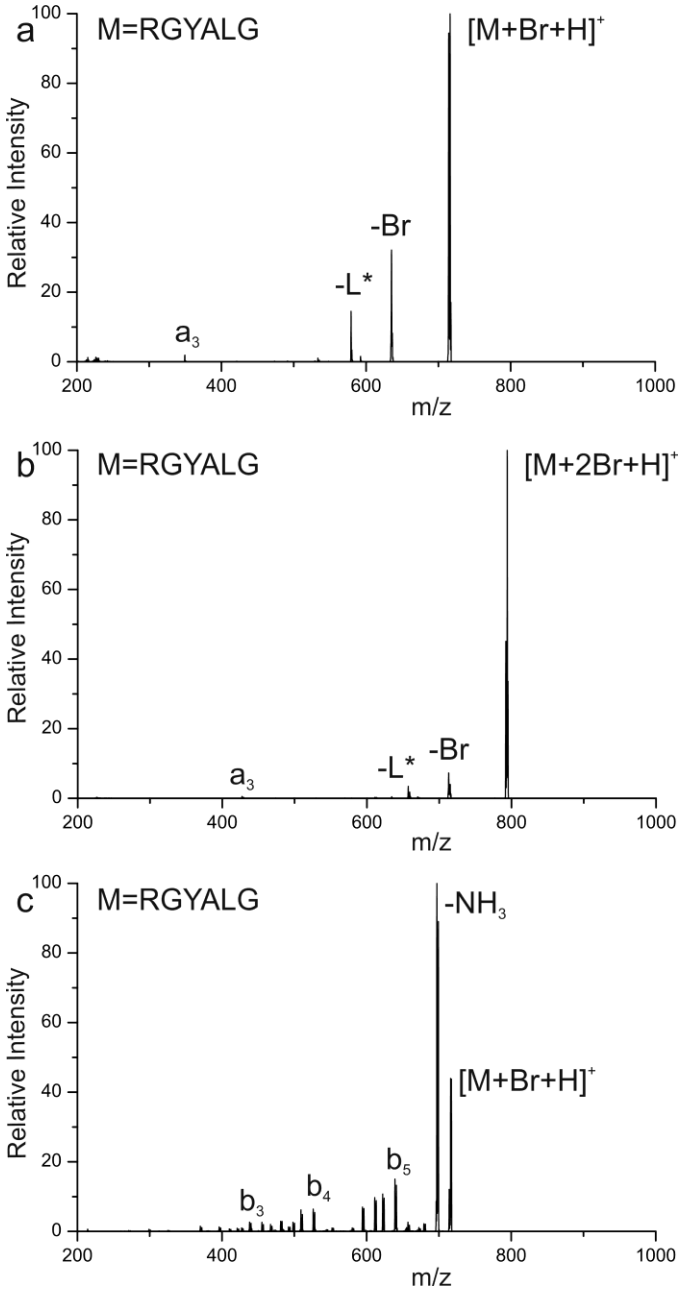

Figure 5.7 a) PD spectrum of singly brominated RGYALG. Loss of bromine is observed along with other radical driven fragmentation b) PD of the doubly brominated RGYALG peptide. c) CID spectrum of singly brominated RGYALG, no Br loss is seen.

Cleavage of the carbon- bromine bond generates a radical on the peptide that can lead to further fragmentation of the peptide. In this case the peptide is small and there is enough remaining energy from the photodissociation process to observe further fragmentation, this has also been observed previously with iodinated species. This radical fragmentation is the cause of the other two peaks in the spectra. Leucine side chain is observed to be lost (-L*) and backbone fragmentation at tyrosine (a_3) is seen. Both are fragments that would be expected based on the predictability of radical directed dissociation (RDD)[28]. These fragments are smaller Figure 5.7b due to lower abundance of radical generated by the photodissociation process. Figure 5.7c is CID of the brominated RGYALG peptide. Loss of bromine does not occur by collisional activation, demonstrating the selectivity of the photodissociation. Photodissociation of this model peptide yielded favorable results, thus experiments were extended to a model protein.

Cytochrome C was successfully brominated by the Chloramine T method. The full MS spectrum of the modified protein is shown in Figure 5.8. A distribution is observed with varying amounts of bromination, from zero to at least 7 bromines. In order to determine the sites of modification, PD-LCMS was utilized. A portion of the same brominated protein was digested by LysC and analyzed by LCMS. The resulting chromatogram is shown in Figure 5.9 along

with the results from searching for neutral loss of bromine during the PD step. The neutral loss search highlighted the points in the chromatogram where loss of bromine occurs in the +1, +2, and +3 charge states by searching for neutral loss 81m/z, 40.5m/z, and 27m/z respectively. This allows simplification of data analysis as only the indicated spectra needed to be analyzed.

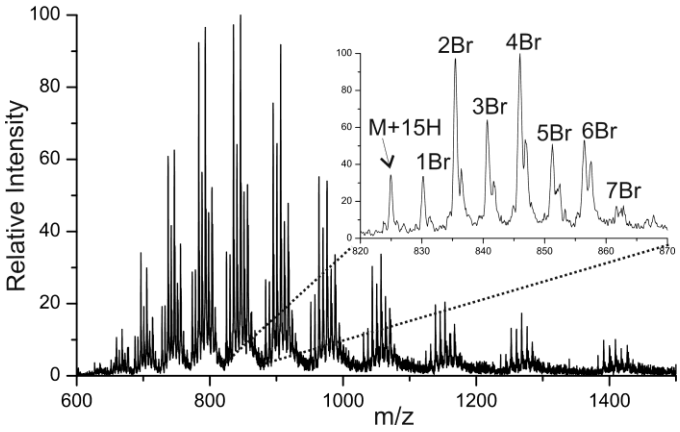

Figure 5.8 Full MS of brominated Cytochrome C. Inset shows distribution of bromine modifications.

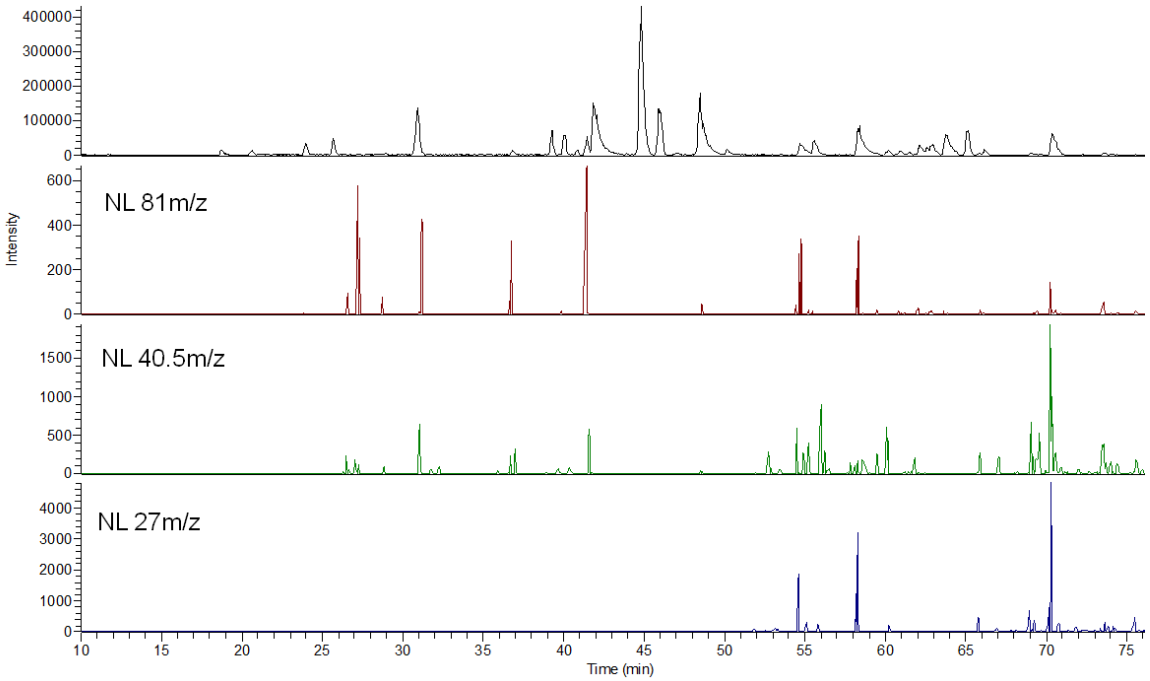

Figure 5.9 LCMS chromatogram of LysC digest of brominated Cytochrome C. TIC is shown in the top panel. Neutral loss (NL) of 81m/z, 40.5m/z, and 27m/z indentify peptides with Br loss by PD.

Examples of the spectra identified in this way are shown in Figure 5.10. These spectra correlate to the points at 27 and 31 minutes. Upon observation of these two spectra it is easy to determine that the peptide in Figure 5.10a contains a single bromine and Figure 5.10b contains two bromines, due to the relative yields of bromine loss. Once the number of bromines is determined, the mass of the peptide can then be used for sequence assignment. The sequences for both spectra were determined to be KYIPGTK, with the single brominated peptide eluting first. Utilizing the neutral loss search method all brominated peptides were identified, analyzed, and summarized in Table 5.2.

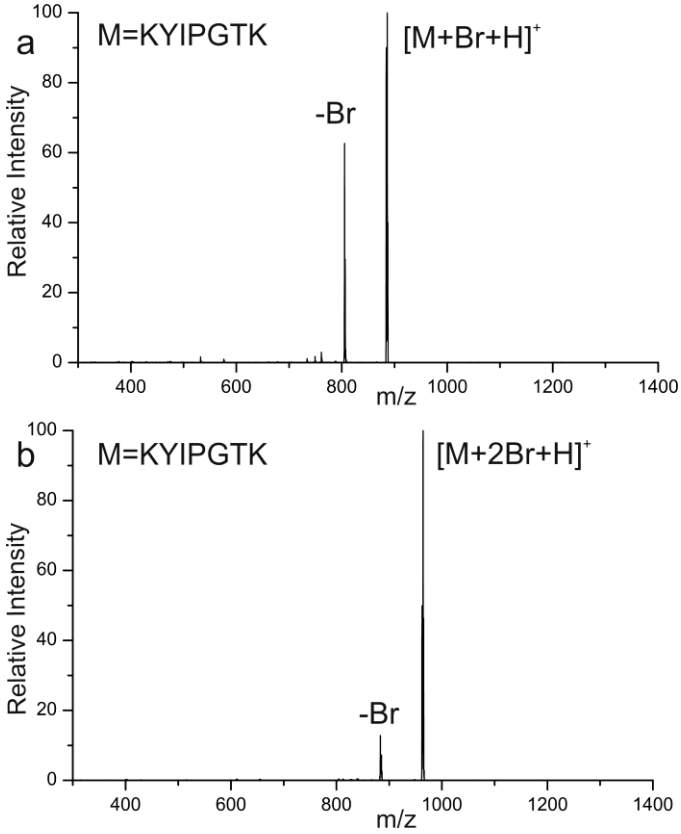

Figure 5.10 a) PD spectrum at 27min from LCMS shown in Figure 5.6. Large bromine loss distinguishes singly brominated peptide. b) PD spectrum at 31minutes. Abundance of –Br peak indicates double bromine peptide. Peptide sequence determined to be KYIPGTK for each.

The abundance of bromination was calculated for all observed peptides. Percent modification is based on ion intensities with the assumption that bromination does not change the ionization of the peptide significantly. From the information contained in Table 5.2 it can be determined that tyrosine 75 was brominated to a greater extent than the other tyrosine residues, and tyrosine 68 was the least modified. There is a peptide observed due to missed cleavage during enzymatic digest containing both tyrosines 68 and 75, which does

influence the ability to distinguish between total amounts of bromination at each tyrosine residue.

Table 5.2: Extent of Tyrosine Bromination in Cytochrome C

#Br	Y	Sequence	%
1	49	TGQAPGFTYTDANK	8.9%
2	49	TGQAPGFTYTDANK	37.3%
1	68	GITWKEETLMEYLENPK	6.6%
1	75	YIPGTK	10.1%
2	75	YIPGTK	78.6%
1	75	KYIPGTK	14.7%
2	75	KYIPGTK	58.3%
1	98	KKTEREDLIAYLK	14.6%
2	98	KTEREDLIAYLKK	45.7%
1	98	KTEREDLIAYLK	13.2%
2	98	KTEREDLIAYLK	47.7%
1	68,75	GITWKEETLMEYLENPKKYIPGTK	33.7%
2	68,75	GITWKEETLMEYLENPKKYIPGTK	22.7%

The ability of this technique to easily distinguish peptides of interest from a complex mixture is advantageous. To demonstrate this, the brominated Cytochrome C digest that is described above was mixed with a Lys C digest of six additional proteins. This digest was also analyzed by PD-LCMS and is shown in Figure 5.11 along with the neutral loss analysis for loss of bromine in the +1, +2, and +3 charge states. Comparison of this data to the neutral loss analysis in Figures 5.9 demonstrates the similarity of the two experiments in terms the level

of data analysis that is needed. By using photodissociation the data analysis is not increased even though the complexity of the sample increased greatly.

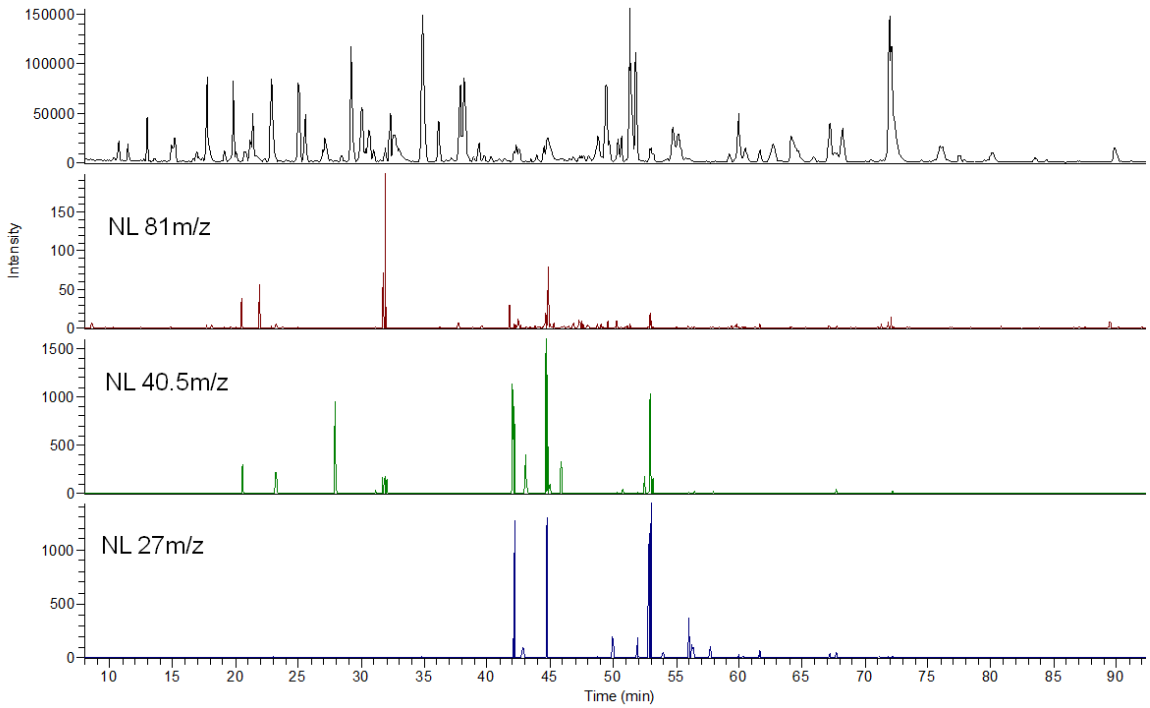

Figure 5.11 LCMS chromatogram of LysC digest mixture of 7 proteins including brominated Cytochrome C. TIC is shown in the top panel. Neutral loss (NL) of 81m/z, 40.5m/z, and 27m/z indentify peptides with Br loss by PD.

The ability of photodissociation to selectively detect chlorinate peptides was also investigated. In order to replicate the type of modifications that would occur due to Myeloperoxidase activity, HOCl was used. The peptide RYLPT was chlorinated and photodissociation produced the spectrum shown in Figure 5.12a. The only peak observed in the spectrum is loss of chlorine from the peptide. Thus homolytic cleavage of the carbon- chlorine bond in tyrosine is also possible

by 266nm photons. Observation of this selective fragmentation makes this another good candidate for analysis by photodissociation. The unique thing about Myeloperoxidase is the ability of this enzyme to produce both HOCl and HOBr. Therefore there is the possibility of creating tyrosine residues or peptides with mixed halogen species.[29] Photodissociation of one such peptide is shown in Figure 5.12b. The peptide RYLPT is modified by a single bromine and a single chlorine atom. Photodissociation of this peptide produces loss of bromine, loss of chlorine, and loss of both halogens. Loss of bromine is the predominant fragment, which holds well with previous observations where yield of homolytic cleavage of Br is higher than that of Cl. Loss of chlorine is present, and also seems to be enhanced by the presence of the bromine. (This observation is based on lower abundance of –Cl in peptides not shown). Backbone fragmentation (c_4) is observed due to the radical peptide generated by loss of bromine, and the c_4 is seen to retain the Cl. The presence of both Br and Cl loss by photodissociation would allow this peptide to be easily identified in a complicated mixture, whereas due to the uniqueness of this peptide modification, identification by standard fragmentation techniques would be difficult.

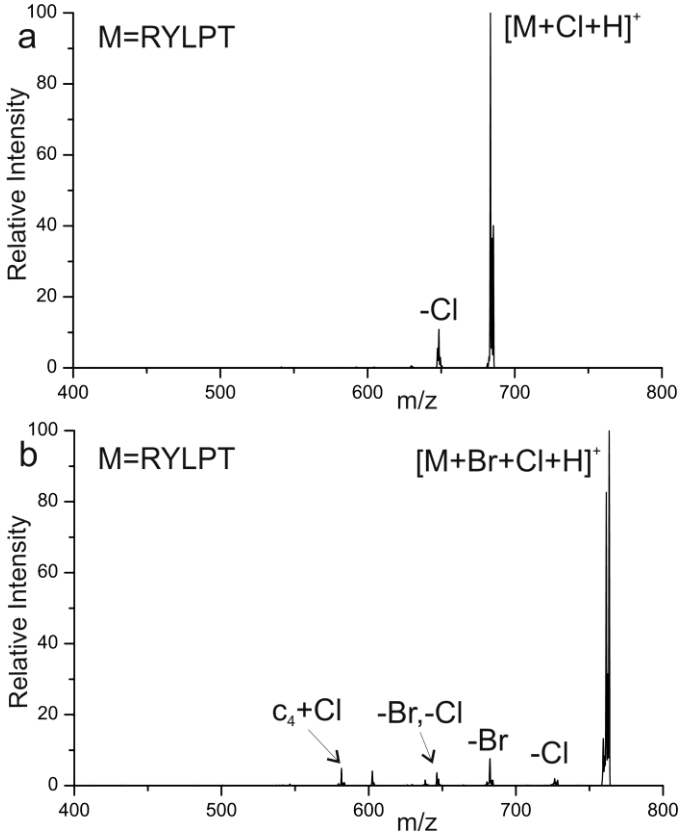

Figure 5.12 a) PD spectrum of singly chlorinated RYLPT. Loss of chlorine is observed due to homolytic cleavage. b) PD of the RYLPT peptide containing both a single bromine and a single chlorine.

5.4 Conclusions

Photodissociation mass spectrometry has previously been shown to be a useful analytical technique for determining protein modifications. Single shot photodissociation in a linear ion trap takes place on the nanosecond time scale making it applicable to automated analysis on a chromatographic time scale. Described herein is the development and application of photodissociation for LC-MS separations. Photo-excitation of proteins or peptide with 266nm laser

light normally does not yield fragmentation. Incorporation of a C-I or C-S bond proximal to a chromophore allows access to direct dissociation pathways resulting in homolytic cleavage of these bonds. Radicals generated through this process can cause further dissociation of the peptide backbone. Two specific applications of this technique are presented herein for identifying reactive metabolites bound to cysteine residues and biomarkers of oxidative stress. Metabolites containing quinones are shown to be reactive with cysteine side chains creating a C-S bond that can be cleaved by photodissociation. Radical directed dissociation (RDD) is useful for identifying the location of the modification sites. Searching PD data for selective mass losses generated by homolytic cleavage allows simplification of data analysis by quickly identifying the peptides of interest in a mixture. Proteins exposed to conditions simulating oxidative stress results in halogenation (I, Br or Cl) of tyrosine residues. Peptides containing these biomarkers of oxidative stress can be easily identified by searching LC-PD-MS data for mass loss of the halogen (due to homolytic cleavage of the carbon-halogen bond). The selective nature of the fragmentation is shown to provide facile identification of PTM sites by greatly simplifying data analysis.

[1] Seo, J.; Lee, K.; *Journal of Biochem and Molec Bio*, **2004**, 37, 35-44.

[2] Shacter, E. *Drug Metabolism Reviews*, **2000**, 32, 307-326.

[3] Heinecke, J. W. *The Journal of Clinical Investigation*, **2000**, 105, 1331-1332.

[4] McDonagh, B.; Sheehan, D. *Proteomics*. **2007**, 7, 3395-3403.

[5] Zamdborg, L.; LeDuc, R. D.; Glowacz, K. J.; Kim, Y.; Viswanathan, V.; Spaulding, I. T.; Early, B. P.; Bluhm, E. J.; Babai, S.; Kelleher, N. L. *Nucleic Acids Research*, **2007**, 35, W701-W706.

[6] Boersema, P. J.; Mohammed, S.; Heck, A. J. R. *J. Mass Spectrom*. **2009**, 44, 861-878.

[7] Jagannadham, V. M.; Nagaraj, *Anal. Chem. Insights.* **2008**, 3, 21-29.

[8] Eyrich, B.; Sickmann, A.; Zahedi, R. P. *Proteomics,* **2011**, 11, 554-570

[9] Cutillas, P. R.; Timms, J. F. *Methods in Molecular Biology*, **2010**, 658.

[10] Ly, T.; Julian, R. R. *J. Am. Chem. Soc.* **2008**, *130*, 351–358.

[11] Diedrich, J. K.; Julian, R. R. *J. Am. Chem. Soc.* **2008**, *130*, 12212–12213

[12] Bookwalter, C. W.; Zoller, D. L.; Ross, P. L.; Johnston, M. V. *J Am Soc Mass Spectrom* **1995**, 6, 872-876

[13] Agarwal, A.; Diedrich, J. K.; Julian, R. R. *Anal Chem*, **2011**, DOI: 10.1021/ac201650v

[14] Dandawate, P. R.; Vyas, A. C.; Padhye, S. B.; Singh, M. W.; Baruah, J. B. *Mini-Reviews in Medicinal Chemistry*, **2010**, 10, 436-454

[15] Diedrich, J. K.; Julian, R. R. *Anal.Chem.* **2010**, *82*, 4006-4014

[16] Chapman, A. L. P.; Skaff, O.; Senthilmohan, R.; Kettle, A. J.; Davies, M. J. *Biochem J*. **2009**, 773-781.

[17] Painter, R. G.; Bonvillain, R. W.; Valentine, V. G.; Lombard, G. A.; LaPlace, S. G.; Nauseef, W. M.; Wang, G. *Journal of Leukocyte Biology*, **2008**, 83, 1345-1353

[18] Schwartz, J.; Leidal, K. G.; Femling, J. K.; Weiss, J. P.; Nauseef, W. M. *J Immunol* **2009**, 183, 2632-2641

[19] Domigan, N. M.; Charlton, T. S.; Duncan, M. W.; Winterbourn, C. C.; Kettle, A. J. *The Journal of Biological Chemistry*, **1995**, 16542-16548.

[20] Mouls, L.; Silajdzic, E.; Haroune, N.; Spickett, C. M.; Pitt, A. R. *Proteomics* **2009**, 9, 1617-1631

[21] Kettle, A. J.; Chan, T.; Osberg I.; Senthilmohan, R.; Chapman, A. L. P.; Mocatta, T. J.; Wagener, J. S. *American Journal of Respiratory and Critical Care Medicine*, **2004**, 170, 1317-1323

[22] Dayon, L.; Roussel, C.; Girault, H. H. *Chimia* **2004,** *58*, 204-207.

[23] Potter, D. W.; Hinson, J. A. *Journal of Biological Chemistry*. **1987**, 262,966-973.

[24] Sun, Q.; Yin, S.; Loo, J. A.; Julian, R. R. *Anal. Chem*. **2010**, 82, 3826-3833.

[25] Bond, G. R. *Clinical Toxicology*. **2009**, 47, 2-7

[26] LaVoie, M. J.; Hastings, T. G. *The Journal of Neuroscience*. **1999**, 19, 1484-1491

[27] Bellomo, G.; Mirabelli, F.; Vairetti, M.; Iosi, F.; Malorni, W. *Journal of Cellular Physiology*, **1990**, 143, 118-128.

[28] Sun, Q.; Nelson, H.; Ly, T.; Stoltz, B. M.; Julian, R. R. *J. Proteome Res.* **2009**,*8*, 958–966.

[29] Henderson, J. P.; Byun, J.; Williams, M. V.; Mueller, D. M.; McCormick, M. L.; Heinecke, J. W. *The Journal of Biological Chemistry*, **2001**, 276, 7867-7875

Chapter 6

CONCLUDING REMARKS

Described in this thesis is the development of radical directed dissociation (RDD) for identification of various types of PMTs in protein and peptide systems. Protein modifications can be grouped into two very broad classifications, selective and nonselective modifications. PTMs which fall into the selective group would include phosphorylation, glycosylation, methylation, disulfide bond formation and such. These are probably the more commonly studied PTMs as they often affect protein function in a desired fashion. Due to their selectivity potential sites of these modifications can be predicted, at least to some extent.

Nonselective modifications however are often not desired or beneficial for protein function, and are often correlated with damage or aging of protein. Additionally modifications such as oxidation, halogenation, or alkylation are often due to exogenous sources. There is often a hierarchy to amino acid sites affected; methione is more susceptible to oxidative damage than other residues

for instance. Thus there is less predictability towards sites that will be modified in this fashion.

Nevertheless an understanding of all these PTMs is of importance. Not only are PTM sites related to proper protein function, but incorrect or damaging PTMs are often related to disease states. Thus to gain a better understanding of disease states we must first understand how it differs from a normal state. Often there are only small differences in location or abundances of PTMs that will differentiate a disease state from a normal one. Thus a robust and selective technique is needed to bring this to fruition.

Techniques presented in this thesis could very well be used in such a way after further improvements. Multiple types of modification were analyzed but each technique focuses on creating a type of fragmentation that was unique to the PTM. Incorporation of a photolabile bond is the key requirement. Two levels of selectivity have been presented in this thesis. Homolytic cleavage of a bond by PD yields a selective mass loss that is useful for identification purposes as well as reducing data analysis. Searching for peptides which contain a PTM of interest is greatly simplified by detecting the presence or absence of the homolytic cleavage. Extending this methodology to applications which meet this requirement alone opens the door to a great number of possibilities. The second

level of selectivity that was presented was that of radical directed dissociation to give selective fragmentation of the peptide. Photodissociation allows preparation of a radical in a desired and known location. The beta position was determined to be the ideal location for generating a radical because of the subsequent backbone dissociation that is favored selectively at the modification site. Other radicals generated by photodissociation, not at the beta position, do give localized fragmentation that can be useful.

An understanding of this chemistry can be utilized to further enhance the efficiency of the modification or to tune the photodissociation properties as desired. Particularly improvement upon the efficiency of some of the reactions would be vital to making photodissociation a viable technique for PTM analysis. Addressing these issues would allow analysis of complicated samples, particularly with the coupling to liquid chromatography. In such a way LC-PD-MS can take full advantage of the selectivity to allow confident identification as well as reduce data analysis.